Garnet-bearing metabasites from the Blastomylonitic Graben, western Galicia, Spain

G. van der Wegen

Wegen, G. van der. Garnet-bearing metabasites from the Blastomylonitic Graben, western Galicia, Spain. — Scripta Geol., 45: 1-95, 29 figs., 6 plates, Leiden, July 1978.

The present study deals with polyphase deformed and metamorphosed basic rocks from the Blastomylonitic Graben. The Blastomylonitic Graben is one of a number of meso- to catazonal complexes of probably Precambrian age in north-western Spain and northern Portugal. The results of the present study are obtained by application of the following methods: optical-mineralogical research, electronprobe microanalysis, X-ray powder diffraction and chemical whole-rock analysis.

It is stated that the metabasites are originally of one, mainly bi-mineralic, rock type, altered by polymetamorphism. The successive phases of metamorphosis and deformation are differently developed locally and belong to two orogenies. The protolith was a rock, in which granoblastic clinopyroxene is intergrown with garnet, white mica, zoisite, kyanite, and quartz. Particularly the amount of white mica, zoisite, kyanite, and quartz is strongly varying in streaks parallel to the general foliation of the rock. The result is a variety of eclogitic and garnet-amphibolitic rocks as we find them in small lens-like bodies in the Blastomylonitic Graben. The true eclogite forms only a small part of the volume of the boudins and conformable interstratified bands of restricted size or the more isometric bodies of larger dimension (i.e. near Bainas).

Two types of garnet appear to occur in the examined metabasites. Firstly a zoned garnet with — from core to rim — increasing Mg, decreasing Ca, varying Fe and rather constant Mn. The garnets are higher in grossular and lower in almandine and pyrope components as compared with the second type, while their spessartine content is always low. Reverse zoning of Mn near the rim is frequently observed. The second type of garnet is not zoned or hardly so, merely variable in composition. Some order exists within the mutual relation between Ca and Fe: Ca-rich correlates with poor in Mg and Fe. It is suggested that the formation of atoll-type garnets and not or hardly zoned garnets with irregular variations in composition is indicative of a special event in the course of the prograde metamorphism.

The clinopyroxene can be differentiated into an older, granoblastic type, and a younger, porphyroblastic one. The former determines mainly the rock foliation. The latter type is late- or post-kinematic (F_1). A zonal structure of omphacite has not been proved. Apart from the crystallographically different pyroxenes, two groups of clinopyroxenes can be distinguished optically and chemically. The total iron content in cpx_{II} is mainly higher than in cpx_I. It is obvious that the total iron content of the bulk rock composition was determining the total iron content of the clinopyroxene that was formed. Cpx_I- and cpx_{II}-bearing metabasites define a magmatic differentiation trend. The spreading of the plots of the metabasites in an AFM-diagram emphasizes the early to middle stage differentiates, i.e. a tholeiitic to alkali-basaltic character and a differentiation trend with decreasing mg.

With regard to the facies of the high-pressure metamorphism: on the basis of Ca-, Mg- and Fe-partitioning in coexisting garnet rim - clinopyroxene pairs, temperature and pressure, prevailing during the culmination of the prograde metamorphism, can be approximated (T= 585-625°C and P= 13-16 kb). The geothermal gradient than should average at 11°C/km, which agrees very well with the formation of the group C-eclogites of Coleman et al. (1965).

Eclogite-amphiboles, i.e. barroisitic hornblendes, are paragenetically related to the critical eclogite-minerals omphacite and pyrope-almandine garnet. A second type of amphiboles, more tschermakitic in composition, is contemporaneous with the stable association albite-epidote. Whereas the former amphibole was formed under higher-pressure conditions, the pressure did not play an important role in the amphibole-epidote-albite paragenesis. A scheme (Table 8) is established in which mineral equilibria during successive metamorphic and deformative phases may be distinguished. Zoisite is syngenetic with the syn-kinematic (F_2) porphyroblastesis of barroisitic hornblende. The F_4-deformation coincides partly with the stable association of blue-green amphibole, albite, and epidote. The impression is gained that the albite-poikiloblastesis took place in the less deformed parts of the eclogitic rock as far as it is syn-kinematic. The formation of boudin-like textures coincides with the development of the albite-amphibole symplectite. The main quartz-veining phase coincides more or less with the uralitisation of the pyroxene. Uralitisation, instability of the garnet, quartz veining, ilmenite formation and magnetite emplacement on cleavages in the garnets point to conditions of deformation (F_3) under a lower pressure.

G. van der Wegen, Rijksmuseum van Geologie en Mineralogie, Hooglandsekerkgracht 17, 2312 HS Leiden, The Netherlands.

Introduction

The investigated rocks derive from the Blastomylonitic Graben in western Galicia (Fig. 1). Western Galicia is situated in the geanticlinal axial zone of the predominantly Hercynian orogen, also known as the Hesperian Massif, of the western Iberian Peninsula. The Blastomylonitic Graben is one of the five meso- to catazonal complexes of north-western Spain and northern Portugal (den Tex & Floor, 1967, 1971).

The area considered in the present publication is situated in the Galician/Castilian paleogeographic zone as distinguished by Lotze (1945). This zone forms the central part of the bilaterally symmetrical orogenic belt of N.W. Spain and Portugal, the history of which lasted from late Precambrian or early Cambrian into the Permian. In the sense of Aubouin (1965) the mentioned zone is the structural hinterland of the geosynclinal development. The evidence for tectonic movements in different parts of the orogen has been compiled a.o. by Matte (1968), Capdevila (1969), and Wagner & Martinez-Garcia (1974). Wagner & Martinez-Garcia concluded that seven major phases of deformation can be correlated from one part of the orogen to another, although the intensity differs in the different units. The older tectonic phases strongly deformed the more internal parts of the geosynclinal complex, to which the present rocks belong, since Middle Silurian times (Wenlock). For further information on the geological history of western Galicia, the reader is referred to Parga-Pondal (1966) and den Tex & Floor (1971), while Engels, Hubregtse, Floor & den Tex (1974), Hubregtse (1973a, b), den Tex & Floor (1967), Anthonioz (1970, 1972), and Vogel (1967, 1969) gave accounts of the meso- to catazonal complexes in particular. The Blastomylonitic Graben contains fine-grained quartzo-feldspathic sediments (den Tex & Floor, 1967) of probably late Proterozoic age, possibly representing the equivalents of the eastern Galician Villaba and Narcea series and the Serie Negra in the southern peninsula. Calc-alkaline to peralkaline granites intruded during the Ordovician (Rb-Sr isochron age: 430-460 Ma, according to Priem et al., 1970) but the metablastesis of their plagioclases was caused by metamorphic recrystallisation of Hercynian age. Van Calsteren (1977b) and Keasberry, van Calsteren & Kuijper (1976) proposed a model assuming mantle-plume development beneath a normal continental crust. The mantle-plume regime started at around 500 Ma (van Calsteren et al., 1977, van Calsteren, 1977c). The meso- to catazonal complexes have suffered a prograde metamorphism. The eclogitic and garnet-amphibolitic rocks investigated in the present study are mafic representatives of this prograde metamorphism.

According to Monster (manuscript thesis, 1967) the mentioned rocks constitute conformably interstratified bands of restricted size in the paragneisses, boudin-like bodies with diameters less than 2 m, or more isometrical bodies of larger dimensions. Rubbens (manuscript thesis, 1963) described an isometrical body with a diameter of about 1 km near Bainas, along the road between Negreira and Berdoyas (Fig. 1). In his preliminary study Monster distinguished the following mafic/felsic rock associations:

A) Eclogites and pyroxene-bearing garnet-amphibolites, set exclusively in polymetamorphic paragneisses (den Tex & Floor, 1967), particularly in the white mica-rich rocks of this group. Their planar to planolinear texture is striking. No mafic rocks are encountered in the ferro-hastingsite-bearing gneisses.

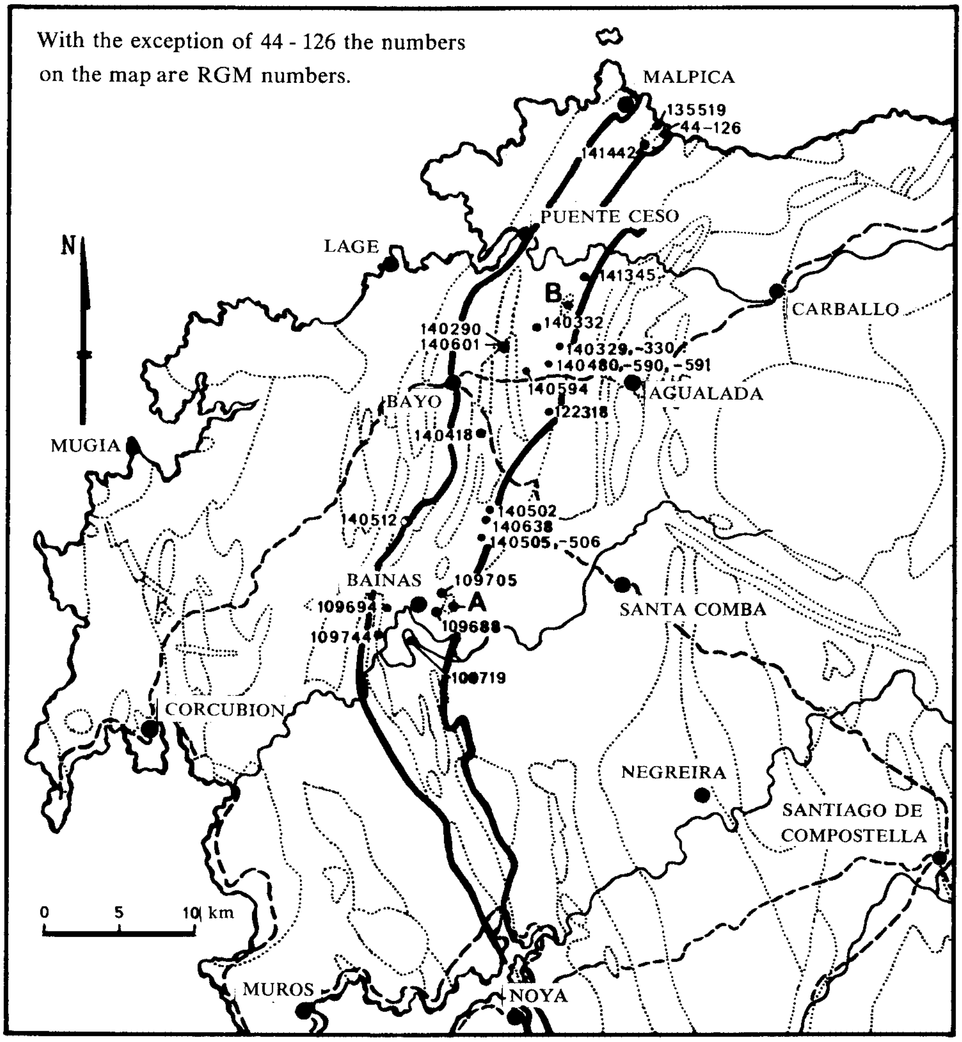

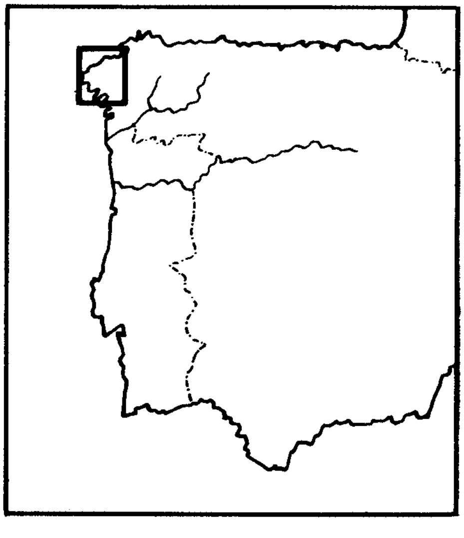

A = Body of metabasites near Bainas: Ru. 5, - 6, - 8, - 11, - 12, - 14, - 15, - 17A, - 17B; RGM 109 669, - 109 669, - 109 681, - 109 682, - 109 684, - 109 685, - 109 723, - 109 773, - 128 219, - 128 225, - 128 226, - 135 506, - 135 507, - 135 508, - 135 509, - 135 510.

B = Metabasite complex between Agualada and Puenta Ceso: RGM 135 523, - 140 322, - 140 323, - 140 379, - 140 380, - 140 383, - 140 385, - 140 389, - 140 615, - 140 617, - 140 622, - 140 623, - 140 647 .

B) Amphibolites with epidote-group minerals, albite, and also garnet are occurring in the same gneisses. These amphibolites are not observed in the peralkaline gneisses.

The Ru-numbers indicate samples derived from the basic body near Bainas collected by Mr H. Koning of the Geological Institute of Leiden University. Sample 44-126 was collected by Mr E. J. H. Rijks, and deposited at the same institute, as are the Ru-samples. Most of the samples enumerated in Table 1 were collected and investigated in the first instance by Messrs I. B. H. M. Rubbens, H. Koning, and G. van der Wegen. The results of Rubbens and Rijks were laid down in unpublished M. Sc. theses for the Department of Petrology of the Geological Institute. A few samples were collected and studied by P. P. Snoep, B. R. van Westreenen and E. J. H. Rijks (unpublished M. Sc. theses, Leiden). The numbers of rock samples deposited and registered in the Rijksmuseum van Geologie en Mineralogie in Leiden (National Museum of Geology and Mineralogy at Leiden) are prefixed with RGM.

The first part of the present publication deals with the results of microscopic investigation, the second part is concerned with the chemistry of minerals and rocks. A brief discussion of the petrogenesis is appended.

Acknowledgements

I want to express my gratitude to Prof. Dr E. den Tex for critically reading the manuscript and for the instructive discussions on the metabasites from the Blastomylonitic Graben. The discussions with colleagues, especially H. Koning and P. Floor were a great support during the preparation of this work.

I am very indebted to Dr C. Kieft of the Working Community for Analytical Chemical Research of Minerals and Rocks (WACOM), who carried out the microprobe analyses. I want to express my thanks to Mr K. M. Stephan, head of the Geochemical Laboratory of the Geological Institute of Leiden University, who kindly performed the whole rock analyses.

Special thanks go to Messrs J. J. F. Hofstra and J. van der Linden for the X-ray powder photographs, to Mr J. Timmers for the drawings, to Mrs C. J. Riethoven-van Leeuwen, for typing the manuscript, and to Messrs T. Veldhuyzen and W. A. M. Devilée for the microphotographs.

Mineralogical investigation

The microscopic examination is limited primarily to those mafic rocks in the area studied, which consist of garnet, clinopyroxene, and rutile, or derivatives of one or more of the mentioned minerals. Moreover, kyanite, white mica, zoisite, porphyroblastic amphibole, and quartz can be present. Products of later metamorphic processes like blue-green pleochroic amphibole, albite, clinozoisite-

---

Fig. 1. Locality map of the metabasites from the Blastomylonitic Graben, Galicia, Spain. The geological contour lines are derived from the 'Carte géologique du nord-ouest de la Péninsule Ibérique' (1:500 000) published by the Geological Survey of Portugal (1967). The Graben is indicated by a heavy outline.

Table 1. List of rock samples of metabasites from the Blastomylonitic Graben, Galicia, Spain (compare Fig. 1).

RGM nr.:	Field nr.:	Collector/report:
	44-126	Rijks, 1968
	Ru 5	Koning
	Ru 6	,,
	Ru 8	,,
	Ru 11	,,
	Ru 12	,,
	Ru 14	,,
	Ru 15	,,
	Ru 17A	,,
	Ru 17B	,,
109 668	R 39B	Rubbens, 1963
109 669	R 40	,, ,,
109 681	R 65	,, ,,
109 682	R 66	,, ,,
109 684	R 68A	,, ,,
109 685		,, ,,
109 688	R 73	,, ,,
109 694	R 84	,, ,,
109 705	R 118	,, ,,
109 710	R 146	,, ,,
109 723	R 153	,, ,,
109 744	R 182	,, ,,
109 781		,, ,,
122 318	155A	Snoep, 1964
128 219	W 78	Van der Wegen, Azopro excursion, 1971
128 225	W 83	,, ,, ,,
128 226	W 83	,, ,, ,,
135 506	10B	,, , 1967
135 507	10C	,, ,,
135 508	10D	,, ,,
135 509	10F	,, ,,
135 510	10G	,, ,,
135 519	18	,, ,,
135 523	26	,, ,,

RGM nr.:	Field nr.:	Collector/report
109 773	R 224	Rubbens, 1963
140 290	44B	Monster, 1967
140 322	20	,, ,,
140 323	21	,, ,,
140 329	36	,, ,,
140 330	37	,, ,,
140 332	40	,, ,,
140 379	130	,, ,,
140 380	131	,, ,,
140 383	133	,, ,,
140 385	135B	,, ,,
140 389	135J	,, ,,
140 418	35	,, ,,
140 480	36A	,, ,,
140 502	16	,, ,,
140 505	24B	,, ,,
140 506	25B	,, ,,
140 512	38	,, ,,
140 590	35A	,, ,,
140 591	35B	,, ,,
140 594	59C	,, ,,
140 601	29C	,, ,,
140 615	112B	,, ,,
140 617	134	,, ,,
140 622	165A	,, ,,
140 623	139C	,, ,,
140 638	13A	,, ,,
140 647	137D	,, ,,
141 345	89	Van Westreenen, 1968
141 442	73C	Rijks, 1967

epidote, chlorite, brown and green biotite, so-called fine-symplectite, ilmenite, titanite, and limonite have been found. Symplectitic intergrowths are associated with garnet, clinopyroxene, and porphyroblastic amphibole of commonly lavender-blue pleochroic colours. Apatite, zircon, pyrite, magnetite, and pyrrhotite may also be present.

One hundred samples of these metabasites have been examined. The results of this study are summarized as follows. The rock samples derive from various places in the Blastomylonitic Graben. Thirty-two samples contain light-coloured amphibole porphyroblasts. A few porphyroblasts of clinopyroxene are found in some of the latter samples. The volume percentage of this amphibole is, roughly estimated, equal or larger than 50 in 11 of the 32 samples. It is remarkable that garnet with atoll-structure is not found in these 11 samples, whereas the rate of occurence of the atoll-garnets is 20 to 100. On the other hand, 24 samples do not or hardly contain porphyroblastic amphibole, but garnets with atoll-structure are observed in 8 of these 24 samples. In a group of about 40 samples from which clinopyroxene has vanished partly or entirely by later alterations, garnet is also strongly affected.

The mineral samples were obtained using mineral separation techniques, such as heavy liquids and the Frantz isodynamic magnetic separator. The magnetic susceptibility of a mineral is established with the aid of the Hess' nomogram (1966) and expressed in 10^{-6}cg units.

Principal characteristics of minerals concerning form, colour, grain-size, and optics are recorded in the next chapter, apart from their mutual relationships. The colour is macroscopically estimated on mineral concentrates with the aid of the Rock-Color Chart, distributed by the Geological Society of America (1963). Refractive index determinations were done on mineral grains with the aid of immersion liquids in transmitted sodium-light, to an accuracy of ± 0.003. The data were continually checked by a Rainer refractometer. Optic axial angles and extinction angles were measured with the aid of a four-axes universal stage.

GARNET

Characteristics

The grain-size of garnet does not only vary between hand specimens, but also within one hand specimen and even within one thin section (from 0.05 to 3 mm). The colour can be indicated according to the Rock Colour Chart from 5YR 7/2 to 5YR 6/4, and is found to be generally colourless to reddish brown in thin sections. Garnets with atoll and more massive structures are to be distinguished. Usually the latter show sieve structure with a massive or an inclusion-poor rim. Garnets with an atoll structure generally show good idioblastic boundaries. It is striking that the atoll-like forms have not been observed in rocks with considerable contents of either dark- or light-coloured, porphyroblastic amphibole. In some instances atoll-garnet is found enclosed in porphyroblastic amphibole (RGM 109 685, 140 647). According to Rast (1965), the atoll-like structure of the garnets in the Central Highlands of Scotland is the result of partial pseudomorphous replacement. Similar structures, well-known to mineragraphers (Schouten, 1934; Edwards, 1960), are supposed to arise from the dissolution of zoned minerals, when selective replacement of the crystal core and of rhythmically varying compositional zones occurs (Smellie, 1974). It has been shown by the present author that the majority of garnets from the metamorphic rocks are zoned. The interior of the present garnets with a well-developed atoll structure is filled with white mica, quartz, and in some places zoisite. In well developed atoll forms, perhaps constituting transitions to the massive garnet type, clinopyroxene is found with (RGM 135 510) or without white mica (RGM 109 781). Light-coloured porphyroblastic amphibole, in places together with remnants of clinopyroxene (RGM 135 506), may occur in the atoll interior. In conclusion it can be said that these

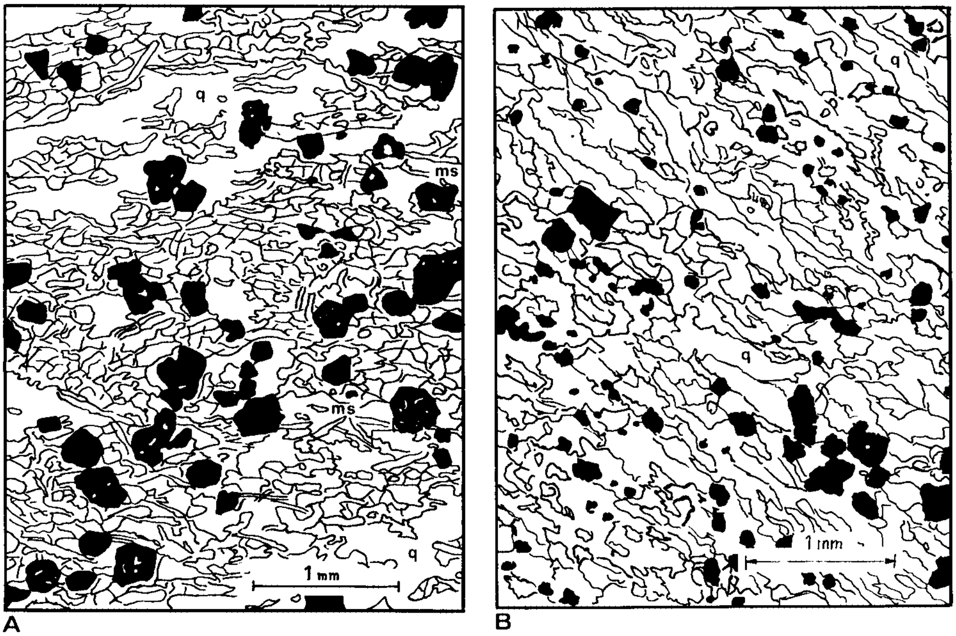

Fig. 2. Distribution of garnets in samples RGM 135 509 (A) and Ru 13 A (B) from the quartz- and mica-rich schistose rocks of the basic body near Bainas. The clinopyroxene is partly uralitised (ms= white mica, q= quartz).

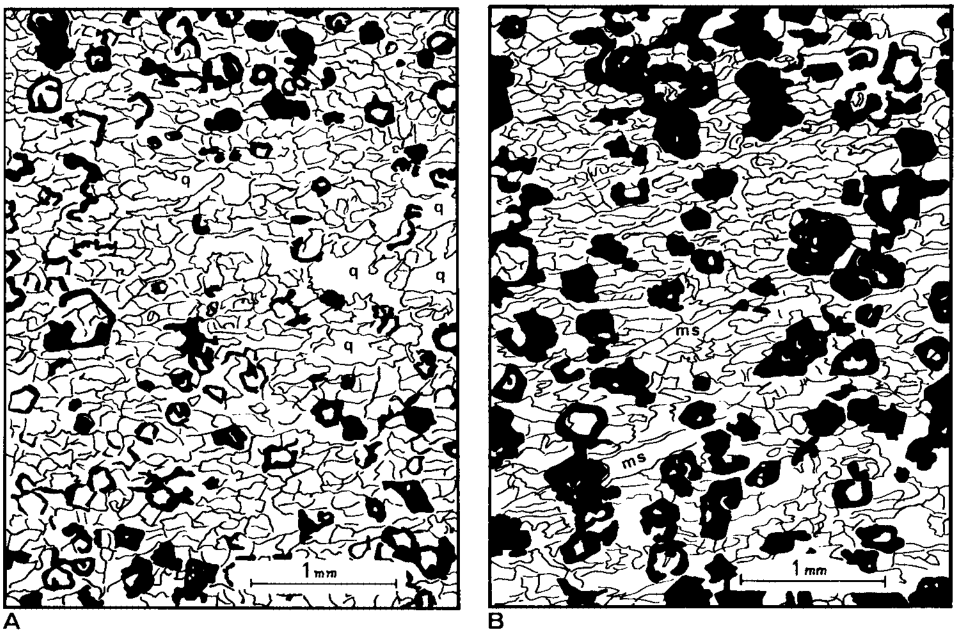

Fig. 3. A. Well-developed atoll-like, euhedral garnets in a groundmass of clinopyroxene with white mica and kyanite. Quartz in streaks parallel to the foliation. The interior of the atoll-garnets is filled with quartz, white mica and some clinopyroxene. Sample RGM 135 506, from the main rock type of the body near Bainas. B. Clotty aggregates of garnet in a groundmass of foliated clinopyroxene and quartz. Atoll garnets can be noticed. Sample RGM 122 318, weakly schistose rock WSW of Agualada.

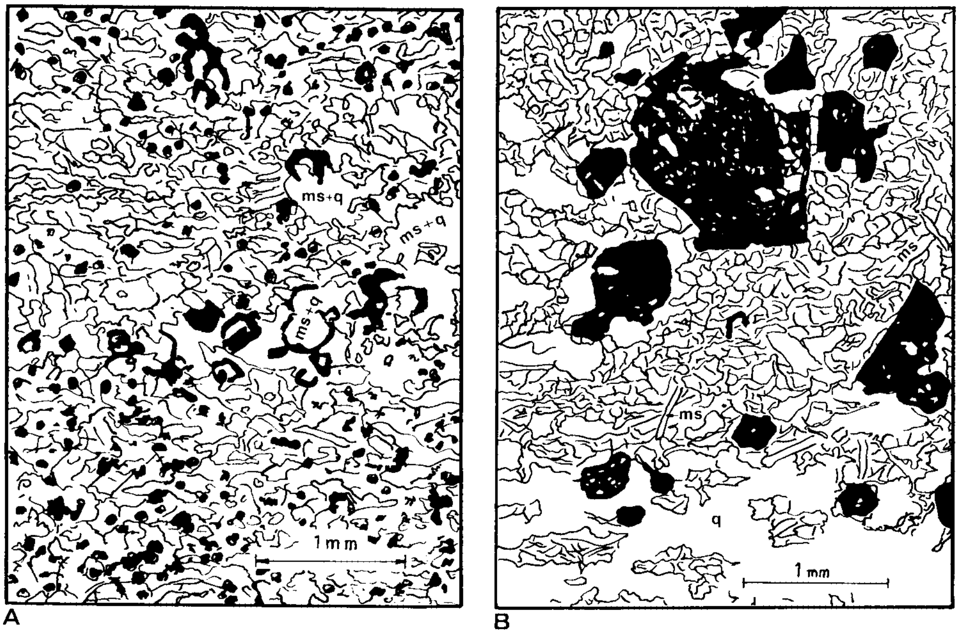

Fig. 4. A. Small, usually anhedral garnets in a groundmass consisting mainly of clinopyroxene. The orientation of the clinopyroxene determines the foliation. Lenticular aggregates of white mica and quartz (ms + q) occur dispersed in the groundmass. The garnet of the lenticules is coarser grained than in the groundmass and shows atoll-like structures. Sample RGM 140 647, from the complex between Agualada and Puente Ceso (see Fig. 1). B. Garnets of unequal grain-size and idiomorphy are surrounded by clinopyroxene, white mica, crystals of the epidote-group, and quartz. The quartz occurs mainly in streaks parallel to the foliation. The garnets show sieve-structures, with some kyanite in addition to inclusions of quartz and epidote-group minerals. Sample RGM 135 508, from the main rock type of the body near Bainas.

atoll forms originate where a garnet core was replaced by white mica, quartz, and possibly zoisite, whereas the porphyroblastic amphibole and the clinopyroxene are inclusion remnants of the pre-existing garnet. The porphyroblastic amphibole is an alteration product of the clinopyroxene. A variant of the atoll-garnet is a garnet with a barrier-reef fabric, i.e. a zone lacking garnet material in between core and rim. This more or less circular zone is also filled with newly formed minerals like white mica, quartz, and zoisite, and the above mentioned inclusion remnants. In many instances core and rim of the garnet are connected (Fig. 8). It may be concluded that during the formation of the assemblage quartz + white mica (+ zoisite) conditions prevailed, in which some garnet compositions were less stable than others. On the other hand Cooper (1972) and de Wit & Strong (1975) refute selective replacement as the cause of atoll formation. They explain these textures in terms of progressive growth features of the garnet (see p. 60).

Textures

An accurate classification of garnet textures can not be furnished; drawings made from microphotographs will, however, give an impression of the different rock types (Figs. 2-8; garnets are indicated in black). Samples not derived from the body near Bainas, are from elsewhere in the Blastomylonitic Graben, as indicated on the map (Fig. 1).

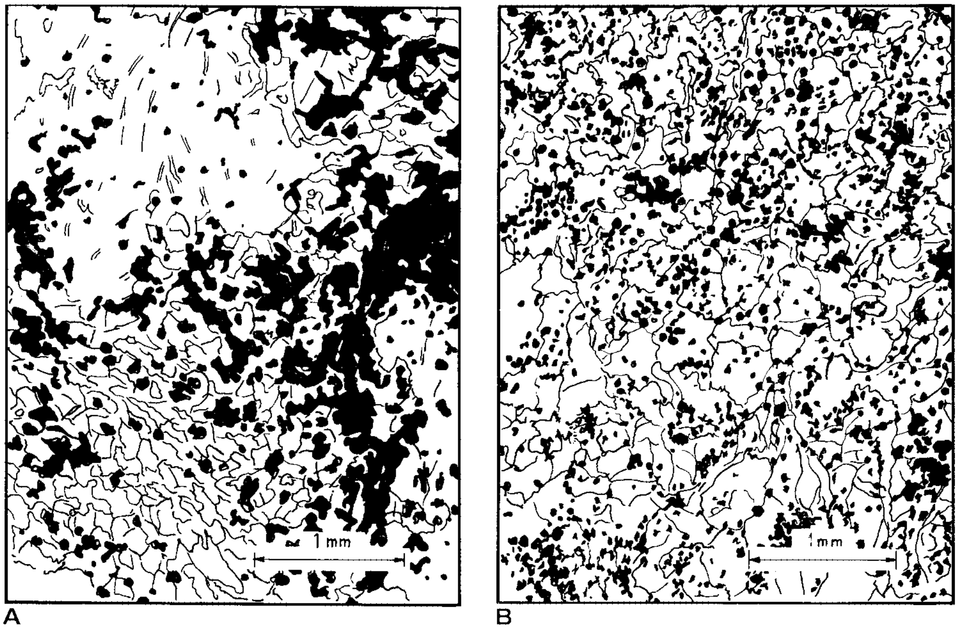

Fig. 5. A. The larger part of the thin section is occupied by light-coloured amphibole of variable grain size. Streaky concentrations of garnet are observed mainly along the coarse-grained amphibole. These streaks follow the wavy foliation in the rock. Helicitic structures show fan-shaped arrangements of zoisite, white mica and some clinopyroxene (see also Pl. 1) in a host of amphibole. This points to synkinematic porphyroblastesis of the amphibole. Sample RGM 109 669, from a dark lens in the body near Bainas. B. Thin section showing very fine-grained, streaky to clotty, scattered garnets. The dispersion pattern seemingly ignores the granular mosaic of the light-coloured amphibole, clinopyroxene, zoisite, and so-called fine-symplectite. Sample RGM 140 329, from the area WNW of Agualada.

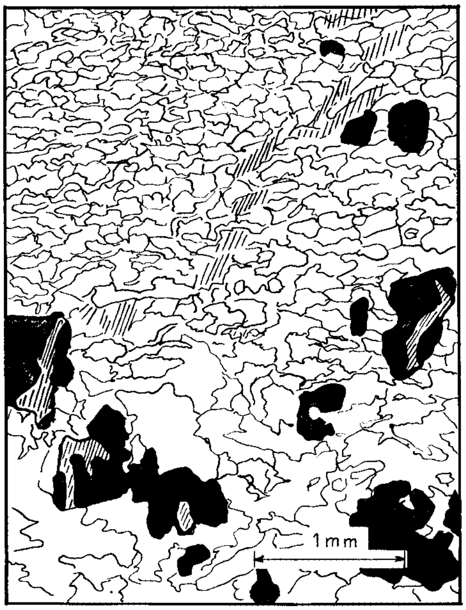

Fig. 6. Section across two thin layers. One layer (left upper part) mainly consists of well-oriented clinopyroxene. The other layer contains dispersed remnants of clinopyroxene occurring together with light-coloured amphibole, white mica and quartz. Relatively large anhedral garnets are mainly found in the latter, whereas the former layer is poor in garnet which is generally smaller in grain size and showing some elongation parallel to the foliation. Sample Ru 17 B, from the body near Bainas.

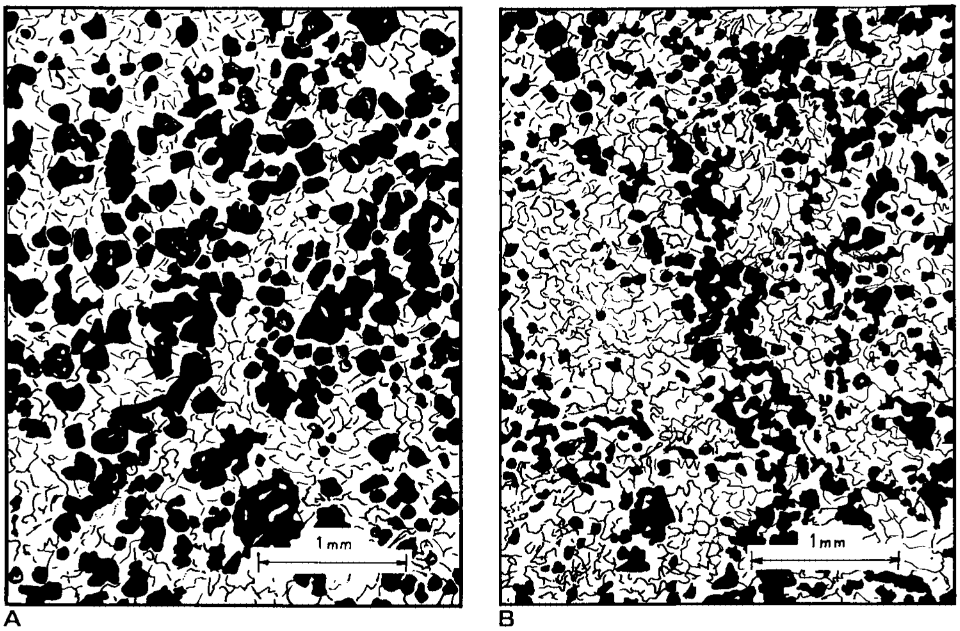

Fig. 7. A. Clotted garnets in a groundmass of clinopyroxene and fibrous symplectite. Blue-green amphibole, albite, titanite with rutile remnants, white mica, and quartz are observed. Sample Ru 11, from the body near Bainas. B. Garnets concentrated in vein-like streaks. Albite blastesis is well-developed together with crystallization of blue-green amphibole, epidote, and titanite. Sample RGM 135 519, from the area ESE of Malpica.

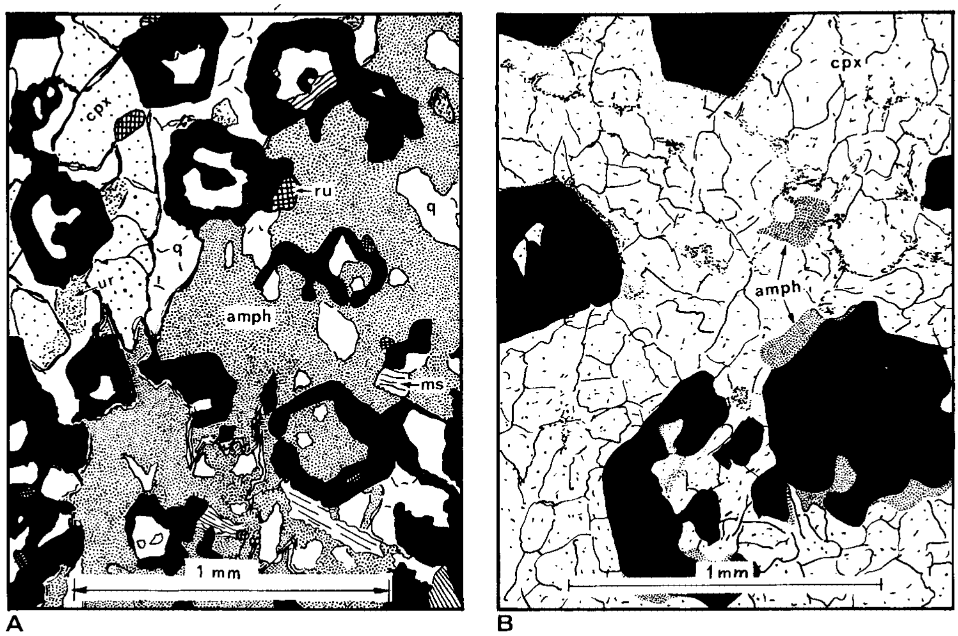

Fig. 8. Garnets with atoll or atoll-with-barrier-reef structures in eclogitic rocks. A. Strongly foliated rock consisting of amphibole poikiloblasts (amph), clinopyroxene (cpx) with uralite (ur), rutile (ru), quartz (q), and white mica (ms). Sample RGM 109 685, from the body near Bainas. B. Drawing from a portion with abundant clinopyroxene. Blue-green amphibole (amph) selectively occurs along the grain-boundaries between garnet and pyroxene as an alteration product of the latter. Sample RGM 109 781, from the vicinity of the body near Bainas.

Alterations

Kelyphite is a common alteration product of garnet in the investigated rocks. In contrast with the generally well-developed kelyphite zones around garnets in eclogitic rocks of the Cabo Ortegal area (Vogel, 1966, 1967; Engels, 1972), the kelyphite of these rocks is restricted to narrow zones. Other alteration minerals are epidote, green and blue-green pleochroic amphibole, sometimes chlorite, brown and green mica, which occur in fractures in the garnets. Apart from the minerals mentioned, finely dispersed opaque minerals are found in a system of parallel joints, or the garnets are entirely replaced by an association of albite,brown or green mica, small sheaves of needle-like amphiboles, some chlorite, and some opaque minerals (RGM 140512, 140505, 140506). The main garnet-replacing mineral — albite — is arranged in a spherulitic manner (Pl. 2, fig. 3).

Deformations

With the exception of a slight elongation parallel to the foliation, the only deformation phenomenon occasionally observed on garnet metablasts is a system of more or less parallel fractures. These fractures can not always be traced into the surrounding clinopyroxene. They are oblique with respect to the foliation.

CLINOPYROXENE

Characteristics

Clinopyroxene occurs predominantly in a granoblastic texture. The grain-size varies from 0.1 to 0.6 mm. Dispersed porphyroblasts found in some of the rock samples hardly measure 2 mm. Smaller clinopyroxene crystals are observed in the pyroxene porphyroblasts of Ru 8. Other examples of porphyroblasts are found in RGM 109688, 140384, and 140617.

The generally well-oriented, short-prismatic crystals define the foliation together with zoisite, white mica, and amphibole. The pyroxene is a solid solution of omphacite composition (see chapter on Mineral chemistry). The optical characteristics of clinopyroxenes from twenty-two samples have been examined. Two groups of clinopyroxenes can be distinguished in the mineral concentrates on account of colour differences (Table 2). The dispersion is usually moderately strong with $r>v$; the dispersion is weak in those cases where $r<v$. A direct relation appears to exist between the refractive index α and the magnetic susceptibility (m.s.) of the clinopyroxene. In Figure 9B one group of clinopyroxenes (cpx_I) occupies a different field from a second group of clinopyroxenes (cpx_{II}). A similar relation holds for the garnets associated with cpx_I and cpx_{II} (Fig. 9A). Plotting the m.s. of the garnets against those of the cpx's (Fig. 9C) the distinction of the two groups remains visible. These data indicate that: 1) the total iron content of both minerals is distinctive for the two groups of metabasites (see further the chapter on Rock chemistry); 2) there is a paragenetic relation between each group of clinopyroxenes and each group of garnets. Textural examinations with the aid of X-ray methods (Mons & Paulitsch, 1970) showed a paragenetic relationship between omphacite, garnet and in addition, quartz in some eclogites from the Muenchberg Gneiss Massif (Bavaria).

Table 2. Optical characteristics and colour of clinopyroxenes from the eclogitic and garnet-amphibolitic rocks of the Blastomylonitic Graben, Galicia, Spain.

A. Greyish yellow-green to weakly yellowish green clinopyroxene (5 GY 7/2 - 10 GY 7/2, according to the Rock Colour Chart).

	α	β	γ	$2V_\gamma$	$\gamma \wedge c$	dispersion
Ru 8	1.663	1.669	1.683	69°	40°	r > v
RGM 109 669	1.667	1.676	1.689	73°	43°	r > v
RGM 135 506	1.669	1.677	1.689	79°		r > v
RGM 135 508	1.670	1.678	1.690	81°	44°	r > v
RGM 135 509	1.670	1.678	1.690	81°	45°	r > v
RGM 109 688	1.667	1.675	1.690	76°	42°	r > v
RGM 109 705	1.669	1.676	1.688	75°	45°	r > v
RGM 109 781	1.673	1.680	1.693	75°	46°	r > v
RGM 122 318	1.668	1.675	1.687	81°	44°	v > r
RGM 135 523	1.670	1.678	1.693	75°		v > r
RGM 140 480	1.668	1.675	1.687	77°	43°	r > v
RGM 140 617	1.673	1.682	1.694	77°	41°	r > v
RGM 140 647	1.665	1.672	1.685	72°		v > r
RGM 141 345	1.666	1.673	1.687	77°	47°	r > v

N.B. The first five samples are from the body near Bainas, the nine others are from elsewhere in the Blastomylonitic Graben.

B. Greyish green clinopyroxene (10 GY 5/2, Rock Colour Chart).

	α	β	γ	$2V_\gamma$	$\gamma \wedge c$	dispersion
RGM 109 723	1.680	1.688	1.702	74°	46°	r > v
RGM 109 773	1.679	1.687	1.701	76°	48°	r > v
RGM 128 225	1.677		1.700			
RGM 135 510	1.675	1.683	1.697	74°	47°	r > v
RGM 140 615	1.675	1.683	1.694	82°	47°	r > v
RGM 135 519	1.684		1.706			
RGM 141 442	1.682	1.692	1.703	86°		r > v
RGM 140 594	1.674		1.690			

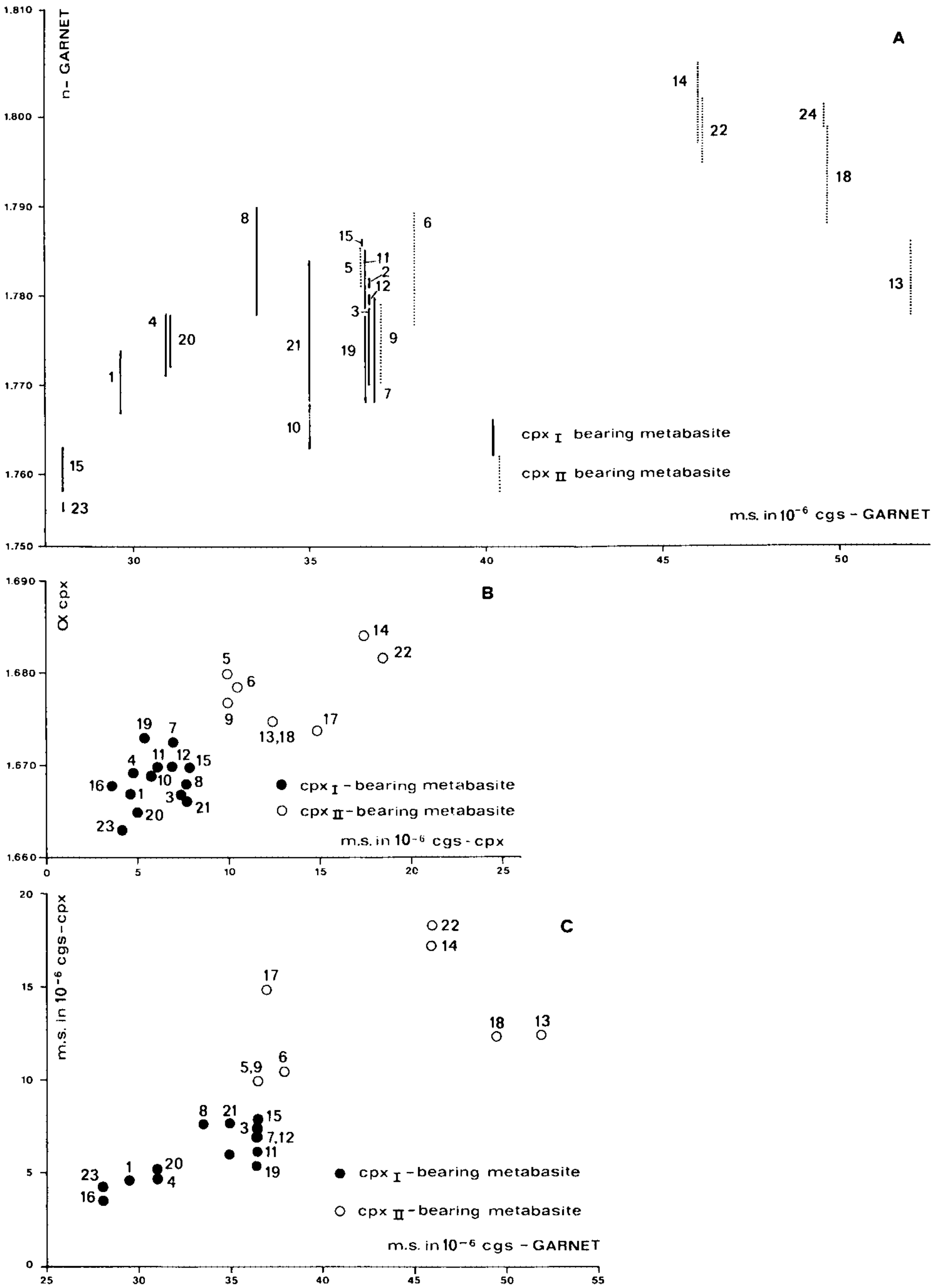

Fig. 9. Diagrams showing the relationship between A: Magnetic susceptibilities (m.s.) and refractive indices (n) of garnets, B: Magnetic susceptibilities (m.s.) and refractive indices (n) of clinopyroxenes, and C: Magnetic susceptibilities (m.s.) of garnets and clinopyroxenes, of 24 metabasites from the Blastomylonitic Graben. The magnetic susceptibility is expressed in cgs x 10^{-6}. The numbers in the diagrams refer to the samples as follows: 1 = RGM 109 669, 2= RGM 109 684, 3= RGM 109 688, 4= RGM 109 705, 5= RGM 109 723, 6= RGM 109 773, 7= RGM 109 781, 8= RGM 122 318, 9= RGM 128 225, 10= RGM 135 506, 11= RGM 135 508, 12= RGM 135 509, 13= RGM 135 510, 14= RGM 135 519, 15= RGM 135 523, 16= RGM 140 480, 17= RGM 140 594, 18= RGM 140 615, 19= RGM 140 617, 20= RGM 140 647, 21= RGM 141 345, 22= RGM 141 442, 23= Ru 8, 24= 44-126.

Textures

Enclosed in the clinopyroxene we find: garnet, euhedral zircon (RGM 135 506), and small euhedral, short-prismatic rutile crystals. Rutile in clinopyroxene, the latter often enclosed itself in amphibole, is fine-grained and finely dispersed, whereas the rutile enclosed in amphibole is more xenomorphous and coarser grained (RGM 140 480). Amphibole and white mica inclusions are never found in the clinopyroxene, but small mica scales are observed in cleavages of the pyroxene (RGM 109 668).

Apart from forming chadacrysts in amphibole, the pyroxene may be enclosed in zoisite, white mica, and kyanite. Inspection of a large number of thin sections reveals that clinopyroxene chadacrysts are generally finer grained and less idiomorphous than the pyroxene outside the oikocrysts. Garnet inclusions are abundant in the clinopyroxene porphyroblasts. These inclusions are more or less euhedral. Comb-like aggregates of garnet, as seen in thin sections, are also sometimes situated festooned in and along large pyroxene crystals. The comb-like structures are possibly thin sections of garnet festoons bordering the capriceous surfaces of the porphyroblasts (Pl. 3, fig. 2).

Alterations

Clinopyroxene crystals are nearly always enveloped by a thin skin of very fine-grained symplectite. It is remarkable that this so-called fine-symplectite is best observed in fresh rocks. In RGM 109 781 clinopyroxene without the fine-symplectite rim occurs, enclosed in white mica. Wherever coarse-symplectite borders

Fig. 10. Two examples of kyanite-bearing eclogitic rock, A: Sample RGM 109 781 from the vicinity of the body near Bainas, B: Sample RGM 135 509 from the body near Bainas; ky = kyanite, cpx = clinopyroxene, ur = uralite, ms = white mica, zoi = zoisite, amph = blue-green amphibole, q = quartz, and ab = albite as thin films along grain boundaries.

the clinopyroxene, a fine-symplectite zone is always found in between. The coarse-symplectite is certainly younger than the fine-symplectite, though there are numerous indications for the fine-symplectite having been formed later than the light-coloured amphibole porphyroblasts (a.o. RGM 109 694, 128 226, 140 638). Blue-green pleochroic amphibole is observed where pyroxene and garnet are in contact. This amphibole is not the result of the formation of garnet-kelyphite but is an alteration product of clinopyroxene.

KYANITE

Characteristics

The grain-size is usually smaller than 1 mm. In sample Ru 14 poikiloblasts as large as 2 mm are seen, whereas strongly deformed kyanite crystals or crystal-aggregates measuring several decimetres across are found in an outcrop of the Bainas-eclogite. The latter kyanite is found intergrown with white mica in a quartz-vein. Generally the kyanites are poikiloblasts with amoeboid boundaries and numerous inclusions. They commonly show strong bending and granulation, while the elongation is not always parallel to the foliation. A subordinate number of kyanites is smaller, allotriomorphous and forms more angular crystals with hardly any or no inclusions. The second type is oriented parallel to the foliation together with clinopyroxene.

Twinning, apparently according to $\{100\}$, is rarely observed in both types.

Textures

Kyanite does not commonly occur in rocks with abundant amphibole, but it is mainly found together with clinopyroxene.

Following Scharbert (1954), Vogel (1967) distinguished typomorphous from post-eclogite kyanite. While Vogel held the opinion that the second generation kyanite is post-eclogitic in the Cabo Ortegal eclogites, Matthes et al. (1970) claimed that this kyanite is of late- rather than post-kinematic crystallization in the Muenchberger Gneiss eclogites. In the latter case simultaneous growth of the poikiloblastic kyanite and garnet is observed. The present author considers the occurrence of quartz-kyanite in crumbled veins, as known from the body near Bainas, to represent a post-eclogitic pegmatoid stage. The pressure during the formation of kyanite should have been at least 4 - 6 kb at 500°C (Fonteilles, 1965; Richardson, Gilbert & Bell, 1969; Althaus, 1967; Newton, 1966; Holdaway, 1971).

The poikiloblastic kyanite may contain inclusions of garnet, clinopyroxene, rutile, quartz, zircon, and apatite. Though kyanite is found in light-coloured amphibole porphyroblasts (Ru 8, RGM 140 480), the mineral has never been seen in clinopyroxene porphyroblasts. This leads to the conclusion that the clinopyroxene blastesis is of pre-kyanite age. Kyanite is found enclosed in garnet (RGM 135 508) and in coarse-grained zoisite (RGM 135 507). The clinopyroxene enclosed in kyanite should originally have been fine-grained (Ru 14) because tiny clinopyroxene crystals, lying close together in a kyanite host-crystal, do not extinguish simultaneously under the microscope in polarised light. The elongation of these inclusions is parallel to the foliation.

Muscovite, zoisite, or amphibole are never chadacrysts of kyanite in the present rock samples. Masses of fine-scaly mica or coarser-grained white mica wrap around and partly replace the kyanite (Fig. 10A). Quartz is nearly always present. Blue-green pleochroic amphibole enclosed by the kyanite (Ru 14) is an alteration product of the clinopyroxene and is younger than the kyanite.

Wherever kyanite shows up in the samples, zoisite is also present. On the other hand, kyanite is not always present when zoisite is found. In three out of seven metabasite samples, other than those from the Bainas-eclogite (Table 2-B), zoisite is present, whilst kyanite is completely absent.

Alterations

Part of a thin section of sample RGM 135 509 is shown in Fig. 10B. Here kyanite and white mica are partly replaced by quartz and albite. The albite occurs as a film between quartz and the former minerals. Kyanite and mica apparently do not form a stable assemblage with quartz and plagioclase. The second generation kyanite was first, and mica is a product of this kyanite. Coarse-symplectite in lobate forms composed of amphibole and albite is found along the boundaries of kyanite and mica. In the author's opinion it is reasonable to assume an intricate replacement of kyanite or muscovite. Kyanite appears to be unstable in association with amphibole or zoisite. Examination of a great many thin sections shows that abundant occurrence of amphibole and/or zoisite is attended by a strong decrease of the kyanite content.

ZOISITE

Characteristics

The grain-size of zoisite may vary considerably, even within one thin section. Zoisite crystals in amphibole porphyroblasts are usually small and euhedral, but they may exceed 2 mm outside the amphibole. Zoisite outside and on the periphery of the amphibole porphyroblasts is more or less elongated in accordance with the general orientation of clinopyroxene and white mica, whereas the chadacryst-zoisites may be arranged in fan-shaped swarms of small prismatic crystals (Pl. 1, fig. 3).

The porphyroblastic zoisite has a zoned structure (Vogel & Bahezre, 1965). A cruciform, or a three-dimensional, hour-glass structure with divergent optical behaviour reveals itself under the microscope in polarised light (Pl. 1, figs. 1 and 2). While searching in the thin sections for crystals that are suitable for further optical examination, it was found that zoisite commonly has a lattice orientation. The best sections are those more or less parallel to the foliation. Generally it appears that the optic axial plane of zoisite is oriented perpendicular to the foliation plane. Moreover, the acute bisectrix of the indicatrix of zoisite, i.e. γ, is also roughly perpendicular to the foliation plane. The porphyroblastic zoisite can be both α- and β-zoisite. A sample containing α-zoisite is RGM 109 688 and one containing β-zoisite is RGM 109 684. According to Deer, Howie & Zussman (1962), α-zoisite has the O.A.P. parallel to $\{100\}$ and β-zoisite parallel to $\{010\}$. The most distinct cleavage is $\{100\}$ while a less pronounced cleavage is parallel to $\{001\}$. Consequently the plane of the main symmetry axes α and β is distinctly parallel to the plane of the foliation.

Table 3. Optical characteristics of α- and β-zoisite as shown in the rock samples of metabasites from the Blastomylonitic Graben.

RGM nr.	α	γ	$2V_\gamma$		dispersion	// b-axis	
109 684	1.696	1.702	core	16°	r > v	y	β-zoisite
			rim	0°			
109 688	1.697	1.704	core	86°	r << v	x	α-zoisite
			rim	57°			

The optical data of porphyroblastic zoisites from RGM 109 684 and 109 688 are given in Table 3. It is technically impossible to distinguish between the refractive indices of core and rim. Estimations of 2V do not give more than a vague idea of the mutual relationship of the R.I.'s. Exact determinations were not feasible through lack of a source of monochromatic sodium-light sufficiently strong for the anomalous interference colours concerned. It is quite possible that $2V_\gamma = 90°$ may also be found. Two characteristics are put forward considered all data: 1) both α-zoisite and β-zoisite may be found in one sample, if not in one thin section; 2) 2V of the rim is always smaller than 2V of the core. The zoned structure is shown in Plate 1, figs. 1 and 2.

Textures

Zoisite porphyroblasts contain inclusions of garnet, clinopyroxene, rutile, quartz, kyanite, and to a lesser extent small prismatic zoisite crystals. It has been observed that white mica is entirely or partly surrounded by zoisite or its later stage substitute epidote (RGM 109 684, 109 773, 135 509). The small prismatic zoisites are commonly found enclosed by amphibole porphyroblasts (RGM 109 669, 140 617, 140 383) whereas porphyroblastic zoisites of zoned structure are situated rather outside than within the periphery of amphibole porphyroblasts (RGM 140 480). It is concluded that the small prismatic zoisite is older than the porphyroblastic zoisite, but that the latter should have been formed during a late- to post-phase of deformation or after the crystallization of amphibole.

Zoisite is particularly present in fresh rocks. The later processes of alteration have obliterated this mineral. In RGM 109 684 the coarse-symplectite formation seems to proceed also at the expense of zoisite. In a few instances epidote is exclusively found enclosed in garnet and zoisite (Ru 8). Table 4 represents a list consisting of the major minerals occuring in a selection of samples, with the exception of clinopyroxene, garnet and rutile. It should be noticed that a cross indicates the ascertained presence of the mineral group concerned, a dash stands for absence or presence of only minute quantities of the mineral shown, whereas an open space signifies that the mineral's presence has not been ascertained. For zoisite it is mentioned whether the α- or β-type is concerned. From the columns it can be deduced that zoisite is lacking in the cpx_{II}-bearing rocks with the exception of two samples, and that kyanite is entirely absent.

Table 4. List of major minerals and mineral groups, with the exception of clinopyroxene and garnet, from the eclogitic and garnet-amphibolitic rocks of the Blastomylonitic Graben, Galicia, Spain.

A. Samples with type I clinopyroxenes:

registration nr.	α- or β-zoisite	kyanite	white mica	amphibole porphyroblasts	quartz	fine-symplectite	coarse-symplectite	albite porphyroblasts	pyrite	pyrrhotite	magnetite	ilmenite	titanite
Ru 8	α	x	x	x	x	x	-	-				x	-
Ru 12	-	-	x	x	x	-	-	-		x		-	-
Ru 15	-	x	x	-	-	-	-	-		x		-	-
RGM 109 669	α	-	x	x	x	-	-	-	x			x	
RGM 109 681	α	-	x	-	x	-	x	-		x		x	-
RGM 109 684	β	-	x	-	x	x	x	-				x	-
RGM 109 688	α	-	x	x	x	-	-	-	x			x	-
RGM 109 705	α	-	x	x	x	x	x	x	x			x	x
RGM 109 781	α	x	x	-	-	-	x	-			x	x	-
RGM 122 318	-	-	x	x	x	-	-	-				x	-
RGM 135 506	α	x	x	x	x	-	-	-				x	-
RGM 135 508	α	x	x	-	x	-	-	-		x		-	-
RGM 135 509	α	x	x	-	x	x	x	-				x	-
RGM 135 523	-	-	x	x	x	x	x	-	x	x		x	x
RGM 140 322	β	-	x	-	x	x	x	-				x	x
RGM 140 385	α	-	-	x	x	x	x	-	x			x	-
RGM 140 480	α	x	x	x	-	x	x	-		x		x	x
RGM 140 617	α	-	x	x	x	x	x	-				x	-
RGM 140 647	-	-	x	-	x	x	x	-			x	x	-
RGM 141 345	-	-	x	x	x	-	x	-		x		x	-

B. Samples with type II clinopyroxene:

registration nr.	α- or β-zoisite	kyanite	white mica	amphibole porphyroblasts	quartz	fine-symplectite	coarse-symplectite	albite porphyroblasts	pyrite	pyrrhotite	magnetite	ilmenite	titanite
RGM 109 723	-	-	x	x	x	-	-	-	x			x	-
RGM 109 773	α	-	x	-	-	-	x	-			x	x	x
RGM 128 225	α	-	-	x	-	-	x	-			x	x	-
RGM 135 510	-	-	x	-	-	-	x	-			x	x	-

registration nr.	α- or β-zoisite	kyanite	white mica	amphibole porphyroblasts	quartz	fine-symplectite	coarse-symplectite	albite porphyroblasts	pyrite	pyrrhotite	magnetite	ilmenite	titanite
Continuation of B. Samples with type II clinopyroxene:													
RGM 135 519	-	-	-	x	x	-	x	x		x		x	x
RGM 140 594	-	-	x	x	-	x	-	-	x			x	-
RGM 140 615	-	-	-	x	x	-	x	-				x	-
RGM 141 442	-	-	x	glauc	x	-	x	-				x	x
C. Samples from which the type of clinopyroxene is unknown:													
RGM 109 719	α	-	-	x	x	x	x	x		x		x	x
RGM 140 290	α	-	-	x	-	x	x	x		x		x	x
RGM 140 502	α	-	-	x	x	x	x	-		x		x	x
44-126	-	-	x	glauc	x	x	x	-	x		x	x	-

AMPHIBOLE

Characteristics

Form, colour, grain-size, and texture differ strongly, often within one thin section. The grain-size varies from tiny patches on fractures in garnet through medium-sized to porphyroblastic crystals. The latter are poikiloblastic to a large extent. Idiomorphous crystal boundaries are moderately to well-developed. The grain-size hardly exceeds 6 mm.

Two types of porphyroblasts can generally be distinguished on account of pleochroic colours. The so-called light-coloured amphibole has: α colourless, β weakly green, and γ weakly lavender blue; $\alpha \leqslant 1.64$. The chemical composition is less variable than that of the so-called dark-coloured amphiboles with $\alpha \geqslant 1.64$. The pleochroic colours of the latter are: α weakly yellow-brown, β olive-green, and γ blue-green.

Colour-differences — even within one crystal — occur, indicating a heterogeneous composition. Especially along the edges and cleavages the colours are darker than in the cores. Blue-green porphyroblasts commonly have cores with light pleochroic colours. Consequently the light-coloured amphibole is older than the dark-coloured one. On the other hand a dark-coloured amphibole is found in the core of the glaucophanitic amphibole from RGM 141442. This latter dark-coloured amphibole is possibly of primary magmatic origin. The characteristics of colour and other optical properties are listed in Table 5 for the various amphibole types reported in this paper. The glaucophanitic amphibole from RGM 141 442 has α weakly yellow, β purple and γ cobalt-blue. The dispersion is weak with v > r. The pleochroic colours of a glaucophanitic amphibole from sample 44-126 are: α weakly-yellow, β purple, and γ purple-blue. The dispersion is moderate with r > v. Yet another has grass-green colours under the microscope. It is considered to be an alteration product resulting from the deformation of porphyroblasts of the light-coloured type (RGM 109 688). An actinolitic amphibole has been identified, associated with albite, quartz, and epidote (RGM 140 647, 141 345).

Textures

Enclosed in the amphiboles are remnants of clinopyroxene, garnet, zoisite, white mica, rutile, and apatite. For a better understanding of the successive stages of metamorphism, causing the alterations of the eclogitic rocks, it is useful to consider the different amphibole types more in detail. Examples of rock samples with porphyroblasts of light-coloured amphibole are: RGM 109 668, 109 669, 109 682, 109 685, 128 219, 140 323, 140 329, 140 332, and 140 590. This type is the earliest of all amphiboles found in the rocks studied with the possible exception of the amphibole found as inclusion in glaucophanitic amphibole in RGM 141 442. The light-coloured porphyroblasts have originated from the omphacitic clinopyroxene. The minerals enclosed in these amphiboles are well-protected against alteration processes (RGM 140 591, 140 622). The fine-symplectite was formed later than the light-coloured amphibole, and the coarse-symplectite is younger than the fine one. It has been established that the fine-symplectite is best developed in those rocks where micro-jointing is most abundant (RGM 140 590). Garnet is commonly present in smaller amounts within than outside fine-symplectite bearing portions. In an advanced stage of fine-symplectite formation the amphibole porphyroblasts were also affected, and consequently became susceptible to later alterations. Such alterations are e.g. the development of coarse-symplectite and of blue-green amphibole (RGM 135 523, 109 719, 109 744, 140 330, Ru 11). It is assumed that the association blue-green amphibole / epidote / chlorite / biotite / albite is a corolary of the formation of blue-green amphibole. The said process is more advanced in the samples RGM 140 330 and 140 601 than in RGM 109 744 and 140 329. While the fine-symplectite developed along with the alteration of rutile to ilmenite (RGM 140 502, 140 617), the paragenesis blue-green amphibole / albite / epidote, etc. is extended with titanite forming after rutile and/or ilmenite (RGM 109 719, 135 519, 109 705, Ru 11).

Coarse-symplectite develops at the expense of the light-coloured porphyroblastic amphibole (RGM 122 318) and possibly also after zoisite (RGM 109 684). The later amphibole of the albite-epidote association and/of the coarse-symplectite, shows variable colours, but it is generally of the blue-green variety (RGM 109 684, 135 509, 135 519). Coarse-symplectite may be microscopically recognised as a symplectitic intergrowth of amphibole and albite. A rod-shaped amphibole is intergrown with albite (RGM 109 719, 135 519, Ru 5, Ru 11). This phenomenon is particularly well visible in the foliation plane, as will be described for RGM 109 684 in the chapter on Petrology. The fine-symplectite is probably not a symplectite in the current usage of the term. Rather it seems to be, in its most simple form, a monomineralic replacement of the clinopyroxene surrounding the latter as a fine-grained aggregate. The replacing mineral is probably amphibole, pos-

Table 5. Optical characteristics and colour of amphiboles from the eclogitic and garnet-amphibolitic rocks of the Blastomylonitic Graben, Galicia, Spain.

sample reg. nr.	α	β	γ	$\gamma\wedge c$	$2V_\alpha$	dispersion	colour (RCC)
A. Light-coloured porphyroblastic amphiboles:							
Ru 8	1.625	1.635	1.644	25°	75°	v > r	5 GY 7/2
RGM 109 669	1.635	1.643	1.649	14°	76°	v > r	5 GY 3/2
RGM 109 688	1.631	1.644	1.653	21°	79°	r > v	5 GY 7/2
RGM 135 506	1.627	1.639	1.647	18°	75°	v > r	5 GY 5/2
RGM 140 617	1.638	1.650	1.658	17°	76°	v > r	5 GY 5/2
RGM 140 647	1.631	1.643	1.651	19°	78°	v > r	5 GY 5/2
B. Dark-coloured porphyroblastic amphiboles:							
RGM 109 705	1.642	1.656	1.662	16°	64°	v > r	10 GY 3/2
RGM 109 723	1.645	1.658	1.663	14°	63°	v > r	10 GY 3/2
RGM 122 318	1.643	1.656	1.662	13°	63°	v > r	10 GY 3/2
RGM 128 225	1.642	1.653	1.660	18°	73°	v > r	10 GY 3/2
RGM 135 519	1.646	1.657	1.663	13°	66°	v > r	10 GY 3/2
RGM 141 345	1.644		1.663				
RGM 141 442 core	1.640	1.653	1.661	16°	61°	v > r	
C. Glaucophanitic porphyroblastic amphiboles:							
RGM 141 442 rim	1.634	1.651	1.653	7°	36°	v > r	5 PB 3/2
44-126	1.619	1.634	1.638	6°	49°	r > v	5 PB 3/2
D. Blue-green hornblende associated with epidote, albite and chlorite:							
RGM 109 684	1.641	1.653	1.661	25°	74°	v > r	10 GY 4/2
RGM 109 744	1.671		1.690	17°	62°	r > v	10 GY 3/2
RGM 109 744 core, $2V_\alpha$ ca 70°; lower R.I.; weaker pleochroic colours.							
RGM 109 781	1.640	1.654	1.662		74°	v > r	10 GY 5/2- 3/2
RGM 135 510	1.653		1.671	> 20°	± 70°	v > r	
RGM 135 523	1.661	1.671	1.680	20°	84°	v > r	10 GY 3/2

sibly of actinolitic type. It is usually colourless, but in some instances blue-greenish in thin section. Uralite would be a better name. This kind of replacement appears to be activated by deformation. It is certainly later than the amphibole poikiloblastesis of the light-coloured type. Uralite rims are apparently less wide where they envelop clinopyroxene that is enclosed in amphibole porphyroblasts (RGM 140 380). Moreover, coarse- and fine-symplectites are hardly distinguishable in thin section. Probably there is a complete gradation from fine- into coarse-symplectite, coarse- is later than fine-grained symplectite, in an advanced state of replacement.

It is concluded that clinopyroxene can be the source of three different types of amphibole developments: a) light-coloured porphyroblasts with rather coarse-grained, euhedral rutile (RGM 109 682, 128 219, 135 523); b) blue-green amphibole often occurring where clinopyroxene borders on garnet, the forming of this blue-green amphibole is apparently older than the fine-symplectite or uralite formation; c) uralite with ilmenite and some titanite.

The porphyroblastic amphibole may alter into: d) amphibole-albite symplectite; e) blue-green amphibole developing along the edges and in the fractures of the porphyroblastic amphibole, it is roughly contemporaneous with the amphibole-albite-epidote association to which the coarse-symplectite mentioned under d also belongs; f) grass-green amphibole forming along joints in the porphyroblastic amphibole.

The development of the grass-green amphibole went together with ilmenite forming after rutile (RGM 109 682). Consequently it is acceptable to assume that the uralitisation and the forming of the grass-green amphibole are synchronous processes.

WEAKLY COLOURED OR WHITE MICA

Characteristics

The grain-size varies from sample to sample, but the white mica flakes do not exceed 1 mm in the majority of them. In some samples (RGM 109 684, 109 773, 109 781, 135 506, 135 508, 135 509, 135 510) much larger mica's have been observed. In composite rocks muscovite prefers zoisite-quartz-rich portions.

Muscovite concentrates usually are silver-white with a greenish tinge. The mica from samples 44-126 and RGM 141 442 is weakly green coloured with brownish patches in thin section and weakly green coloured in concentrates. The paragonite or margarite share in the white mica is considerable (p. 64). No other parameters than β and $2V\alpha$ (Table 6) of the micas of some of the samples have been determined.

Table 6. $2V_\alpha$ and β of micas from the eclogitic and garnet-amphibolitic rocks of the Blastomylonitic Graben, Galicia, Spain.

Sample reg. nr.	$2V_\alpha$	β
RGM 109 684	25^o	1.594
RGM 109 773	45^o	1.595
RGM 109 781	50^o	1.597
RGM 122 318	39^o	1.596
RGM 135 508	46^o	1.594
RGM 135 509	39^o	1.597
RGM 140 647	34^o	1.593
RGM 141 442	ca. 0^o	1.600
44-126	ca. 0^o	1.599

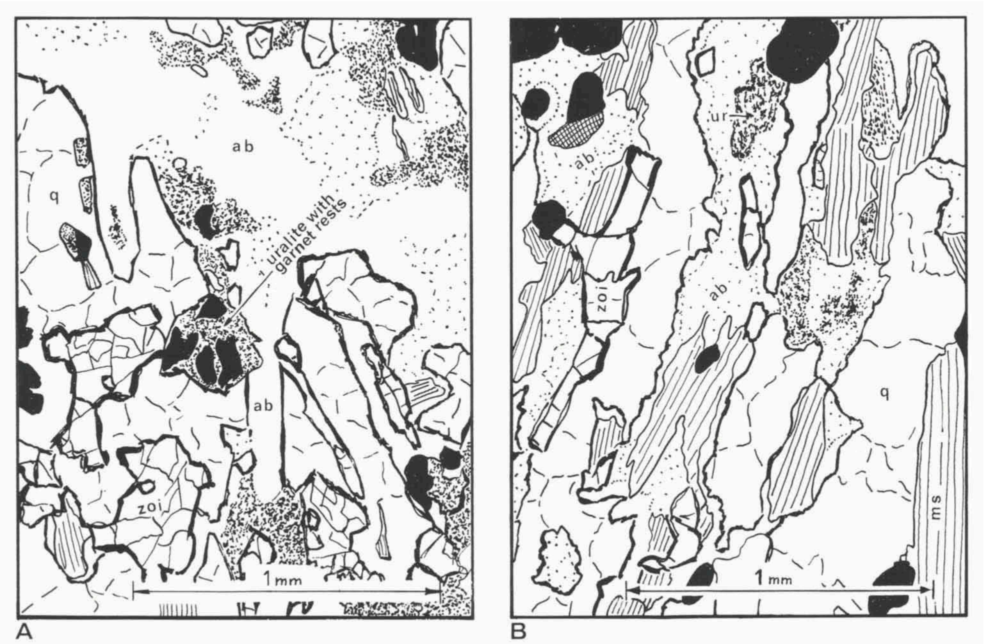

Fig. 11. A. Albite penetration from a quartz-albite veinlet into the host rock, and replacing the white mica. Sample RGM 140 323, from the complex between Agualada and Puente Ceso. B. Albite metablastesis along the grain boundaries of quartz and white mica. Sample Ru 6, from the body near Bainas. For the symbols see Fig. 10.

Textures

Inclusions in white mica are: garnet, clinopyroxene, rutile, and zoisite. Amphibole, epidote, and apatite have never been observed as chadacrysts in the micas. Epidote and zoisite are likewise found partly enveloping the muscovite. This phenomenon goes along with extensive development of albite along the grain-boundaries of minerals like quartz, mica, and zoisite. Albite-amphibole symplectite is encountered in the vicinity. Albite is observed replacing mica in Ru 6 and RGM 140 323 (Fig. 11A, B).

Many of the present rock samples show composite textures, i.e. rock compositions alternate in thin layers or lenses. Mica preferably occurs together with zoisite (RGM 109 669, 140 385), light-coloured amphibole (RGM 109 669), and quartz (RGM 109 773, 140 380) in portions poorer in pyroxene. When the kyanite-content varies in the different lenses or layers, white mica is found preferably in the kyanite-rich portions (RGM 109 781). In RGM 122 318 it is observed that the coarsest mica crystals appear in the quartz-rich rock portions, albeit exceptionally. White mica may occur enclosed in clinopyroxene porphyroblasts (Ru 8) but quartz never does so.

ALBITE

The intergranular albite film, mentioned in the preceding pages, is found between quartz and other minerals. The author considers this kind of albite occurrence to be the first stage of albite metablastesis (RGM 109 684, 135 509). White mica is one of the first minerals to be subjected to progressive albite replacement (RGM 140 323, Ru 6). An advanced stage of albite formation is present where albite porphyroblasts, exceeding 1 mm, are dispersed throughout the rock (RGM 140 389) (Pl. 2, figs. 1, 3; Pl. 3, fig. 1). Small oval quartz remnants are among the chadacrysts of these albite poikiloblasts (RGM 109 705). RGM 140 379 is an example of a rock fabric in which synkinematic albite-metablastesis took place. A rotation of less than 90° has caused the weakly S-shaped arrangement of tiny zoisite prisms. Metasomatism is a prerequisite for this type of albite metablastesis. The albite film is a product of the chemical activity of an intergranular fluid. This process has been discussed in detail by Wegmann (1935) and Spry (1969). The ionic migration of sodium, is not necessarily a long distance affair. Omphacitic clinopyroxene originally present in the investigated rocks is partly or entirely uralitized. In that instance uralitisation and albite blastesis need to be successive stages of one process. The observations mentioned suggest a progressive process of albite-metablastesis by the formation of albite films on the grain boundaries. But is is quite possible that ultimate albite-porphyroblastesis is not part of the same process as the initial development of albite films. It has been mentioned already that albite is paragenetically associated with epidote, blue-green amphibole, titanite, etc. The anorthite-content of the plagioclase never exceeds 10% and is often less than 5%. Another mode of albite occurrence is in veinlets usually together with epidote (pistacite in RGM 140 647), actinolite, and quartz (Pl. 3, fig. 3). There is no reason to assume that this latter albite belongs to another phase of metamorphism.

MINERALS OF THE EPIDOTE GROUP

The epidote group minerals of the present rocks are rather variable in composition, as indicated by optical determinations. The optical data of the epidote from RGM 109 781 are:
$\alpha = 1.718, \gamma = 1.735, 2V\alpha = 92°$.

The atomic proportions obtained by electron-microprobe analysis, executed under the direction of Dr C. Kieft in the W.A.C.O.M.-laboratory at the Free University in Amsterdam, on one grain indicates an endmember composition of 55 mol.% clinozoisite against 45 mol.% epidote. The theoretical R.I.'s derived from this composition, according to Tröger's tables (1971), should be:
$\alpha = 1.717, \gamma = 1.732, 2V\alpha = 83°$.

These values agree reasonably well with the above mentioned measured R.I.'s. The results of several optical measurements are listed below. They demon-

Table 7. Optical measurements obtained from epidote-group minerals in various samples from the Blastomylonitic Graben, Galicia, Spain.

RGM nr.	α	γ	$2V_\alpha$	remarks
109 684	1.705	1.722	90°	clinozoisite envelopping white mica
109 744	1.727	1.754	80°	epidote
109 773	1.721	1.743	85°	epidote from the groundmass outside the garnet
109 773			92°	epidote from within the garnet
128 225	1.716	1.731	90°	epidote

strate the variety in composition of the epidote-group minerals (see Table 7).

Minerals of the epidote group occur in the present rocks as follows: 1) together with dark-coloured amphibole, with or without albite in the groundmass (RGM 109773, 135508, 128225, Ru 15); 2) as pistacite together with actinolitic amphibole, with or without albite and quartz in veinlets (see below); 3) in joints and cavities of garnets with sieve structure together with blue-green amphibole (RGM 109773, 109781) and muscovite (RGM 135510); 4) along the edges of muscovite (RGM 135510, 140323, 140594, 140615, Ru 5) or zoisite (RGM 109684), usually separated from quartz by an albite film.

QUARTZ

Quartz of various generations is frequently found in the present rocks in highly variable quantities. It occurs as follows:
1) as angular and somewhat rounded inclusions in garnet, kyanite, zoisite, and amphibole, the grain-size does not exceed 0.1 mm; 2) as a few dispersed or aggregated grains in the rock, the grain-size is usually smaller than 0.2 mm; 3) as thin bands arranged parallel to the foliation, reminding the ribbon-quartz texture lacking preferred lattice orientation which is characteristic of syntectonic recrystallization in certain granulites; the mutual grain boundaries of the equidimensional quartz show an amoeboid texture; these lenticular, commonly coarse-grained quartz layers conform — as to grain-size, texture and form — to the intermediate type of mylonitic schists distinguished by Bellière (1971) in his classification of mylonitic rocks; 4) in veinlets with albite or adularia.

Extensive quartz injection was a corrolary of the development of type 3. This injection was certainly later than the amphibole metablastesis, and probably syn- to post-uralite formation. The clinopyroxene is never invaded by quartz, a skin of uralite is always found between the clinopyroxene and the quartz (RGM 140615). Clinopyroxene, garnet, white mica, zoisite, and amphibole commonly show signs of resorption where bordering quartz. Egg-like quartz grains are found as remnants in albite poikiloblasts (RGM 109705). In other samples quartz is restricted to boudin-like bodies together with white mica, zoisite, and some garnet (RGM 140385, 140647). The white mica is more coarse-grained than in the groundmass. The minerals of the groundmass, consisting mainly of garnet and clinopyroxene with minor mica and amphibole, show wavy foliation, while the boudins have been rotated (type 2). A good example of deformation is the microfold of RGM 109 684 (see p. 31 and 32). The quartz intrusion, as represented in this rock sample, is almost syn-kinematic (F_3 in Table 8).

The fact that some quartz-grains occur as inclusions in minerals like garnet, kyanite, zoisite, and amphibole indicates that a generation of quartz older than the quartz of the injection-phase is present (type 1). Yet, all quartz appears to be later than the clinopyroxene. Moreover, quartz is ubiquitously found associated with kyanite, zoisite, and white mica. The latest quartz generation is present in veinlets with chlorite and adularia.

OPAQUE AND OTHER DARK MINERALS

Rutile and other titanium minerals occur in the investigated rocks. In the chapter on amphiboles it has been emphasized that uralitisation goes together with ilmenite formation (RGM 109 694, 135 523, 140 380, 140 638). The next stage subsequent to the development of albite + epidote + blue-green amphibole often though not always (RGM 140 506) shows extensive titanite (RGM 109 705, 140 290, 140 418, 140 502, 140 505, 140 506, 140 623). However, sample RGM 109 705, described in detail in the chapter on Petrology, proves that the titanite is older than the mentioned ab + ep + amp paragenesis. In RGM 135 519 uralite is for the most part replaced by albite-amphibole symplectite. Skeleton crystal configurations of titanite-ilmenite-rutile are scattered all over the rock; the titanite is situated in the rim, the rutile in the core and the ilmenite in between. Ilmenite is post-amphibole poikiloblastesis, which is proved by wide zones of ilmenite enveloping rutile outside the poikiloblasts (RGM 109 669).

Tiny, short-prismatic, angular or more roundish rutile grains, not exceeding 0.35 mm and often smaller than 0.20 mm, are frequently found enclosed in clinopyroxene and garnet. More exceptional are such inclusions in zoisite (RGM 109 684), white mica (RGM 109 685, 109 781), kyanite (RGM 135 507), and poikiloblasts of amphibole (Ru 8, RGM 109 705). This rutile did not survive the formation of albite-amphibole symplectite. More coarse-grained and less idiomorphic rutile grains, varying in size from 0.4 to 1.6 mm, are generally situated along the grain boundaries of clinopyroxene, garnet, kyanite, white mica, and zoisite, but they can also be enclosed in the poikiloblastic amphibole. Consequently it is likely that the coarse-grained, xenomorphic rutile is younger than the angular and idiomorphic, fine-grained rutile. Moreover, the latter are more regularly dispersed in the rock, but usually more or less oriented in accordance with the foliation (RGM 135 507, 135 508, 135 509, 135 510).

The younger rutile is arranged in interrupted strings, more or less after the foliation. Other strings form incomplete rings. The rings are oval-shaped with the long axis about parallel to the foliation (Ru 8, 10, 12) and several millimetres long. The coarse-grained, xenomorphic rutile may also occur enclosed in the garnet cores together with blue-green amphibole, epidote, apatite, and quartz (Ru 14). Ilmenite bordering uralite may form skeleton crystals. These are always situated outside the amphibole poikiloblasts (RGM 109 688, 109 694, 109 719, 135 523, 140 502, 140 505).

Other opaque minerals mentioned in Table 4 are magnetite, pyrrhotite, and pyrite. In most cases identification was done with the aid of the X-ray powder-diffraction method. Magnetite was identified in six of the thirty-two mineral concentrates. It may occur in other samples as well. The quantities are always very minute. Uralitisation of the clinopyroxene is rather advanced particularly in the six samples mentioned above. The ilmenite clearly forms rims enveloping rutile, whereas titanite is hardly of importance. Magnetite is found in fractures of the garnet in sample RGM 135 510. These fractures are disposed at an angle to the foliation.

Pyrite and pyrrhotite, usually in larger quantities than magnetite, occur associated with blue-green amphibole, epidote, chlorite, and apatite. Hydrated iron-oxide minerals, such as goethite, are frequently found as alteration rims around the sulfides mentioned.

Petrology

ROCK DESCRIPTIONS

In this chapter the results of the microscopic investigation of selected samples of the eclogites and garnet-amphibolites of the Blastomylonitic Graben in Galicia (Spain) is dealt with. The concluding remarks pertain to the chapter on Mineralogy as well.

If most of the rocks were not on the scale of a hand specimen, the author would have applied the classification of amphibolitic and eclogitic rocks, as used for instance by Lange (1963), but this classification is too detailed for the present study. The rocks form a series starting with a rock type in which granoblastic clinopyroxene is intergrown with garnet, white mica, zoisite, kyanite, and quartz. This rock is called eclogite. When light-coloured amphibole is added, it is called amphibole-eclogite. Later deformation and metamorphism caused the development of epidote, albite, symplectites, and other amphiboles. Through eclogitic amphibolites one comes to garnet-amphibolites. Garnets are hardly present in the most altered rocks. One can recognize all these rock types in one small outcrop and even one hand specimen may contain two or more of these rock types.

Eclogitic rocks — The rock of sample Ru 17B is of composite texture (see Fig. 6); it consists of several bands of different composition exceeding 1 cm in thickness. Clinopyroxene-rich bands or portions can be distinguished from bands or portions poor in pyroxene but with abundant amphibole. The long axes of the pyroxene crystals are oriented parallel to the banding planes. The garnet of the clinopyroxene-rich bands is usually smaller and slightly elongated by deformation parallel to the foliation. The amphibole is somewhat granoblastically intergrown and of the light-coloured type (α = 1.635, β = 1.654; colour according to the R.C.C. = 5GY 3/2). The larger garnets from the amphibole-rich bands contain many inclusions which are arranged in such a way that a helicitic texture can be vaguely discerned. The enclosed minerals are mainly light-coloured amphibole, white mica, some clinopyroxene, rutile, and kyanite. In addition, darker coloured amphibole, biotit, epidote, and an opaque mineral are found in fractures in the garnet. The darker coloured amphibole, biotite, and epidote are certainly alteration products of the garnet. The opaque mineral is likely to be magnetite. Kyanite is found in both types of bands, although apparently more abundant in the ones rich in pyroxene. On the other hand white mica is coarser grained and observed more frequently in the parts of the rock rich in amphibole. In the clinopyroxene-rich bands the kyanite is crystallographically oriented together with clinopyroxene and well individualised, whereas in the amphibole-rich bands kyanite occurs as very small, euhedral grains enclosed in white mica and garnet. Epidote is often bordering white mica. The epidote and albite development is more advanced in sample Ru 17A than in sample 17B.

Although sample Ru 17B shows resemblance to sample RGM 135 510, with respect to the mineral composition, pyroxene and garnet are rather different in chemical composition as demonstrated by the physical properties. These differences are the more remarkable because both samples have been taken close to each other in the body near Bainas. The clinopyroxene of Ru 17B is of type I (α = 1.670, β = 1.690, m.s. = 7.2 x 10^{-6} c.g.s. and the colour is 10 GY 7/2), whilst the pyroxene of sample RGM 135 510 is of type II (see Fig. 9B and Table 4). The physical properties with respect to the Ru 17B garnet are: n = 1.766-1.773, a = 11.56 Å, m.s. = 35 x 10^{-6} c.g.s. For the garnet of RGM 135 510 reference is made to Fig. 9A. Sample Ru 17B contains a lot of kyanite, whereas RGM 135 510 does not. Finally it should be noted that both samples are the only chemically analysed rocks which contain some normative nepheline (see Table 19).

Ru 12 represents an example of an older type of deformation (Pl. 4, fig. 1) as shown by the arrangement of the light-coloured poikiloblasts in the foliated groundmass. Here the younger type deformation and its accompagnying alteration have hardly had any influence.

Garnet-amphibolitic rocks — RGM 109 773 is a sample of a strongly foliated, dark-coloured rock with a weak schistosity caused by mica concentrated in thin layers. The laminae, each only a few millimetres thick, consist alternatively of either clinopyroxene and garnet or garnet, amphibole, and white mica. The amphibole is the type associated with epidote and albite. This amphibole originated probably from uralite. The most intensely cleaved rock portions show presence of abundant uralite. The cleavage system crosses the foliation. It is obvious that amphibole and epidote are locally younger than the uralite. In other places it can be observed that uralite resisted the epidote-amphibole blastesis rather well. A fine amphibole-albite symplectite developed along the uralite. A lot of epidote and amphibole crystals grew with their long axes parallel to the clinopyroxene elongation. The albite is confined to thin films along the white mica and quartz boundaries.

The garnet contains — particularly in the cores — a lot of inclusions of blue-green coloured amphibole and epidote, which are probably alteration products of this garnet. Partly limonitised magnetite occurs frequently on the fracture planes in the garnet crystals. White mica is not always elongated after the foliation. Some α-zoisite prisms are crystallographically oriented parallel to the foliation plane. A plausible explanation for the fluctuating contents in amphibole and pyroxene of the alternating laminae is a primary difference in mica-content. As mentioned before (p. 25) white mica seems to be the preferred environment for the albite-epidote-amphibole development. Subsequently mica-rich layers are those rock portions in which percolation of the intergranular fluid preferably took part. Another sample showing this phenomenon in an excellent way is RGM 140 380.

RGM 109 669 is a sample of a greyish green coloured, spotted rock. The dark-coloured patches are roughly planolinear aggregates, not exceeding 1 cm, containing amphibole in a fine-grained groundmass consisting predominantly of clinopyroxene, garnet, and zoisite. The weak schistosity is due to the occurrence of white mica. Under the microscope the rock shows a heterogeneous composition. Alteration (uralitisation of the pyroxene) and deformation are especially represented in the garnet-pyroxene portion, whereas the portion which consists mainly of white mica, amphibole, zoisite, and quartz is less altered. White mica, quartz, and amphibole are hardly found in less fresh portions of the rock. Amphibole poikiloblasts are observed with inclusions of zoisite, white mica, and pyroxene as shown in figures 3 and 4 of Pl. 1. In one of the thin sections these enclosed minerals are arranged in such a way (Powell & Treagus, 1970) that the rotational axis of the synkinematically grown poikiloblasts is situated approximately in the plane of the thin section (see Fig. 5A).

The rock sample RGM 109 705 is an eclogite which is altered by successive stages of metamorphism. Clinopyroxene remnants wrapped by uralite, strongly rounded garnet, and rutile — consecutively altered into ilmenite and titanite — are still found. The rock consists mainly of amphibole of the dark-coloured porphyroblastic type. Variable pleochroism within individual crystals indicates a heterogeneous composition. Zoisite and quartz occur intergranularly with respect to amphibole. Besides uralite, strings of rutile-ilmenite-titanite are observed outside the porphyroblastic amphibole (Pl. 3, fig. 3). The albite, which in this case is certainly younger than quartz, is initially developed at the quartz grain boundaries. Titanite obviously belongs to an earlier stage than albite (1) and possibly also than amphibole. Moreover, zoisite is older than the cleavage and its stuffing with albite, amphibole, and epidote. The epidote continued to grow onto the broken crystal of zoisite (2). Consequently this amphibole is partly or entirely synchronous with the albite and epidote, as may be expected. The abundant titanite is older than the above mentioned paragenesis. Finally, sulfide minerals are frequently observed together with ilmenite and titanite.

RGM 109 744 is a sample of a greyish green coloured, spotted rock. Under the microscope the rock is fine-grained and appears composite. The dark patches consist of uralite with strings of rutile and ilmenite and to a lesser extent titanite. Unlike the boudins the patches lack garnet. They contain albite, epidote, greenish and brown biotite, some chlorite, some quartz, and deformed blue-green amphibole. The colour of the core of the amphibole is often lighter than the rim. Apatite is frequently found in both portions. In conclusion we can say that the garnet — enclosed in the poikiloblastic, light-coloured amphibole — has survived the uralitisation stage of the clinopyroxene better than the garnet outside these poikiloblasts.

Well-developed poikiloblasts of albite occur also in the comparable rock sample of RGM 140 290 (Pl. 3, fig. 1; Pl. 4, fig. 2). The garnets of the latter, likewise found only in the epidote-biotite-albite rock portions, are smaller in size and less abundant than in RGM 109 744. In the albite-rich portions of sample RGM 140 290 biotite and micro-folded, fibrous amphibole occur enclosed in the albite poikiloblasts (Pl. 3, fig. 1). Cleavages in the deformed amphibole porphyroblasts are also filled with albite. Consequently the albite-epidote development is apparently late- to post-kinematic (i.e. blastic stage of the boudinage). Without any doubt the light-coloured amphibole, garnet, zoisite, and uralite are of the prekinematic stage. This can also be said of apatite prisms which are broken and deformed. Apatite is likewise found included in blue-green coloured amphibole. The colour change of the amphibole from light to blue-green has taken place most probably during the albite-epidote blastesis.

Sample RGM 140 646 represents an example of intricate deformation with subsequent — though less advanced — alteration, as described from sample RGM 109 705 and 140 290. Clinopyroxene and garnet are still present in the uralite part of RGM 140 646. Moreover, the light-coloured amphibole poikiloblasts with chadacrysts of zoisite, garnet, pyroxene, and rutile, as situated outside the uralite-white mica portions, may clearly be recognized. The uralite portions with remains of pyroxene show wavy foliation around the boudin-like rock parts consisting mainly of albite, epidote, and amphibole.

RGM 109 684 is another example of a composite rock. The most striking element is a folded, garnet-rich, more or less s-shaped band of centimetre-size.

Four different types of zones can be distinguished within the garnet-rich band A 2 mm wide zone containing more than 30 vol. % of garnet surrounded by quartz (type 1). Some blue-green coloured amphibole, amphibole-albite symplectite, zoisite, albite, epidote, and white mica are also observed. It is remarkable that the apatite is exclusively found in this zone. Apatite is also included in the zoisite of this zone. The second zone, not exceeding 1 mm in width, contains even more garnet (type 2). The garnet, in comparison with this mineral outside mentioned band, is fine-grained and equigranular. Zoisite is lacking. The third zone is again of type 1, but it lies outside the figure of Pl. 6. Thus a central garnet-rich zone is bounded on both sides by a zone of type 1. The apatite does only occur in one of those zones of type 1. Outside the garnet-rich band and particularly so at its periphery the rock is rich in zoisite. A division can be made in one zone containing, besides zoisite, a lot of uralite with clinopyroxene remains (type 3), and another zone rich in albite-amphibole symplectite and less abundant garnet (type 4). Wherever present the uralite is surrounded by coarse-symplectite. Under the microscope the amphibole of this symplectite is lighter coloured than the small blasts of blue-green amphibole which are scattered throughout the rock. The changing colour of the latter amphibole reveals a heterogeneous composition. White mica, most abundantly occurring in the zone of type 4, is frequently partly wrapped by zoisite and epidote. Epidote is subsequent to zoisite. Besides uralite, the albite-amphibole symplectite seems also to be derived from zoisite. Wherever white mica borders quartz albite is observed in between. An albite film is continually found on the grain boundaries, such as between quartz and mica, quartz and zoisite, or even quartz and quartz.

The properties of the minerals, with respect to composition or texture, are for the greater part mentioned elsewhere in the present paper, however some remain to be emphasized. It can be concluded from electronprobe microanalyses that the garnet outside the zone of type 2 shows a capriceous distribution, while this mineral within the zone of type 2 is obviously zoned. A system of fine, parallel fractures occurs in the plane of the thin section mentioned. These fractures are particularly well-developed in the garnets of zones of types 1 and 2. It is reasonable to suppose that the fracture system represents some stage of the tectonic phase resulting in the micro-folding of this sample.

Zoisite is to a large extent crystallographically oriented. This property became evident from search for zoisites in the thin sections on which optical determinations could be done. Some sections turned out to be more suitable for the purpose than others. The orientation of the indicatrix is that of β-zoisite, i.e. β is parallel to the crystallographic b-axis. The position of the b-axis conforms best with the folding axis of sample RGM 109684. Consequently the optic axial plane in this case is perpendicular to the folding axis. In the thin section zoisite shows locally parasitic folding with the b-axis as the axis of rotation. It is striking that the symplectite is likewise oriented, which results in a rod-shaped amphibole intergrowth with albite especially observable in the direction of the folding axis. Across this direction an amphibole aggregate forms a symplectite prism not exceeding 1 mm together with one or more albite blasts. The length of such a prism, coinciding with the direction of the folding axis, is a multiple of its width. Rotation of garnet with dragging of clinopyroxene, though sporadic and weak, can be recognized in this thin section.

CONCLUDING REMARKS

A substantial difference in chemical composition between garnets and clinopyroxenes does not exist for the metabasites from in- and outside the body near Bainas. Fresh eclogite rocks are found more frequently within the large body than in the smaller lenses and boudins elsewhere. Consequently the metabasites of Bainas were for the greater part appropriate for this investigation. Besides, no substantial difference in chemical composition exists between garnets from rock samples mentioned by Monster under a and b (see p. 3). According to Rubbens the body near Bainas consists predominantly of a more or less schistose, quartz-rich eclogite in which white mica causes the schistosity. Dark lenses, 0.5 to 10 m long, are arranged in a fluidal fashion in the lighter coloured main mass. The dark, more massive, though still foliated rock contains a lot of porphyroblastic amphibole. The present author starts from a rock in which granoblastic clinopyroxene is intergrown with garnet, white mica, zoisite, kyanite, and quartz. Particularly white mica, zoisite, kyanite, and quartz are strongly varying in streaks parallel to the general foliation of the rocks. In the case of the body near Bainas the rocks are moderately dipping to the east. The clinopyroxene-rich rock may change into thin bands or lenses of a darker rock rich in lighter and darker coloured porphyroblastic amphibole. The amphibole developed at the expense of the clinopyroxene and kyanite.

Clinopyroxene can be divided into an older, granoblastic type and a younger, porphyroblastic one. The former determines extensively the rock foliation. The younger type is late- or post-kinematic (F_1). It is quite possible that the pegmatoid- and atoll-garnet formation should be considered synchronous rather than consecutive. Clinopyroxene is found as inclusion in garnet, garnet as inclusion in pyroxene, small kyanite grains are enclosed in garnet, poikiloblastic kyanite is containing garnet as well as pyroxene. The occurrence of atoll-garnets, zoned or otherwise heterogeneously composed, point to an intricate development of garnet in the investigated rocks. It is a development of repeated growth under changing conditions of pressure and temperature, and changing composition of intergranular fluid solutions. Besides growth, resorption of garnet happened at least once, as is demonstrated by the occurrence of atoll shapes.

During the blastesis of the light-coloured amphibole some garnet was also formed in stable association with this type of amphibole. As shown in the chemical part of the present paper, the garnet of the glaucophane-bearing rock sample 44-126 is usually rich in almandine, which agrees well with garnets from the so-called blueschists. In another sample (Ru 17B), the garnet shows vaguely a helicitic structure with chadacrysts of light-coloured amphibole, white mica, clinopyroxene, and kyanite. No chemical data are available of this garnet.

The composition of the light-coloured, porphyroblastic amphibole appears to be barroisitic. Consequently, pressure played an important role in the formation of this amphibole type.

Synkinematic blastesis of β-zoisite from sample RGM 109684 is followed by uralitisation. This zoisite is syngenetic with the synkinematic (F_2) porphyroblastesis of light-coloured amphibole. The F_4-deformation coincides partly with the stable association of blue-green amphibole, albite, and epidote. The impression is gained that the albite-poikiloblastesis took place in the less deformed parts of the eclogitic rock, as far as it is synkinematic. The formation of the boudin-like textures coincides with the development of the albite-amphibole symplectite. The

Table 8. Mineral equilibria during successive metamorphic and deformative phases as shown in the polymetamorphic eclogitic and garnet-amphibolitic rocks from the Blastomylonitic Graben, Galicia, Spain.

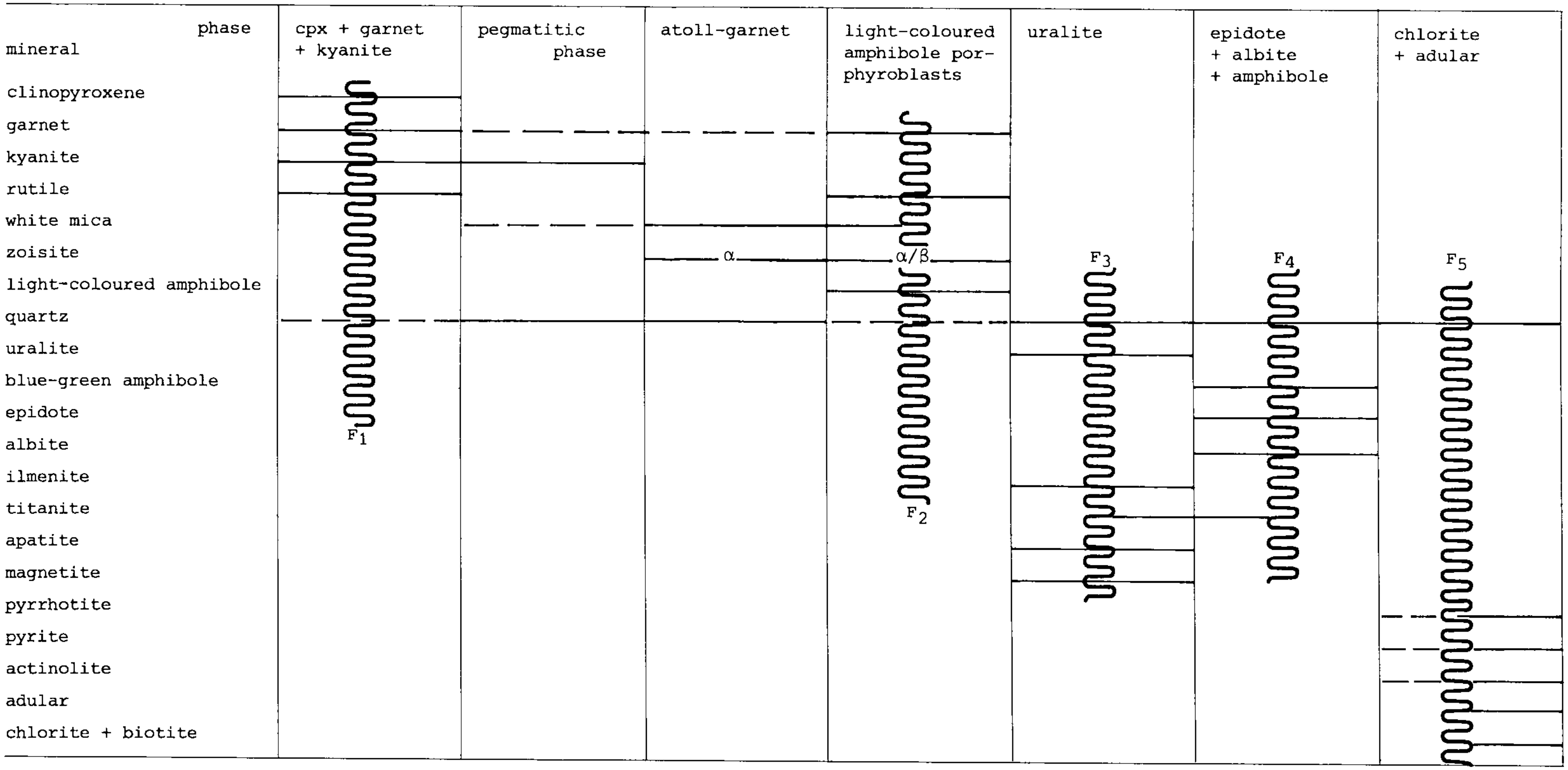

phase / mineral	cpx + garnet + kyanite	pegmatitic phase	atoll-garnet	light-coloured amphibole porphyroblasts	uralite	epidote + albite + amphibole	chlorite + adular
clinopyroxene	—						
garnet	—	- - -	- - -	—			
kyanite	—	—					
rutile	—			—			
white mica		- - -	—	—			
zoisite			— α —	— α/β —			
light-coloured amphibole				—			
quartz	- - -	—	—	- - -	—	—	—
uralite					—		
blue-green amphibole						—	
epidote						—	
albite						—	
ilmenite					—		
titanite					—	—	
apatite					—		
magnetite					—		
pyrrhotite							- - —
pyrite							- - —
actinolite							- - —
adular							—
chlorite + biotite							—

main phase of quartz veining coincided more or less with the uralitisation of the pyroxene. Uralitisation, instability of garnet, quartz veining, ilmenite formation, and magnetite emplacement on fractures in garnet indicate conditions of deformation (F_3) under lower pressure.

Mineral and rock chemistry

First of all the chemistry of minerals such as amphibole, garnet, omphacite, and zoisite in the eclogitic and garnet-amphibolitic rocks from the Blastomylonitic Graben is treated. Microprobe analyses of these minerals were performed on the GEOSCAN of the Institute of Earth Sciences of the Free University at Amsterdam. The raw data were corrected on the basis of a computer program (modified according to Springer, 1967).

X-ray investigation was carried out by means of X-ray powder photographs in order to check the chemical compositions of the minerals concerned. These diagrams were prepared using FeKα-radiation and a Debye-Scherrer camera with a diameter of 114.6 mm for single record. A Guinier camera of de Wolff (1948) for the simultaneous exposure of four powder patterns was used to fix the d_{221}-spacing of omphacites. CuKα-radiation was used in the latter technique.

It would have been useful, in the present study, to employ X-ray diffraction methods for various reasons. One of the principal motives is to determine unit-cell parameters, in particular of amphibole and pyroxene. These determinations procure means to assess the positions of the cations in the crystal latice of the minerals studied. For amphiboles according to Heritsch & Kahler (1961), Binns (1967), Borg (1967), Gibbs & Prewitt (1968), and Ross, Papike & Weiblen (1968) and for clinopyroxenes e.g. after Clark, Appleman & Papike (1968).

Twenty whole rock samples of eclogite and garnet-amphibolite were analysed in the Geochemical Laboratory of the Geological Institute of Leiden University (head K. M. Stephan).

MINERAL CHEMISTRY

Amphiboles

The general structural formula for the half unit-cell of the amphiboles is: $A_{0\text{-}1}X_2Y_5Z_8O_{23}.H_2O$ in which 6-8-fold coordinated (X-) cations are situated in position M_4, octahedrally coordinated (Y-) cations in positions M_1, M_2 and M_3, and tetrahedrally coordinated (Z-) cations in positions Si_I and Si_{II}. M_1, M_2, M_3 and M_4 are the positions of all cations with the exception of Si- or its replacing Al^{IV}-ions. X-cations are Na and Ca; Y-cations are Mg, Ti, Fe^{2+}, Fe^{3+}, Mn, Cr, and Al^{VI}-ions. The A-situations, which are occupied by the 10-12 fold coordinated cations Na, K and H, may remain empty. For a better understanding of the crystal chemistry of amphiboles the reader may referred to Deer, Howie & Zussman (1962) and Ernst (1968).

In Table 9 eighteen microprobe analyses of amphiboles are given. The atomic values for the half unit-cell were computed from the oxide-values on the

Table 9. Results of electronprobe microanalyses of 18 amphiboles from the metabasites of the Blastomylonitic Graben, Galicia, Spain.

analysis nr.:	(1)	(2)	(3)	(4)	(5)	(6)	(7)	(8)	(9)	(10)	(11)	(12)	(13)	(14)	(15)	(16)	(17)	(18)
oxide value / sample nr.	109 669	109 688	109 688	140 647	140 647	44-126	109 684	109 705	109 705	109 781	135 508	135 508	135 509	135 510	135 510	140 615	140 615	140 615
SiO_2	49.6	53.05	51.75	49.55	50.5	54.7	43.35	50.8	47.45	43.15	43.35	38.95	43.0	39.55	50.5	47.35	45.6	48.45
Al_2O_3	12.05	7.65	9.65	13.0	12.85	10.7	15.6	9.4	13.1	16.7	15.9	18.9	16.25	18.35	12.1	15.1	14.55	14.05
TiO_2	0.35	0.1	0.2	0.25	0.3	0.15	0.5	0.3	0.35	0.35	0.35	0.45	0.6	0.3	0.15	0.45	0.3	0.3
Cr_2O_3	0.0	0.0	0.0	0.0	0.0	0.0	0.0	<0.05	<0.05	0.0	0.0	0.0	0.0	0.0	0.0	0.0	0.0	0.0
MnO	<0.05	0.0	0.0	0.05	0.05	<0.05	0.0	0.05	0.15	0.1	0.1	0.15	0.25	0.0	<0.05	0.05	0.1	0.05
MgO	15.15	17.3	15.95	14.6	14.8	8.25	9.65	15.0	12.35	10.3	11.4	8.85	8.5	7.6	12.95	9.85	8.7	10.25
FeO	7.3	6.95	7.4	7.4	6.85	14.55	14.85	8.35	11.4	12.25	11.6	14.8	16.2	17.0	9.5	12.5	15.8	12.2
CaO	8.5	9.35	8.85	8.2	7.7	1.25	9.8	9.6	9.35	8.65	8.6	9.55	8.5	9.15	6.15	5.4	4.85	4.85
Na_2O	3.85	2.75	3.25	3.8	4.2	7.1	3.15	3.0	2.85	5.45	4.3	4.3	4.5	4.45	5.05	6.25	6.5	6.35
K_2O	0.4	0.2	0.25	0.35	0.3	0.0	0.95	0.35	0.45	0.05	0.85	0.1	0.15	0.0	0.1	0.4	0.45	0.35
total	97.2	97.35	97.4	97.2	97.55	96.7	97.85	96.85	97.45	97.0	96.45	96.0	97.95	96.4	96.5	97.35	96.85	96.85
for Fe^{3+} [1]	0.4	0.45	0.35	0.4	0.35	0.4	0.35	0.1	0.45	0.15	0.45	0.6	0.5	0.6	0.5	0.3	0.65	0.35

[1] N.B. the Fe^{2+}/ Fe^{3+}- ratio is chosen in such a way that Y = 5.00 (see Table 10).

Table 10. The atomic values for the half unit cell of the amphiboles of Table 9, computed from the oxide values on the basis of 23 oxygens.

Ana-lysis nr.:	Sample nr.:	$A_{0-1.00}$		$X_{2.00}$		$Y_{5.00}$							$Z_{8.00}$		Niggli mg	Type amphibole
		K	Na	Na	Ca	Mg	Mn	Ti	Cr	Fe^{2+}	Fe^{3+}	Al^{VI}	Al^{IV}	Si^{Si}		
1	RGM 109 669	0.07	0.31	0.73	1.27	3.16	0.00	0.04	0.00	0.42	0.43	0.95	1.04	6.96	0.79	*
2	RGM 109 688	0.04	0.12	0.61	1.39	3.58	0.00	0.01	0.00	0.34	0.46	0.61	0.64	7.36	0.79	*
3	RGM 109 688	0.05	0.19	0.68	1.32	3.31	0.00	0.02	0.00	0.48	0.39	0.80	0.79	7.21	0.80	*
4	RGM 140 647	0.06	0.25	0.77	1.23	3.04	<0.01	0.03	0.00	0.44	0.43	1.06	1.08	6.92	0.78	*
5	RGM 140 647	0.05	0.28	0.85	1.15	3.05	<0.01	0.03	0.00	0.45	0.35	1.11	1.00	7.00	0.79	*
6	44-126	0.00	0.13	1.81	0.19	1.73	0.00	0.02	0.00	1.32	0.40	1.53	0.25	7.75	0.36	*
7	RGM 109 684	0.18	0.43	0.46	1.54	2.10	0.00	0.06	0.00	1.44	0.37	1.03	1.66	6.34	0.54	●
8	RGM 109 705	0.07	0.28	0.54	1.46	3.18	<0.01	0.03	0.00	0.88	0.11	0.80	0.78	7.22	0.24	*
9	RGM 109 705	0.08	0.22	0.57	1.43	2.62	0.02	0.04	0.00	0.89	0.47	0.96	1.24	6.76	0.34	*
10	RGM 109 781	0.01	0.90	0.64	1.36	2.25	0.02	0.04	0.00	1.36	0.14	1.20	1.68	6.32	0.45	●
11	RGM 135 508	0.15	0.60	0.66	1.34	2.47	0.02	0.04	0.00	1.92	0.50	1.05	1.68	6.32	0.52	○
12	RGM 135 508	0.01	0.77	0.47	1.53	1.97	0.02	0.05	0.00	1.18	0.66	1.12	2.20	5.80	0.37	○
13	RGM 135 509	0.03	0.60	0.67	1.33	1.85	0.03	0.07	0.00	1.40	0.58	1.07	1.72	6.28	0.48	●
14	RGM 135 510	0.00	0.75	0.54	1.46	1.69	0.00	0.04	0.00	1.46	0.67	1.14	2.09	5.91	0.44	●
15	RGM 135 510	0.02	0.31	1.07	0.93	2.72	0.00	0.02	0.00	0.60	0.53	1.13	0.88	7.12	0.71	●
16	RGM 140 615	0.07	0.58	1.17	0.83	2.10	<0.01	0.05	0.00	1.20	0.30	1.35	1.20	6.80	0.49	●
17	RGM 140 615	0.08	0.59	1.25	0.75	1.89	0.01	0.03	0.00	1.20	0.72	1.15	1.35	6.65	0.58	●
18	RGM 140 615	0.06	0.52	1.25	0.75	2.19	0.01	0.03	0.00	1.10	0.37	1.31	1.06	6.94	0.60	●

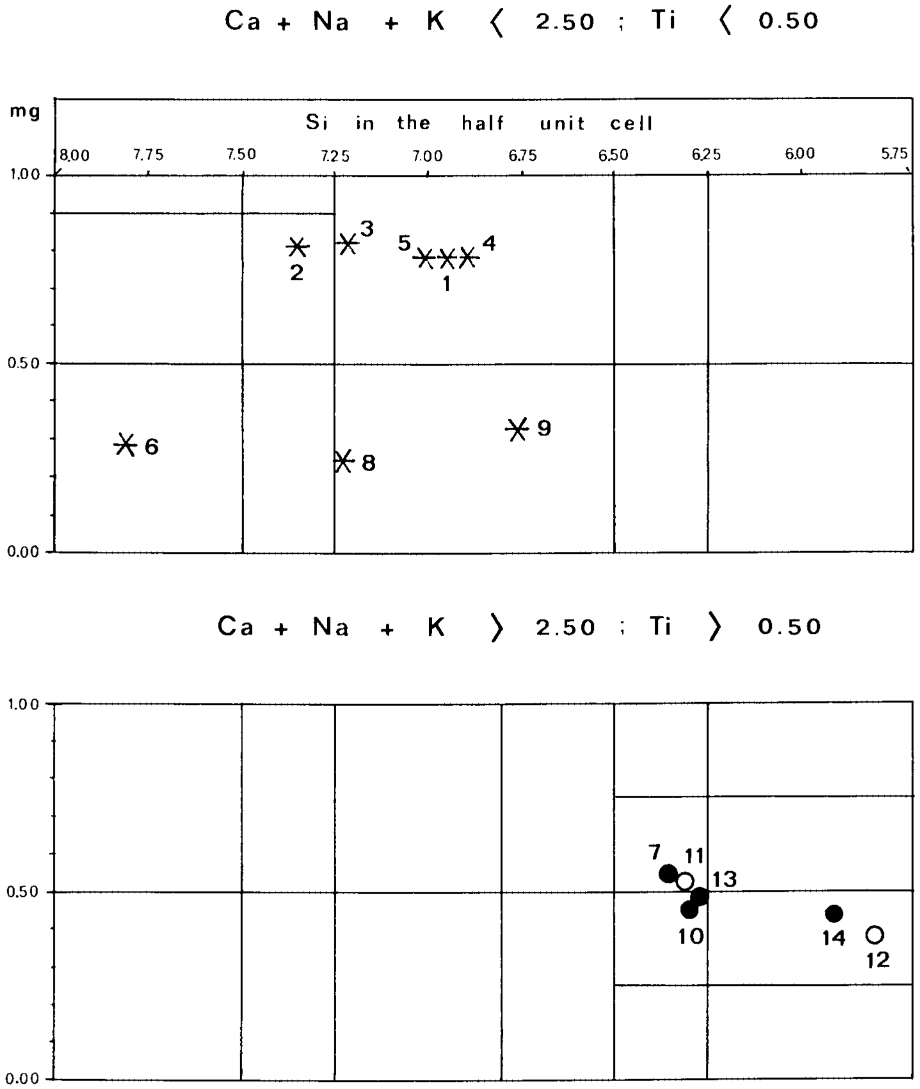

Fig. 12. The calciferous and sub-calciferous amphiboles from Table 10 are subdivided in accordance with Leake (1968).

basis of 23 anions (O) (Table 10) for lack of data on water content of the analysed amphiboles. This shortcoming is inherent in electronprobe microanalysis. Ernst (1968) computed his analyses on the basis of 23 (O), assuming that 1 H_2O (2 OH^-) is present. The result of water analyses, obtained in the conventional manner, is unreliable and would not elucidate the O-OH relation. The degree of occupation of the A-sites remains an unsolved problem. According to Ernst, the only correct solution is to determine unit-cell volume and specific gravity of the amphibole concerned. Such data, combined with chemical analyses, may result in a definite structural formula of the amphibole. However, the present author has only chemical and optical data at his disposal. His first assumption is that the minerals concerned are no oxy-amphiboles. In oxy-amphiboles hydroxyl-groups have been replaced by oxygen atoms; that is to say more cation combinations per unit-cell might be possible. It is agreed with Phillips (1963), that Ti may replace Mg (see Table 10).

The analyses 1-5, 7-14 are those from sub-calciferous amphiboles (Leake, 1968), for which $Ca = 1.00$ is the minimum value. The analyses 6 and 15-18 are those from calcium-poor amphiboles.

Analytical results marked with an asterisk are those from the porphyroblastic (either weakly or strongly pleochroic, light- or dark-coloured) amphibole; those marked with a dot are from grains of amphibole associated with albite and epidote, whereas those results marked with a circlet are from other small grains of amphibole which occur exclusively on cleavages in the garnet. The analyses numbers 1 to 5 are from light-coloured porphyroblastic crystals. Nr. 6 deals with glaucophane and the amphiboles of the remaining numbers are of the blue-green pleochroic type.

In accordance with Leake's (1968) nomenclature of sub-calciferous and calciferous amphiboles (Fig. 13) the microprobed minerals are:

1, 3, 4, and 5	magnesiohornblendes;
2	actinolitic hornblende;
8 and 9	ferro-hornblendes;
7, 10, 11, and 13	ferro-pargasitic to magnesiohastingsitic hornblendes;
12 and 14	magnesiohastingsites.

It is remarkable that both the light-coloured and the blue-green coloured porphyroblastic amphiboles plot in the upper part ($Ca + Na + K < 2.50$) of the diagram in Fig. 12, whereas the small grains associated with epidote and albite plot in the lower part of this diagram. Besides, $Ca + Na + K < 2.50$ corresponds with higher Si-values and $Ca + Na + K > 2.50$ with lower Si-values.

The results of analyses 12 and 14 are similar to that of mboziite, a mineral in metamorphic rocks of Alpine age from the Sierra de los Filabres (S.E. Spain), described by Linthout & Kieft (1970). Mboziite (Brock, Gellatly & von Knorring, 1964) is an endmember mineral belonging to the sub-calciferous amphiboles with low Si-values and $Ca + Na + K > 2.50$. The amphiboles of numbers 12 and 14 are even richer in Ca, Al, and Mg than the mboziite of Linthout & Kieft (see Table 11).

Amphibole nr. 6 and three out of four calcium-poor amphiboles, i.e. numbers 16, 17 and 18, contain Na_2O-values exceeding 6 wt.%, whereas nr. 15 exceeds 5 wt.%. These five analyses indicate alkali-amphiboles which are named

Table 11. Analyses 12 and 14 (Table 10) chemically compared with mboziite from the Sierra de los Filabres, SE Spain (Linthout & Kieft, 1970).

	K+Na	Na+Ca	R^{2+}	R^{3+}	Al^{IV}	Si
Type mboziite from nepheline syenite	100	100-100	300	200	200	600
Mboziite from the Sierra de los Filabres	64	76-124	294	208	190	610
Analysis 12	78	47-153	317	183	220	580
Analysis 14	75	54-146	315	185	209	591
Tschermakite (theor.)	0	0-200	300	200	200	600

Table 12. Calcium-poor and sodium-rich amphiboles from the metabasites of the Blastomylonitic Graben, chemically compared according to Miyashiro (1957).

Analysis nr. (Table 10):	Si	R^{2+}	R^{3+}	Fe^{2+}/R^{2+}	Fe^{3+}/R^{3+}
6	775	305	195	0.43	0.20
15	712	332	168	0.18	0.32
16	680	330	170	0.17	0.18
17	665	310	190	0.39	0.38
18	694	330	171	0.33	0.22

according to Miyashiro (1957) (Table 12). Analysis nr. 6 is of a glaucophane, whereas the other alkali-amphiboles fall within the arfvedsonite to riebeckite-glaucophane fields. However, the amphibole nr. 6 seems to belong to an older metamorphic stage than the other alkali-amphiboles mentioned, the latter being associated with albite and epidote. The alkali-amphiboles are Mg-rich (Fe^{2+}/R^{2+} < 0.5).

The light-coloured porphyroblastic amphiboles strongly resemble barroisites from Naustdal in Norway as described by Binns (1967), from Shikoku in Japan (Banno, 1964) and from New Caledonia (Coleman et al., 1965). Barroisite, a name proposed by Murgoci (1922), is an amphibole variety with a composition between normal hornblende and glaucophane (Binns, 1967; Morgan, 1970). Our barroisites are obviously richer in Mg and poorer in Fe^{2+}, which most probably causes the lower indices of refraction. The pleochroic colours are mostly weak. The amphiboles of numbers 8 and 9 are so-called blue-green porphyroblastic amphiboles. They differ from the light-coloured porphyroblastic amphiboles in having a smaller mg-number, which signifies that they are poorer in Mg and richer in Fe^{2+}.

Finally, the amphiboles of numbers 7, 10, 11, and 13 are, according to Leake, ferro-pargasitic to magnesiohastingsitic hornblendes, though they differ slightly from ferro-pargasites and magnesiohastingsites as described by Gilbert (1966).

As regards chemical composition and genesis Leake (1965a, 1971) has drawn a number of conclusions from an empirical examination of about 1500 analyses of amphiboles derived from the literature since 1890. One of the most definite conclusions is that, within wide variation of pressure and temperature, the composition of amphibole is mainly controlled by the rock composition (Leake, 1965b). This is particularly emphasized in the mg-ratio. The high mg-ratios, varying from 0.78 to 0.80, of the light-coloured porphyroblastic amphiboles is remarkable. The mg-ratios of the secondary amphiboles are distinctly lower and vary strongly. The former ratios are more in agreement with corresponding values in the chemical analyses of host rocks.

TiO_2-percentages of our eclogitic rocks are mostly a multiple of those of the amphiboles in the same rocks. The Ti-values for the half unit-cell are smaller than 0.10. On condition that excess TiO_2 is present in the rock the TiO_2-content of the amphiboles, is only dependent on the degree of metamorphism (Leake, 1965a). The small Ti-values of the present amphiboles point to comparatively low

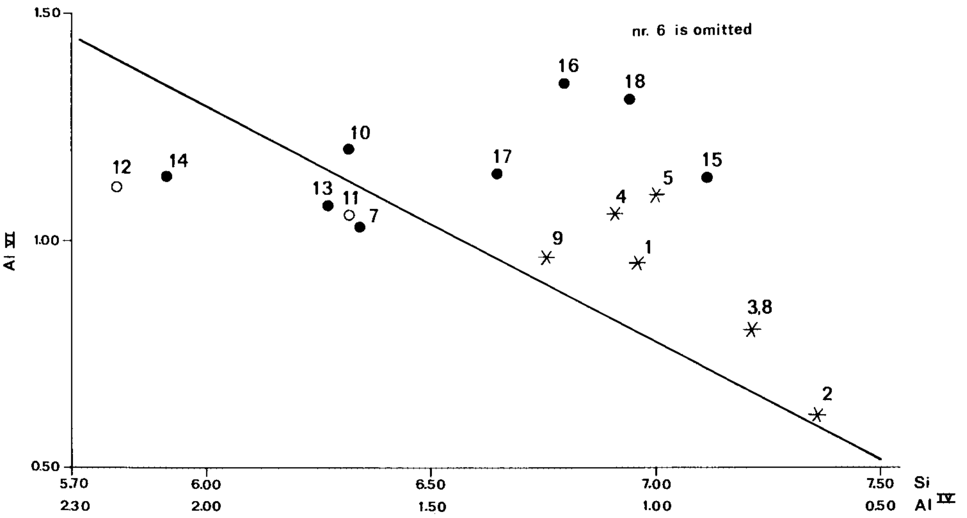

Fig. 13. Plot of octahedral Al in the half unit cell against tetrahedral Al (or Si) on the basis of 23 oxygens (Leake, 1965b) for the amphiboles from the metabasites of the Blastomylonitic Graben (see Table 9 for the explanation of the symbols). The suggested maximum possible for Al^{VI} is shown by the line drawn across the figure.

temperature conditions. This certainly holds for our primary amphiboles, marked with an asterisk (primary signifies here of older age than secondary). Apart from low temperature, high pressure is indicated by the Al^{VI}/Si-ratio as condition for the primary amphiboles (Raase, 1974). Considering the temperature in particular, the grade of metamorphism would agree with the greenschist-amphibolite facies transition. The plot of the Al^{VI} against Si in the half unit-cell for the so-called primary amphiboles, are not far away (Fig. 13) from the line indicating the maximum value of Al^{VI} for the corresponding Si-values. High pressure must have been an important condition (Leake, 1965a). Moreover, all points plot well within the field of metamorphic amphiboles. The light-coloured amphiboles show lower Al^{VI}-values than the other ones. It is quite possible that the rock composition in general and the composition of the older or light-coloured amphibole in particular, are responsible for the composition of the secondary amphibole. That is to say, the relevance of the above mentioned conclusion of Leake could be less stringent for the secondary amphiboles. It is beyond the scope of this paper to examine this matter more fully.

Mottana & Edgar (1969) are of the opinion that eclogite-amphiboles, on the basis of new chemical and X-ray data and data from the literature, can be differentiated in groups depending on the conditions of formation of the eclogite. Consequently eclogite-amphiboles are paragenetically related to the critical eclogite-minerals such as omphacite and pyrope-almandine garnet. However, it appears from extensive microscopic investigation of the present amphiboles that even the so-called primary amphiboles must be younger than the actual eclogite formation. A time lag appears to exist between eclogite formation and the primary amphibole blastesis, unless both are considered as stages in a plurifacial development resulting in eclogite first and amphibolite in a later stage. For the eighteen amphiboles studied, Figure 14 shows the plot of Al^{IV} against Al^{VI}, with field divisions for eclogitic amphiboles after Mottana & Edgar. The primary amphiboles (nrs. 1-5, 8,

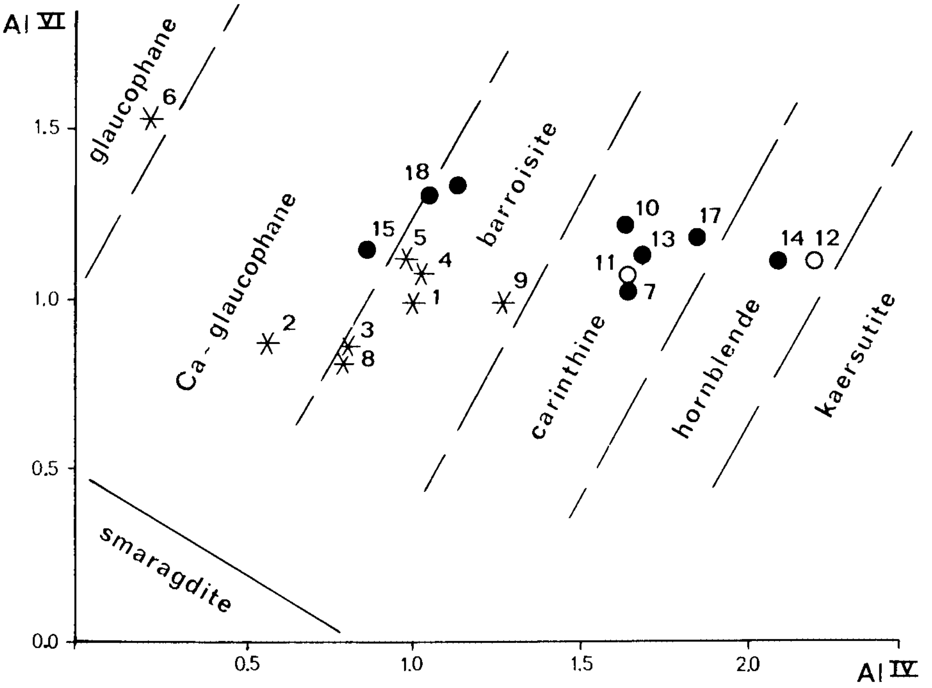

Fig. 14. Al^{VI}-A^{VI} in the half unit cell on the basis of 23 oxygens for the 18 amphibole electronprobe microanalyses of Table 9, plotted in the amphibole fields according to Mottana & Edgar (1969). For explanation of the symbols see Table 9.

and 9) appear to be in the fields of the barroisites and Ca-glaucophanes. Nr. 6 is even lying in the field of the true glaucophanes. With the exception of the nrs. 15, 16, and 18 the blue-green amphiboles (associated with albite and epidote) are restricted to the carinthine and hornblende fields of eclogitic amphiboles. The author realises, with Mottana & Edgar, that Al- and Si-values are largely inaccurate. Nevertheless, it is noteworthy that the Al^{VI} against Al^{IV} plot of the primary amphiboles form such a limited cluster. On the basis of data from the literature the conditions of formation of these amphiboles are supposed to be:
4 - 5 kb and 100° - 300° C for Ca-glaucophane;
6 - 8 kb and 400° C for barroisite;
6 - 8 kb and 200° - 300° C for glaucophane.

The secondary amphiboles show some resemblance with the tschermakitic hornblendes mentioned by Wenk, Schwander & Stern (1974). The latter hornblendes are confined to the meta-sedimentary belt south of the Gotthard Massif. They are characterised by high Al^{VI}-content and low mg-ratio, and despite the high Al-content they can hardly be related to high pressure conditions. One dark-coloured and one light-coloured amphibole, possibly both belonging to the same paragenesis, can be distinguished in the thin sections of samples RGM 109684 and 135510. Further examination is needed to prove the existence of two amphibole assemblages, in the sense of Klein (1968, 1969), Himmelberg & Papike (1969), and Leake (1972), in the amphibole-epidote-albite association.

Clinopyroxenes

Omphacite, the clinopyroxene of the eclogitic rocks in the present study, can be determined within the system jadeite-acmite-diopside-hedenbergite-tschermakite and expressed in the structural formula (Clark & Papike, 1968): M_2M_1 (Si, Al)$_2$ O_6, in which polyhedrally coordinated (X-) cations are situated in position M_2; and octahedrally coordinated (Y-) cations in M_1. The tetrahedrally coordinated (Z-) cations are Si and Al^{IV}. X-cations are Na and Ca, Y-cations are Mg, Fe^{2+}, Fe^{3+}, Cr, and Al^{VI}.

The chemical composition of omphacite from seven rock samples was established with the aid of the microprobe. The results are averages of several point-measurements in one or more mineral grains in a thin section (Table 13). The atomic values in the half unit-cell are computed on the basis of 6 (O) (Table 14). The molecular values of the five theoretical end member minerals of omphacite can easily be computed (Yoder & Tilley, 1962) from the atomic values (Table 15). Despite the likely inaccuracy of the SiO_2 and the Al_2O_3 determinations (Smith, 1966), and consequently of the Al^{IV}/Al^{VI} ratio, the conformable plot for the present omphacite analyses is clearly situated within the eclogite field of Aoki & Kushiro's (1968) diagram (Fig. 15). The Si-value in the half unit-cell corresponds

Table 13. Results of electronprobe microanalyses of 7 clinopyroxenes from the metabasites of the Blastomylonitic Graben, Galicia, Spain.

	(1)	(2)	(3)	(4)	(5)	(6)	(7)
oxide value: sample nr.	109 669	109 705	109 781	135 506	135 509	135 510	140 615
SiO_2	56.3	55.8	56.0	56.45	55.6	56.0	56.25
Al_2O_3	10.5	8.65	11.9	12.55	12.5	11.8	12.5
TiO_2	0.1	<0.1	0.1	0.1	0.1	0.1	0.1
Cr_2O_3	0.0	0.7	0.0	0.0	0.0	0.0	0.0
FeO	2.8	3.75	5.5	3.15	4.7	6.75	6.4
MnO	<0.05	<0.1	<0.05	<0.05	<0.05	0.0	0.05
MgO	9.3	9.8	7.1	7.7	7.0	6.4	5.9
CaO	14.1	15.2	11.65	11.75	11.45	10.6	9.65
Na_2O	6.75	5.85	7.8	7.95	8.05	8.05	8.9
K_2O	0.0	0.0	0.0	0.0	0.0	0.0	0.0
sum	99.85	99.85	100.05	99.75	99.4	99.7	99.75
for Fe^{3+} 1)	0.15	0.2	0.25	0.15	0.3	0.25	0.35

1) The Fe^{2+}/ Fe^{3+}-ratio is chosen in such a way that Y = 1000 (see Table 14).

Table 14. The atomic values for the half unit cell of the clinopyroxenes of Table 13, computed from the oxide values on the basis of 6 oxygens (x 1000).

analysis nr.:	X_{1000}			Y_{1000}					Z_{1000}		Niggli	
	Na	Ca	Mg	Mg	Fe^{2+}	Fe^{3+}	Cr	Al^{VI}	Al^{IV}	Si	mg	cpx_I or cpx_{II}
1	465	535	0	490	35	45	0	430	10	1990	0.86	I
2	405	580	15	505	90	25	20	360	0	2000	0.72	I
3	535	445	20	355	95	65	0	485	15	1985	0.56	I
4	545	445	10	395	55	35	0	515	10	1990	0.82	I
5	555	435	10	360	60	80	0	500	25	1975	0.73	I
6	560	405	35	305	135	65	0	495	0	2000	0.65	II
7	615	365	20	290	95	95	0	520	5	1995	0.62	II

Table 15. Omphacite composition in percents of the end members jadeite, acmite, tschermak's molecule, hedenbergite, and diopside (Yoder & Tilley, 1962; White, 1964) from metabasites of the Blastomylonitic Graben, Galicia, Spain.

Analysis nr.	Jd	Ac	Tsch	Hd	Di
1	42.2	4.5	1.1	3.5	48.7
2	36.9	4.6	0.0	9.3	49.2
3	47.8	6.8	1.5	9.7	34.2
4	51.2	3.5	1.1	5.5	38.7
5	48.1	8.1	2.6	6.1	35.1
6	49.5	6.5	0.0	13.5	30.5
7	52.1	9.5	0.3	9.5	28.6

with the expectation for omphacite that the cationic positions in the tetrahedron are exclusively occupied by this ion.

The plots of the compositions of seven clinopyroxene solid solutions, obtained along two different ways, show a striking resemblance (Fig. 16A and B). The seven microprobed clinopyroxenes are plotted in Coleman's et al. (1965) triangle. Refractive index β and D_{221}-spacing have been measured from the same clinopyroxenes. According to Essene & Fyfe (1967) the combination of these measurements will provide the determination of sodic-pyroxenes. It should be noticed that this rapid determination method only holds, if the components $NaCrSi_2O_6$ (cosmochlore) and $CaAlSiAlO_6$ (Ca-tschermak's molecule) can be neglected. It appears from the chemical part of the investigation that the clinopyroxene of RGM 109 705 contains 0.7 wt% of Cr_2O_3, representing 2.0 wt% of cosmochlore besides 2.6 wt% of acmite. The Cr_2O_3-percentage lies within the range of similar contents found in clinopyroxenes from wehrlite, pyroxenite, and lherzolite inclusions in basalts and in crystal lapilli and the tuff from Dreiser Weiher in the Eifel district of Western Germany (Aoki & Kushiro, 1968). The above mentioned clinopyroxene from RGM 109 705 is an omphacite with the lowest jadeite and highest hedenbergite-diopside content of the microprobed pyroxenes, i.e. 36.9 and 58.5 mol% respectively.

The measurements of the d_{221}-spacing and the refraction index β of the clinopyroxenes from seventeen rock samples are given in Table 16 with the observation whether the clinopyroxene is of the cpx_I or of the cpx_{II} type (see p. 6). Figure 16C is a plot of the data from Table 15 into the triangle of Essene & Fyfe for sodic-pyroxenes. The jadeite is from Upper Burma and the diopside from Zillertal in Austria (Zwaan, 1955).

It has been proved that zoned structures exist in omphacites. Comparing the chemistry of the present omphacites with that of clinopyroxenes from similar rocks in the Muenchberg Gneiss Massif, Bavaria, Western Germany (Matthes, Richter & Schmidt, 1969), it is striking that the average Na/Ca-ratio of the seven

Table 16. d_{221}-spacing and refraction index β of 17 omphacites from the metabasites of the Blastomylonitic Graben and two clinopyroxenes added for comparison. For the clinopyroxenes of the present study is indicated whether they are of type I or II.

from sample:	d_{221} in Å	R.I.β	cpx_I or cpx_{II}
1. RGM 109 669	2.966	1.676	I
2. RGM 109 705	2.972	1.676	I
3. RGM 109 781	2.965	1.680	I
4. RGM 135 506	2.956	1.677	I
5. RGM 135 509	2.955	1.678	I
6. RGM 135 510	2.967	1.683	II
7. RGM 140 615	2.955	1.683	II
8. Ru 8	2.969	1.669	I
9. RGM 109 688	2.971	1.675	I
10. RGM 109 723	2.965	1.688	II
11. RGM 109 773	2.960	1.687	II
12. RGM 122 318	2.967	1.675	I
13. RGM 135 523	2.965	1.678	I
14. RGM 140 480	2.967	1.675	I
15. RGM 140 617	2.959	1.672	I
16. RGM 140 647	2.959	1.682	I
17. RGM 141 345	2.966	1.673	I
jadeite from Upper Birma (RGM 78 526)	2.922		
diopside from Zillertal, Austria (RGM 24 594)	2.992	1.676	

Table 17. Composition of clinopyroxenes from the Muenchberg Gneiss Massif, Bavaria, Western Germany.

	Jd	Ac	Tsch	He	Di
minimum	18	1	0	2	34
average (71)	32.7	5.9	4.7	6.6	48.9
maximum	50	11	10	13	70

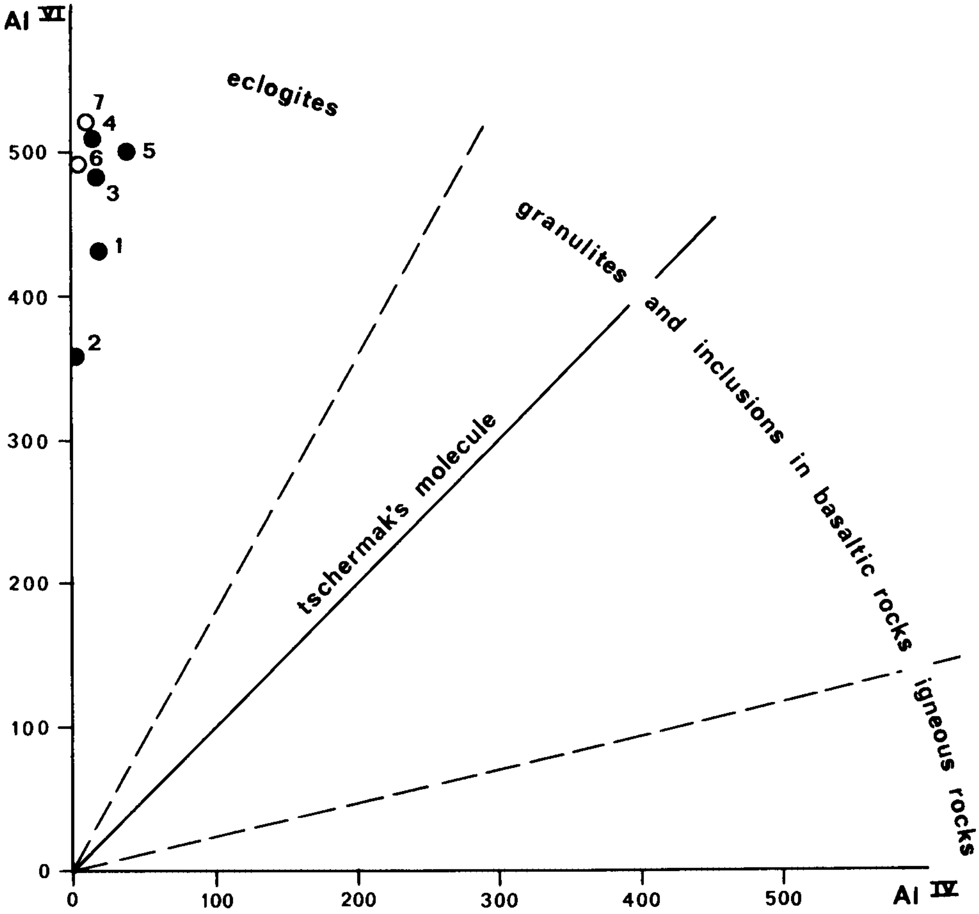

Fig. 15. Plot of the octahedral Al in the half unit cell against tetrahedral Al on the basis of 6 oxygens (x 1000) for the clinopyroxenes from the metabasites of the Blastomylonitic Graben (see Table 14) in Aoki & Kushiro's (1968) diagram.

omphacites analysed is 1.14, whereas the average of the corresponding ratio of seventy-one clinopyroxene analyses from the Muenchberg Gneiss Massif is 0.71 (Table 17). Consequently the jadeite-content of the present omphacite is remarkably higher, while the average content of the diopside component is a little lower than in those from the Muenchberg Gneiss Massif.

From experimental study Kushiro (1965) found that the pyroxene components jadeite and Ca-tschermak's molecule are important indicators of the physical conditions. The componental share of jadeite exceeds excessively that of Ca-tschermakitic clinopyroxenes from rocks formed under Kushiro's notion of eclogite facies conditions.

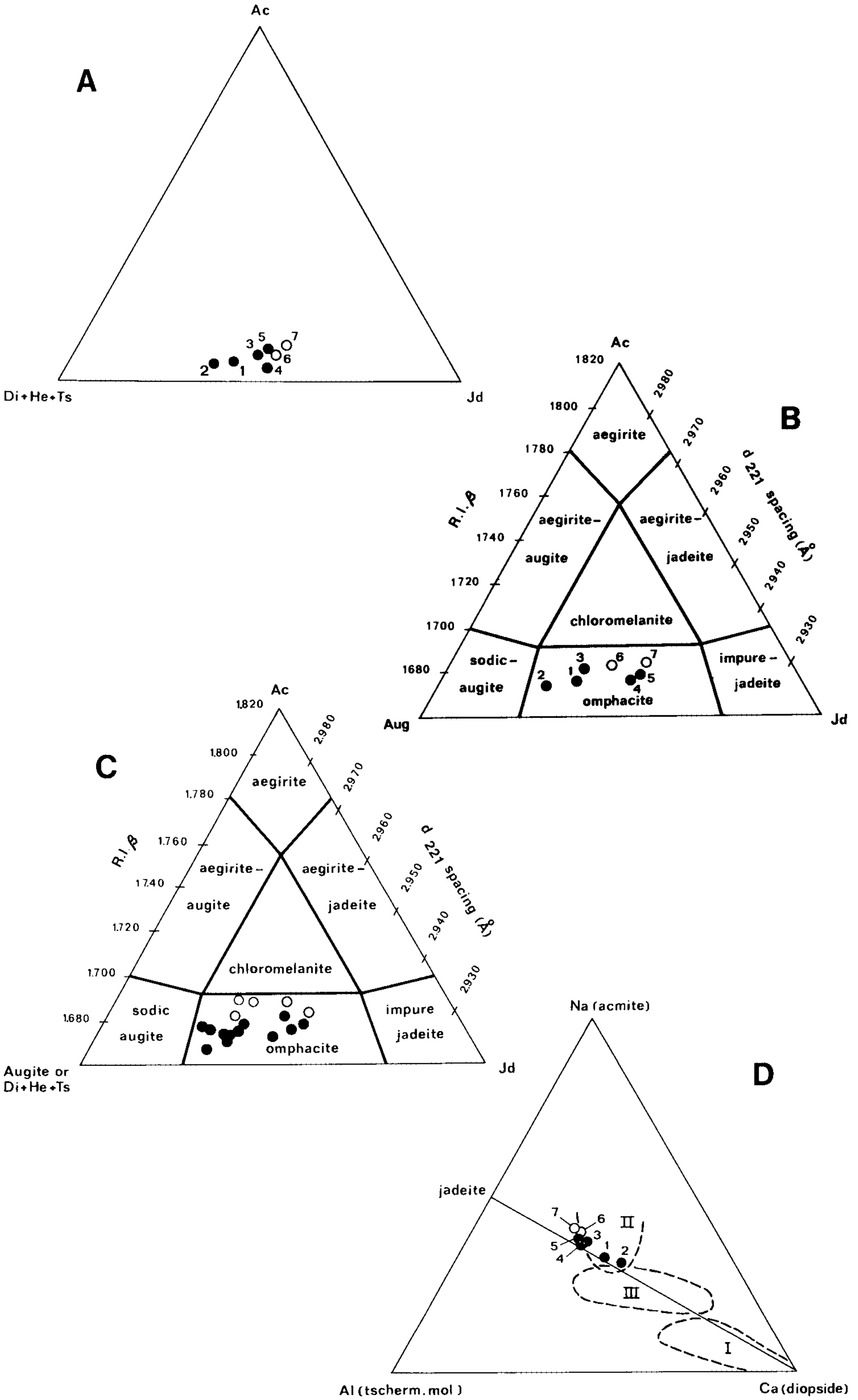
A
Ac
Di+He+Ts
Jd
1
2
3
4
5
6
7
B
Ac
Aug
Jd
R.I. β
1820
1800
1780
1760
1740
1720
1700
1680
d 221 spacing (Å)
2.980
2.970
2.960
2.950
2.940
2.930
aegirite
aegirite-augite
aegirite-jadeite
chloromelanite
sodic-augite
omphacite
impure-jadeite
C
Ac
Augite or Di+He+Ts
Jd
R.I. β
1.820
1.800
1.780
1.760
1.740
1.720
1.700
1.680
d 221 spacing (Å)
2.980
2.970
2.960
2.950
2.940
2.930
aegirite
aegirite-augite
aegirite-jadeite
chloromelanite
sodic augite
omphacite
impure jadeite
D
Na (acmite)
jadeite
Al (tscherm. mol)
Ca (diopside)
I
II
III

Garnets

Stockwell (1927) proved that three different properties, namely the unit-cell dimension, the index of refraction and the specific gravity, are useful to identify the composition of garnets. A number of scientists, a.o. Heritsch (1927), Wright (1938), Tröger (1959), and Schmid (1966), found a relation between garnet composition and rock type. Within thermodynamic restrictions (Saxena, 1968), this relation appears to be important to solve petrogenetic problems.

The general structural formula for the unit-cell of garnet is: $X_3Y_2Z_3O_{12}$, in which Z represents the tetrahedrally coordinated Si and replacing Al, Fe^{3+}, and probably Ti. Y stands for the octahedrally coordinated trivalent cations Al, Fe^{3+}, Ti, and Cr, and X for the likewise octahedrally coordinated uni- and bivalent cations Mg, Fe^{2+}, Ca, Na, and K, which are situated in the interstices within the Si-Al framework. The chemical composition of garnet is commonly expressed in the proportions of the six important end member components of the garnet group: almandine, pyrope, grossular, spessartine, andradite, and uvarovite.

The majority of forty-one microprobe analyses are only performed on the elements Fe (expressed as Fe^{2+}), Mg, Mn, and Ca. Moreover, the results of Si and Al measurements are mentioned in a few instances and some Ti-values are added. The analyses represent the average of two or more measurements per garnet grain (Table 18). The number of cations is computed on the basis of 12 oxygen atoms. Iron is expressed as Fe^{2+}. The proportion of Fe^{2+} that remains after filling up the X-positions, is converted tot Fe^{3+}. The garnet composition in the present paper is based on five components in stead of six, because the Cr-content is very low where measured. Spessartine and andradite are found to be subordinate to almandine, pyrope and grossular. According to the analytical results, they form more than 90 mol.% of the garnet composition. The index of refraction n and the length of the unit cell a of this cubic mineral are derived from the five-component composition for each of the forty-one analyses (Skinner, 1956; Deer, Howie & Zussman, 1962). With regard to the accuracy of the X-ray emission microanalysis, Knowles et al. (1969) state that variations of upto a few percent are common.

Refractive indices and unit cell dimensions have been estimated as a check on the composition of the microprobed garnets. The garnet samples were obtained by mineral separation techniques as mentioned on p. 5. The often clearly zoned structure of the garnets results in maximum and minimum indices of refraction for each sample. X-ray powder photographs were obtained from the same samples. The unit-cell dimensions in Å were diagrammetrically calculated (Zwaan, 1961) from the high-angle reflections 10 4 0, 10 4 2, and 8 8 0. The dimension a of the majority of the samples varies continuously between two values. Generally the variation in chemical composition is so small that the reflection lines of a sample

---

Fig. 16. Omphacites from metabasites of the Blastomylonitic Graben. A. Seven electron-microprobed clinopyroxenes (see Table 14) plotted in Coleman's et al. (1965) diagram for omphacite components. B. Plot of the refractive indices β and d_{221}-spacing of the seven electronmicroprobed clinopyroxenes in Essene & Fyfe's (1967) diagram for sodium-pyroxenes. C. Plot of the refractive indices β and d_{221}-spacing of 17 omphacites from Table 15. D. Plot of the seven electronmicroprobed clinopyroxenes in Smulikowski's (1968) Na-Al-Ca diagram. According to the Na-Al-Ca ratios the present clinopyroxenes are situated in and near the field of ophiolitic eclogites. I= cpx-field of garnet-pyroxenites, II= cpx-field of ophiolitic eclogites, III= cpx-field of normal eclogites.

Table 18. Results of electronprobe microanalyses and computations of end member compositions of garnets in metabasites from the Blastomylonitic Graben, Galicia, Spain.

sample nr.:	44-126					109 669		109 684						109 688		109 705	109 781			135 506
analysis nr.:	1	2	3	4	5	6	7	8	9	10	11	12	13	14	15	16	17	18	19	20
	1: core	1: core	2: atoll	5: core	5: rim	3: core	3: rim	1-6: lowest Fe, highest Ca	1-6: highest Fe, lowest Ca	7-11: lowest Fe, highest Ca	7-11: highest Fe, lowest Ca	garnet-rich band, core	garnet-rich band, rim	core	rim	1 - 3	1-2: average	1-2: Ca-rich	1-2: Ca-poor	
SiO_2						39.35	39.1	38.0	38.3	38.3	38.0			38.6	38.9					39.9
Al_2O_3						22.05	22.3	21.1	21.4	21.1	21.1			21.7	21.8					22.5
TiO_2						<0.05	<0.05													
FeO	29.65	32.35	31.3	32.5	30.55	23.2	21.9	24.1	27.0	26.2	26.6	23.25	24.7	24.5	23.7	23.5	24.05	24.05	24.05	22.75
MnO	0.85	0.6	0.55	1.05	0.5	0.6	0.5	0.5	0.3	1.1	0.5	2.3	0.5	0.5	0.3	0.55	0.8	0.8	0.8	0.7
MgO	1.8	2.6	3.0	2.05	4.4	7.85	9.05	3.2	4.4	3.3	4.2	2.9	4.35	4.0	8.1	5.45	6.4	5.25	7.45	9.4
CaO	8.75	5.1	6.45	7.65	6.1	7.55	6.9	13.4	9.8	10.3	9.3	11.2	10.35	11.0	7.8	9.75	8.35	9.9	7.15	5.6
total						100.6	99.75	100.3	101.2	100.3	99.7			100.3	100.6					100.85
Si						3.00	2.98	2.965	2.94	3.00	3.00			3.00	2.97					3.00
Al^{IV}						0.00	0.02	0.035	0.06	0.00	0.00			0.00	0.03					0.00
Al^{VI}						1.98	1.98	1.905	1.945	1.955	1.95			1.99	1.93					1.99
Ti						0.00	0.00	0.00	0.00	0.00	0.00			0.00	0.00					0.00
Fe^{3+}						0.02	0.00	0.06	0.00	0.05	0.07			0.01	0.04					0.00
Fe^{2+}	1.98	2.195	2.05	2.07	1.965	1.46	1.395	1.51	1.73	1.67	1.68	1.55	1.605	1.59	1.46	1.53	1.535	1.54	1.525	1.43
Mn	0.06	0.045	0.04	0.07	0.035	0.04	0.03	0.03	0.02	0.07	0.03	0.155	0.035	0.03	0.02	0.035	0.05	0.05	0.05	0.05
Mg	0.21	0.315	0.36	0.235	0.50	0.89	1.03	0.375	0.50	0.39	0.49	0.345	0.50	0.47	0.92	0.625	0.73	0.60	0.845	1.06
Ca	0.75	0.445	0.55	0.625	0.50	0.61	0.565	1.12	0.805	0.87	0.79	0.95	0.86	0.91	0.63	0.81	0.685	0.81	0.58	0.46
on the basis of 12 oxygens																				
pyrope	7.0	10.5	12.0	7.8	16.7	29.5	34.1	12.1	16.4	12.8	16.0	11.5	16.7	15.6	30.0	20.8	24.4	20.0	28.2	35.3
almandine	66.0	73.2	68.3	69.0	65.5	48.5	46.2	48.8	56.6	54.8	54.9	51.7	53.6	52.8	47.5	51.0	51.2	51.3	50.8	47.7
spessartine	2.0	1.5	1.4	2.3	1.1	1.3	1.0	1.0	0.7	2.3	1.0	5.2	1.2	1.0	0.7	1.2	1.6	1.7	1.7	1.7
grossular	25.0	14.8	18.3	20.9	16.7	20.2	18.7	36.2	26.3	28.5	25.8	31.6	28.5	30.3	20.5	27.0	22.8	27.0	19.3	15.3
andradite						0.5	0.0	1.9	0.0	1.6	2.3			0.3	1.3					0.0
mg	0.09	0.12	0.15	0.10	0.20	0.37	0.42	0.19	0.22	0.18	0.22	0.23	0.17	0.17	0.38	0.18	0.32	0.27	0.35	0.42

Continuation of Table 18.

sample nr.:	135 508		135 509				135 510			140 615				140 647							
analysis nr.:	21	22	23	24	25	26	27	28	29	30	31	32	33	34	35	36	37	38	39	40	41
	1: core	1: rim	5: core	5: rim	7: core	7: rim	core	rim	outermost rim	1: core	1: rim	4: core	4: rim	5: core	5: rim	7: Ca max., Fe min.	7: Ca min., Fe max.	A: average	B: average	B: high Ca, low Fe	B: low Ca, high Fe
SiO_2			38.25	38.65	37.75	37.9															
Al_2O_3			21.45	21.7	21.15	21.5															
TiO_2					0.2	<0.05															
FeO	26.25	22.6	23.7	25.05	28.3	27.45	25.5	25.6	24.75	26.9	28.5	27.1	27.6	21.2	24.1	20.5	23.4	22.7	20.95	19.8	23.0
MnO	1.0	0.25	1.75	0.35	0.85	0.4	0.7	0.45	0.7	0.75	0.65	0.8	0.65	0.6	0.6	0.6	0.6	0.6	0.65	0.65	0.65
MgO	5.15	7.35	4.65	6.95	3.55	5.6	5.3	6.0	6.35	2.4	5.2	2.5	4.85	5.7	7.7	5.7	8.3	8.85	6.9	6.9	6.9
CaO	7.0	8.45	10.2	7.15	8.45	6.8	8.3	7.6	7.6	10.3	5.2	10.1	6.6	11.2	5.4	11.75	6.0	6.05	9.6	11.3	6.9
total			100.0	99.85	100.25	99.65															
Si			2.98	2.99	2.97	2.97															
Al^{IV}			0.02	0.01	0.03	0.03															
Al^{VI}			1.95	1.97	1.935	1.955															
Ti			0.00	0.00	0.01	0.00															
Fe^{3+}			0.03	0.02	0.035	0.15															
Fe^{2+}	1.74	1.45	1.515	1.60	1.83	1.785	1.655	1.65	1.595	1.79	1.90	1.80	1.825	1.375	1.59	1.325	1.51	1.455	1.36	1.27	1.57
Mn	0.065	0.015	0.115	0.02	0.055	0.025	0.055	0.03	0.045	0.05	0.045	0.055	0.045	0.04	0.04	0.04	0.04	0.04	0.04	0.04	0.04
Mg	0.605	0.84	0.54	0.80	0.42	0.65	0.61	0.69	0.73	0.28	0.61	0.285	0.57	0.655	0.91	0.66	0.96	1.01	0.80	0.775	0.805
Ca	0.59	0.695	0.85	0.59	0.715	0.57	0.69	0.63	0.63	0.88	0.445	0.86	0.56	0.93	0.46	0.96	0.49	0.495	0.80	0.915	0.58
on the basis of 12 oxygens																					
pyrope	20.2	28.0	17.7	26.4	13.7	21.3	20.5	23.0	24.5	9.3	20.3	9.5	19.0	21.8	30.3	22.1	32.0	33.7	26.7	25.8	26.9
almandine	58.0	48.3	49.7	52.7	59.9	58.6	55.5	55.5	53.5	59.7	63.3	60.0	60.8	45.8	53.0	44.4	50.3	48.5	45.3	42.3	52.4
spessartine	2.2	0.5	3.8	0.7	1.8	0.9	1.5	1.0	1.5	1.7	1.7	1.8	1.5	1.4	1.4	1.3	1.4	1.3	1.3	1.4	1.4
grossular	19.6	23.2	27.8	19.5	23.5	18.7	22.5	20.5	20.5	29.3	14.8	28.7	18.7	31.0	15.3	32.2	16.3	16.5	26.7	30.5	19.3
andradite			1.0	0.7	1.1	0.5															
mg	0.25	0.37	0.25	0.33	0.18	0.26	0.26	0.29	0.30	0.13	0.24	0.13	0.23	0.30	0.36	0.33	0.38	0.40	0.37	0.37	0.33

of heterogeneously composed garnets show only vaguely deliminated bands on the photographs. Usually, the composition from zone to zone differs gradually though abrupt changes do occur. The accuracy of the measurements is ± 0.005 Å. The n and a values and their variations are estimated for garnets from the twelve rock samples. The contents of pyrope, almandine, and grossular may be obtained with the aid of the triangular diagrams of Sriramadas (1957). The garnets from each of these rock samples were microprobed. The proportions of pyrope, almandine, and grossular of each sample, were converted to a total of 100 mol% and were plotted in the same diagram. It appears that the plots of the computed and the estimated values of refractive index and unit-cell dimension do not coincide. With respect to each other, plots of corresponding points deviate a few per cent. This deviation is the obvious result of neglecting the contents of andradite and spessartine.

Garnets from twelve rock samples were electron microprobed in various degrees of intensity (Table 18). Forty-one analyses have been executed in total.

Two preparations of garnet grains (866 and 867) obtained from sample RGM 109688 by heavy liquid separation and with the aid of the Frantz isodynamic magnetic separator, demonstrate a small difference in magnetic susceptibility. X-ray powder photographs were made from these preparations. The lenght of the unit-cell of the magnetically stronger garnet (866) varies between 11.614 and 11.619 Å and that of the magnetically weaker one (867) varies between 11.581 and 11.609 Å. Their lowest and highest indices of refraction are 1.770 and 1.778 respectively. Most n-values of preparation 866 are closer to 1.778, whereas in preparation 867 most n-values are measured closer to 1.770. It appears from the tables of Winchell (cf. Deer, Howie & Zussman, 1962) that relatively small changes in the almandine-pyrope content cause conspicuous deviations in the indices of refraction. The unit-cell dimensions are hardly influenced by these changes of composition. However, the cell edges change considerably when the grossular content varies. This change of the cell edge dimensions hardly influences the refractive index, provided the almandine-pyrope ratio remains unchanged. The garnets of the above mentioned rock have a distinctly zoned structure with the following characteristics: Fe and Mn weakly decreasing, Ca obviously decreasing, and Mg increasing from core to rim. Consequently, preparation 866, as compared with 867, contains more components of almandine and grossular, i.e. more material from the core of the grossular garnet. Assuming that the highest of the pertinent a and n-values agree with the variations of the pyrope and the grossular contents respectively (high n corresponds with high almandine and high a corresponds with high grossular), the latter values can be arranged as given in Table 19.

It is probably needless to say that estimated and calculated values of n and a are distinguished here. The estimated n is derived from immersed grains and a

Table 19. Computed and estimated values of a and n for garnets from rock sample RGM 109 688.

	computed values:		estimated values:	
	a	n	a	n
core (analysis 14)	11.617	1.783	11.619	1.778
rim (analysis 15)	11.580	1.776	11.581	1.770

from X-ray powder photographs, both from the same preparations. The calculated values of n and a are obtained from the electronprobe microanalyses performed on these sections (see also Table 19).

Six garnet grains from the garnet-rich band of sample RGM 109 684 and 5 grains from outside of the same band (p. 32) were microprobed. The garnets have zoned structure with the following characteristics: garnet-rich bands (1-6); Mn and Fe diminishing weakly, Ca decreasing clearly, and Mg increasing strongly from core to rim. Outside the garnet-rich band (7-11); Mn and Fe vary weakly, Ca decreases clearly, and Mg increases clearly from core to rim.

The calculated size of the unit-cell of analysis 8 (see Table 20) stands out compared with all of the forty-one analyses. Its high value is the result of the relatively high grossular content, whereas the calculated small size of the unit-cell of analysis 9 holds good for the low grossular-content. Besides, two partial analyses (12 and 13) were made from a garnet not belonging to the garnet-rich band. The composition appears to be irregular (see Table 20).

Estimated refractive indices of garnets from the garnet-rich band range from 1.773 to 1.783 and the garnets outside the band from 1.779 to 1.785. The estimated a values of the same garnets are respectively 11.586 - 11.599 Å, and 11.576 - 11.625 Å. Consequently, in accordance with the calculated a and n values for both garnet types, it turns out that the grossular content must be relatively high when the almandine content is relatively low. The alternative is that the almandine content must be high when the grossular content is low. The extremes of the estimated values should be arranged as in Table 20. The arrangement of estimated values suggests that the almandine-pyrope content of garnets varies less outside the garnet-rich band than within. The calculated values are not decisive with respect to this suggestion.

In sample 44-126, no systematic difference in composition has been observed between garnets enclosed by and those outside the amphibole (glaucophane). Garnet 1, enclosed in amphibole, has a zoned structure with obviously decreasing Ca and increasing Mg from core to rim. Fe and Mn are less variable. Garnet 5, from outside the amphibole, is also zoned. The latter zonality only

Table 20. Computed and estimated values of a and n for garnets from rock sample RGM 109 684.

	computed values:		estimated values:	
	a	n	a	n
grains 1-6 (within the garnet-rich band):				
core (analysis 8)	11.646	1.782	11.599	1.773
rim (analysis 9)	11.601	1.786	11.586	1.783
grains 7-11 (outside the garnet-rich band):				
core (analysis 10)	11.621	1.788	11.625	1.779
rim (analysis 11)	11.612	1.788	11.576	1.785
core (analysis 12)	11.626	1.785		
rim (analysis 13)	11.609	1.783		

consists of a core and a rim. Garnet 2, an atoll-type garnet, enclosed in amphibole, is hardly zoned. The garnet of sample 44-126 seems to be almandine-rich and poor in pyrope in comparison with the other analysed garnets (see Table 21).

Table 21. Computed and estimated values of a and n for garnets from rock sample 44-126.

	computed values:		estimated values:	
	a	n	a	n
1 - core (analysis 1)	11.604	1.797	11.602	1.799
5 - core (analysis 4)	11.591	1.802		
1 - rim (analysis 2)	11.568	1.803	11.562	1.802
5 - rim (analysis 5)	11.570	1.794		
atoll-type (analysis 3)	11.579	1.800		

The estimated n values vary between 1.799 and 1.802 and a between 11.562 and 11.602 Å (see Table 21). It is not easy to make a decision between the combinations: $n_{max.}$ with $a_{min.}$ or $n_{max.}$ with $a_{max.}$, because of the fluctuating nature of Fe. However, a feasible wrong choice does not yield important mistakes, for the difference between $n_{max.}$ and $n_{min.}$ is small.

Sample RGM 141 442 is from another glaucophane-bearing rock. Results of electronprobe microanalyses for minerals of the mentioned sample are not available. Provided that the general rule for these garnets holds, i.e. that the grossular content is highest in the core and the pyrope-almandine content in the rim, the estimated values can be arranged as in Table 22.

Table 22. Estimated values of a and n for garnets from rock sample RGM 141 442.

	a	n
core	11.605	1.795
rim	11.536	1.802

Samples RGM 135 506, 135 508, 135 509, and 135 510, are part of six samples, taken from an extensive exposure of the basic body near Bainas. The well-banded rocks are dipping 30-40° to the ESE. The first (RGM 135 506) and the last (RGM 135 510) of these samples, taken perpendicular to the banding, are only about 2.5 m apart. Atoll-type garnets observed in sample RGM 135 506 have been tested for zoning with the aid of electron microprobe sample-scanning. Only a faint zoning has been ascertained with respect to Mn. The Mn-content varies from 0.4% in the core to 0.55% in the rim. The examined garnet from RGM 135 508 has a clearly zoned structure with decreasing Fe and Mn, and increasing Ca and Mg from core to rim. Particularly the significant increase of Ca from core to rim is remarkable. Though we are dealing here with an increase in grossular of less than 5 mol%, further investigation of this sample is warranted (see Table

23). The garnet from RGM 135 509 is irregularly structured. The increase of Mg and decrease of Ca and Mn from core to rim is obvious. The Fe-content is variable.

Table 23. Computed and estimated values of a and n for garnets from rock samples RGM 135 508, 135 509 and 135 510.

	computed values:		estimated values:	
	a	n	a	n
Sample RGM 135 508:				
core (analysis 21)	11.578	1.787	11.560	1.785
rim (analysis 22)	11.583	1.775	11.587	1.779
Sample RGM 135 509:				
core (analysis 23)	11.613	1.782		
rim (analysis 24)	11.576	1.781	11.551	1.778
core (analysis 25)	11.601	1.792	11.582	1.780
rim (analysis 26)	11.576	1.787		
Sample RGM 135 510:				
core (analysis 27)	11.587	1.784	11.598	1.786
rim (analysis 28)	11.578	1.783	11.568	1.778
outermost rim (analysis 29)	11.578	1.781		

The garnet from RGM 135 510 generally has a zoned structure. A specially examined garnet grain presents the following properties: Mg increases from core to rim. Though tending to be higher in the core, Fe is rather constant. Ca is distributed irregularly, possibly partly due to inclusions just below the surface of the microprobed slice. However, it is quite possible that this irregularity is typical for Ca of this garnet (see also RGM 135 508). Mn decreases from core to rim and increases again in a very thin outermost rim. The Mn-content varies as follows: core 0.75%, rim 0.4%, outermost rim 0.7 - 0.9%. An X-ray emission photograph (Pl. 5, fig. 1) shows the Mn-increase in the rim very clearly.

Fe is rather homogeneously distributed in the garnets from sample RGM 140 615. A small increase towards the rim can usually be established. Mn diminishes a little near the rim, Ca clearly decreases from core to rim. Calculated values and estimated values from the extremes are given in Table 24.

Sample RGM 140 647 contains two types of garnet, i.e. a large atoll-type in the micaceous rock (A) and a smaller massive garnet in the amphibole-rich portion (B). Five grains were measured at two points from each type of garnet. Type A is more homogeneous than type B. In fact different compositions were established for type B: an average one with higher Ca and lower Fe, and an incidental one with lower Ca and higher Fe. Other distinctions are: the Fe- and Mg-contents are highest in type A whereas the Ca-content is highest in type B. Though the compositions of both types are partly overlapping, the mentioned

Table 24. Computed and estimated values of a and n for garnets from rock sample RGM 140 615.

	computed values:		estimated values:	
	a	n	a	n
core (analysis 30)	11.617	1.791		
core (analysis 32)	11.615	1.791	core: 11.603	1.788
rim (analysis 31)	11.562	1.792	rim: 11.585	1.799
rim (analysis 33)	11.575	1.790		

differences were established by measurements on many grains. The garnets of type B display a clear, sometimes irregular and abrupt, zonality: Mn is constant and low, whereas Fe, Mg, and Ca are rather variable. The variation is largest for Ca. Ca decreases and Fe and Mg increase from core to rim in several instances. The element distribution in other grains is irregular to such a degree that higher Ca-contents are also found in the rim. Hence microprobe results are furnished from Ca-richer and Ca-poorer types, in stead of compositional changes from core to rim, e.g. garnet 7. Calculated values and estimated values of the extremes are given in Table 25.

Table 25. Computed and estimated values of a and n for garnets from rock sample RGM 140 647.

	computed values:		estimated values:	
	a	n	a	n
5 - core (analysis 34)	11.613	1.775		
5 - rim (analysis 35)	11.557	1.780		
7 - Ca$_{max.}$ (analysis 36)	11.617	1.773	core/ Ca-rich, Fe-poor:	
7 - Ca$_{min.}$ (analysis 37)	11.559	1.777	11.608	1.773
A - average (an. 38)	11.558	1.775	rim/ Ca-poor, Ca-rich:	
B - average (an. 39)	11.596	1.773	11.554	1.778
B - Ca$_{max.}$ (analysis 40)	11.609	1.770		
B - Ca$_{min.}$ (analysis 41)	11.572	1.780		

Much work has been done on the investigation of variations in the composition of garnet grains by means of electronprobe microanalysis (Hollister, 1966, 1969; Fediukova & Vejnar, 1971; Bryhny & Griffin, 1971; Kurat & Scharbert, 1972). Although the results of the microprobe are evidently less precise, a source of error, not to be neglected, is hidden in the sample preparation of the conventional chemical analyses. The bulk composition of the separated garnet fraction is not in proportion with the chemical variation in the garnet grains. Mineral separation methods appear to work selectively in such a way that the bulk composition of the garnet sample agrees more with the core material (Harte & Henley, 1966), whereas the gross composition of the other garnet is more in accordance with the rim material (Dudley, 1969). At the moment the electronprobe microanalysis is the only method to estimate characteristics of the chemical variation of zonally built garnets. Generally one may distinguish regular and irregular zoning (Kurat & Scharbert, 1972). In an early stage it was already pointed out that the boundaries between the chemically varying parts are usually not sharp (Harte & Henley, 1966). The existence of interrupted zoning as a result of resorption and subsequent (eventually zonal) recrystallisation is supposed (Atherton & Edmunds, 1966; Harte & Henley, 1966). Abrupt variations could be defined in the latter instance. The early investigators of zoned structure of garnets had the opinion that Ca and Mn were decreasing, and Mg and Fe were increasing from core to rim, in addition to which Ca and Mg are often varying. This was called normal zoning as opposed to reverse zoning. The garnets in question derive from mesozonal pelitic schists and are almandine-rich. However, the chemical variations found in garnets of eclogites and granulites are not yet quite understood.

With regard to the present investigation, it generally may be said that there is a compositional variation between the elements Fe, Mg, Ca, and Mn. Iron appears to be mainly bivalent. In cases of obvious zoning Ca is decreasing and Mg is increasing from core to rim, whereas Fe and Mn behave more capriciously. The atoll-type garnets display the slightest variation. They are relatively Mg-rich and poor in Ca.

Figure 17A represents the almandine-pyrope-grossular diagram according to Sriramadas (1957). It may be seen that the fields of the calculated and the estimated compositions of material from core and rim respectively are overlapping for the greater part. The fields of estimated values from core as well as rim material shifted pyrope-wards compared with the fields of the computed values of the same samples. Moreover, both fields of core material overlap mutually, as do both fields of rim material of the garnets from selected rocks. The data of garnets with extreme compositions, such as those of the pyrope-rich garnet from sample RGM 135 506 and the almandine-richer garnets from 44-126 and RGM 141 442 can not be accommodated in the diagrams of Fig. 17. The garnet from RGM 140 615 also does not fit, especially concerning its rim.

In accordance with garnet composition (alm + spess; gross + andr; pyr) the present eclogitic rocks belong to the group C-eclogites of Coleman et al. (1965) (Fig. 17B), i.e. eclogites associated with glaucophane schists. The atoll-type garnets from RGM 135 506 and 140 647-A are more in agreement with those from group B-eclogites. The latter eclogites are associated with migmatites and gneisses. A linear correlation exists between the parameters FeO + MgO and CaO + MnO with increasing degree of metamorphism (Sturt, 1962; Nandi, 1967). This correlation is valid only under condition that the trivalent positions in the crystal lattice are occupied by Al. This condition is generally fulfilled. The andradite component is of less importance in all of the garnets under consideration. Replacement of the cations Ca and Mn by Fe and Mg is based on Miyashiro's rule (1953) that the molecular volumes of garnets decrease with increasing pressure, or that larger cations are replaced by smaller ones. In accordance with current opinion it is concluded that the zoned structure of the garnets in question is the result of prograde metamorphism under non- or imperfect equilibrium conditions (Fig. 18). It is quite possible that the abrupt variations indicate interruption or even resorption in a succession of garnet forming phases.

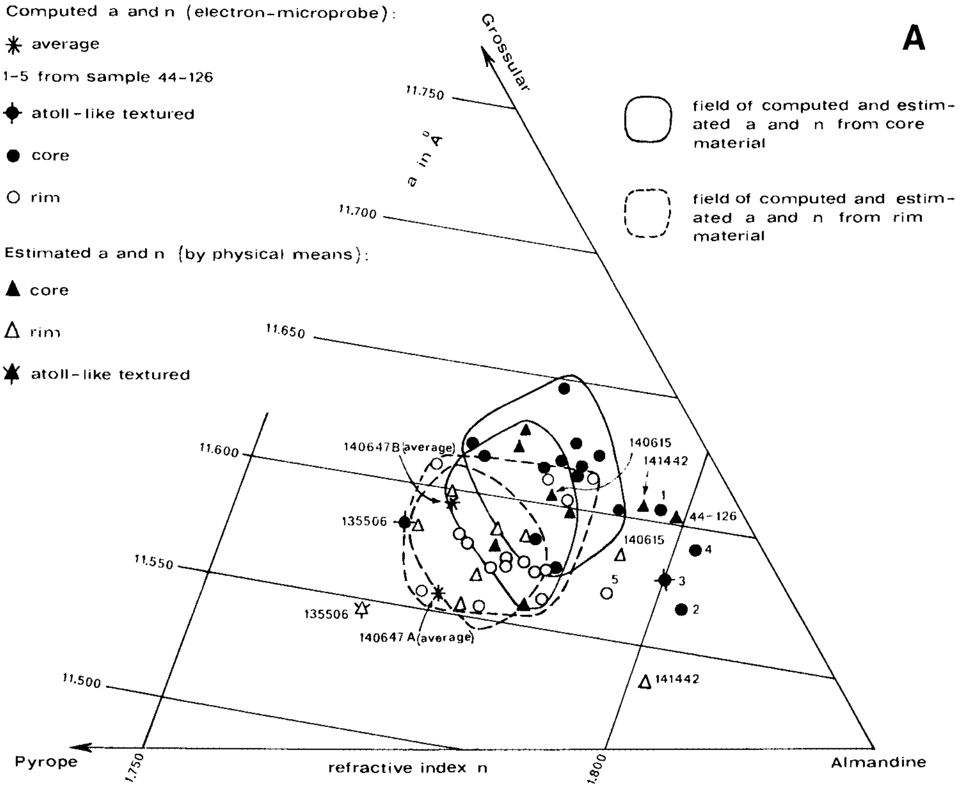
Computed a and n (electron-microprobe):
✳ average
1-5 from sample 44-126
✦ atoll-like textured
● core
○ rim
Estimated a and n (by physical means):
▲ core
△ rim
atoll-like textured
A
field of computed and estimated a and n from core material
field of computed and estimated a and n from rim material
Grossular
a in Å
11.750
11.700
11.650
11.600
11.550
11.500
140647B (average)
135506
140647 A (average)
140615
141442
1
44-126
4
3
2
5
Pyrope
1.750
refractive index n
1.800
Almandine

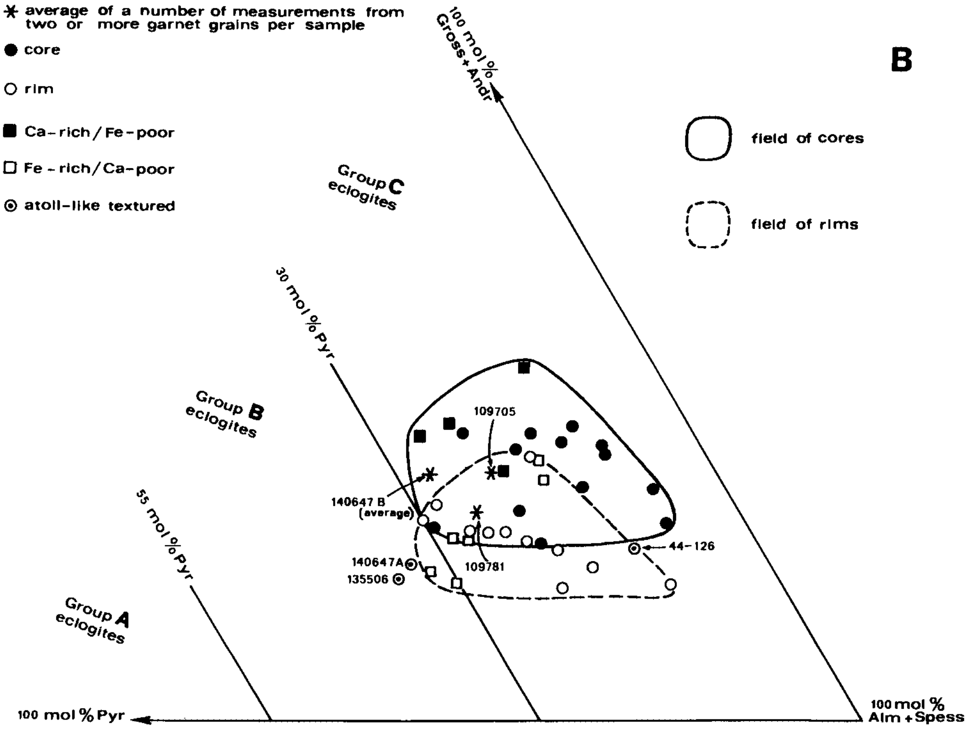
✳ average of a number of measurements from two or more garnet grains per sample
● core
○ rim
■ Ca-rich/Fe-poor
□ Fe-rich/Ca-poor
⊙ atoll-like textured
B
field of cores
field of rims
100 mol% Gross+Andr
Group C eclogites
Group B eclogites
Group A eclogites
30 mol%Pyr
55 mol%Pyr
109705
140647 B (average)
140647A
135506
109781
44-126
100 mol%Pyr
100 mol % Alm+Spess

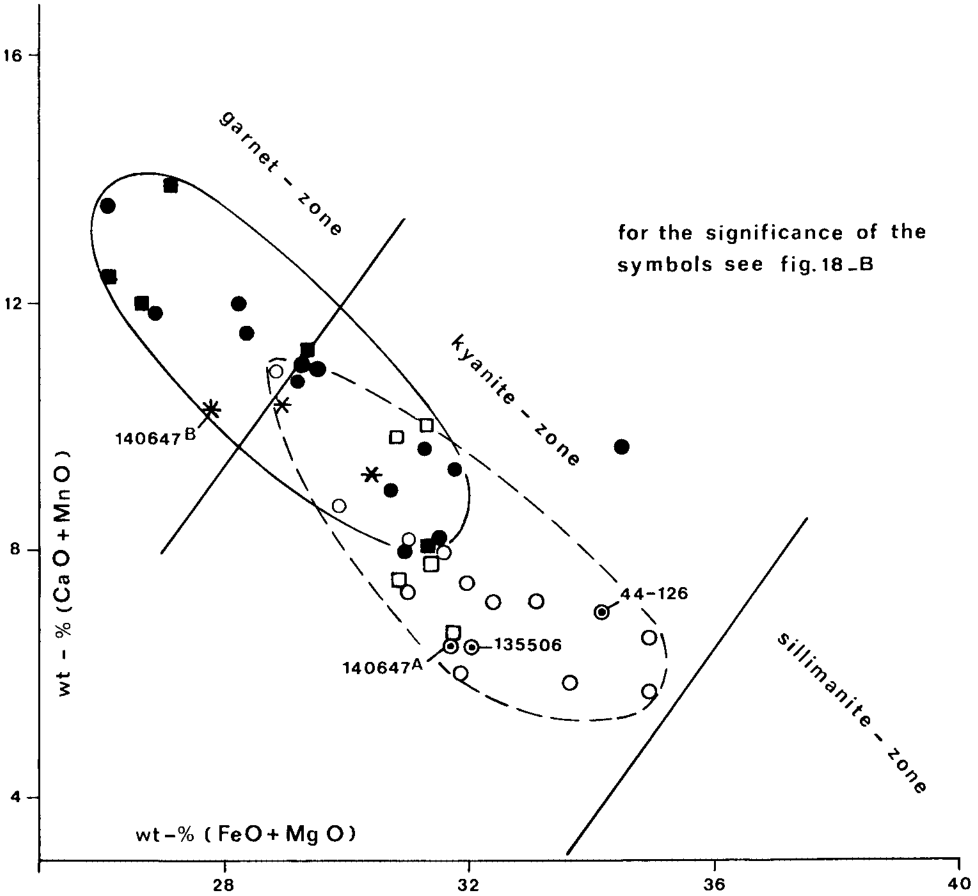

Fig. 18. Plot of the proportions (CaO + MnO) and (FeO + MgO) (Nandi, 1967) of the electronmicroprobed garnets from the Blastomylonitic Graben. The distribution of the points in partly overlapping fields of core and rim garnets manifest a prograde metamorphism when assuming that Ca-rich, Fe-poor and Fe-rich, Ca-poor garnets respectively represent core and rim material.

Fig. 17. Garnets from metabasites of the Blastomylonitic Graben. A. Plot of n and a, in accordance with Sriramadas (1957), expressing the composition for garnets in the alm-pyr-gross diagram as estimated from mineral preparations. The electronprobe microanalyses of garnets from the same rock samples are plotted in the triangular alm-pyr-gross diagram. The parameters n and a can accordingly be read from the plot; these are called computed values in the text. The full line defines the field of the estimated and computed plots of the garnet cores from most of the samples. The dashed line does the same for the garnet rims. 1-5 are analysis numbers of garnets from sample 44-126 (see Table 18). B. Plot of the electronprobe microanalyses in the triangular diagram according to Coleman et al. (1965) showing relative proportions of (alm + spess), (gross + andr), and pyr garnet endmembers with indication of the fields for core and rim.

General conclusions — Two types of garnet appear to occur in the examined eclogitic rocks. Firstly, a zoned garnet with increasing Mg, decreasing Ca, varying Fe, and rather constant Mn from core to rim. These garnets plot within Tröger's (1959) field of eclogite-garnets and amphibole-garnets. Also these garnets are higher in grossular and lower in almandine and pyrope components as compared with the second type, while their spessartine content is always low. Reverse zoning of Mn near the rim is frequently observed. According to Kurat & Scharbert (1972) this would point to a drop of temperature during the final phase of garnet development. The second type of garnet is not or hardly zoned, merely variable in composition. Some order exists within the mutual relation between Ca, Mg, and Fe: Ca-rich against poor in Mg and Fe. The clearly zoned garnets seem to have a lower pyrope content than the second type of garnets, which is also expressed in the Niggli-value mg.

It is the author's opinion that the formation of atoll-type garnets and not or hardly zoned garnets with irregular variations in composition is indicative of an event in the course of the prograde metamorphism. Subsequently a part of the already formed garnets became instable. In the instance of the atoll-type garnets, this event could have happened before the end of the garnet growth, i.e. garnet crystallisation continued after a certain period of interruption. The core replacement of garnets from the aureole of the Ardara pluton, Co. Donegal, Ireland (Smellie, 1974) occurred mainly in those garnets enclosed by quartz or quartz-rich groundmass, which is generally in agreement with observations on the rocks described in the present publication. Judging from the replacing minerals in the core of the atoll-like garnets an important agent should be water supply. The garnet replacing minerals are mainly muscovite and quartz, as well as porphyroblastic amphibole and some zoisite. Clinopyroxene which is sometimes observed here, could be a remnant of an inclusion in the garnet.

The reasons for the suggestion that atoll-garnets are merely documents of prograde metamorphism are not valid here. Features mentioned by Cooper (1972) and de Wit & Strong (1975), as far as occurring in the present rocks, are not concomitant: 1) plagioclase occurs as albite and belongs to a later stage of alteration; 2) fine-symplectite in relation with clinopyroxene is ubiquitous and coincides more or less with deformative circumstances together with the development of coarser grained epidote-albite-amphibole symplectite (F_3 and F_4 of Table 8); 3) biotite development is of no importance; 4) kelyphitic rims around garnets are not observed.

Minerals of the epidote-zoisite group

X-ray powder photographs of likely zoisite from a number of rock samples definitely show the pattern of reflection lines of this mineral. With the available X-ray method the present author was not able to distinguish between α- and β-zoisites.

Optically zoned porphyroblasts were microprobed to establish the Fe, Al, Mn, Ti, and Cr content (samples RGM 109684 and 109688). Ti and Cr were only estimated as traces. The Ca-content behaved stoichiometrically. Variations were only found in the Fe/Al-ratio. The maximum content of Fe_2O_3 is 3.2 and the minimum one is 1.4. The weight percentages are highest in the core of the zoisite. All iron in the zoisite is, as usual, expressed as Fe_2O_3. The variation of the Fe_2O_3/Al_2O_3-ratios seems to be responsible for the differences in the optical characteristics of the zoisites (see p. 19). The chemistry and optics of some epidotes are discussed on p. 26.

ROCK CHEMISTRY

Twenty whole-rock samples have been chemically analysed. One group of fifteen and another group of five samples were analysed with an interval of about half a year. The standard deviation (σ) of the duplicates of the two groups were calculated to get an impression of the accuracy of the analytical results (Table 26).

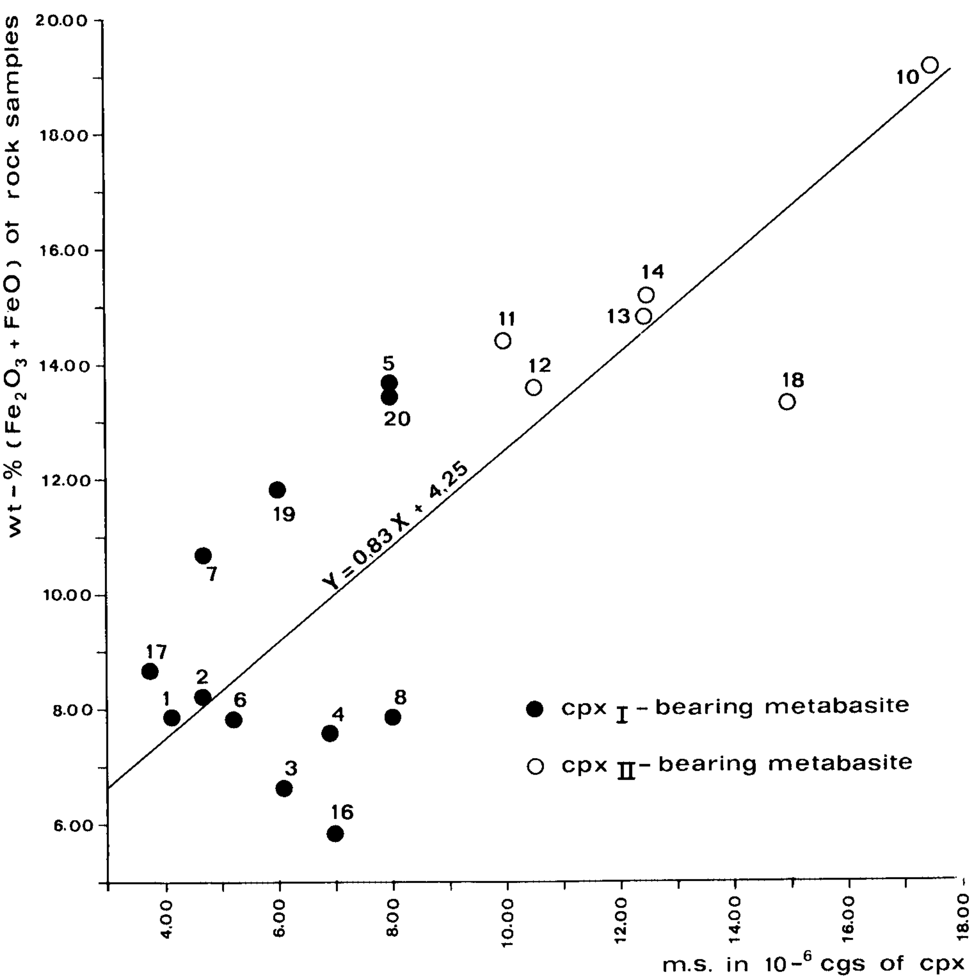

Fig. 19. Relationship between total iron in wt % (Fe_2O_3 + FeO) of rock samples and magnetic susceptibilities (m.s.) of the clinopyroxenes from the corresponding samples of metabasites from the Blastomylonitic Graben. For explanation of the symbols see Table 26. The statistical parameters are:

	stand deviation	mean
abcissa: m.s.	3.93	9.34
ordinate: wt % (Fe_2O_3 + FeO)	3.76	11.17

The correlation coefficient is 0.79. The progressive regression m.s. depends on total iron, which fulfils the equation $y = 0.83 + 4.25$.

Table 26. Chemical analyses, QLM-values, Niggli-values and katanorms of 20 rock samples from metabasites of the Blastomylonitic Graben, Galicia, Spain.

	1	2	3	4	5	6	7	8	9	10	11	12	13	14	15	σ	16	17	18	19	20	σ
	Ru.8	109 669	135 508	109 781	135 523	140 647	109 705	Ru.17B	44-126	135 519	109 723	109 773	135 510	140 615	145 505		135 509	140 480	140 594	140 617	141 345	
SiO_2	49.625	48.940	61.620	51.355	46.985	54.250	48.140	48.405	54.310	47.290	48.175	48.360	45.215	51.480	49.815	0.18	64.495	47.375	47.150	49.510	49.140	0.14
Al_2O_3	16.255	16.225	15.365	18.755	15.095	14.555	15.030	21.140	14.720	12.235	13.925	16.695	20.215	14.725	13.945	0.10	14.660	16.700	15.145	15.510	15.260	0.04
Fe_2O_3	1.675	1.990	1.900	2.930	2.100	1.760	2.315	2.545	3.075	5.035	4.140	4.585	3.660	3.665	1.805	0.08	1.465	2.475	4.715	1.915	2.765	0.09
FeO	6.160	6.200	4.720	4.600	11.695	6.145	8.455	5.285	10.575	14.230	10.335	9.020	11.180	11.480	11.700	0.11	4.300	6.230	8.675	10.025	10.665	0.05
MnO	0.150	0.155	0.130	0.145	0.285	0.185	0.225	0.065	0.245	0.375	0.300	0.275	0.220	0.295	0.290	0.02	0.150	0.175	0.265	0.225	0.265	0.04
MgO	10.725	9.075	4.000	5.565	6.650	8.840	7.875	7.950	3.525	5.075	5.635	5.700	8.075	4.110	6.100	0.14	3.450	9.680	6.515	7.335	7.735	0.08
CaO	11.475	12.300	7.400	9.940	9.325	7.050	11.475	8.220	6.000	7.495	9.945	9.875	6.865	7.690	9.650	0.11	5.575	11.095	10.000	9.765	9.735	0.05
Na_2O	2.500	3.175	3.110	4.925	3.075	2.750	2.325	4.460	4.445	2.475	2.915	4.325	2.975	4.100	2.075	0.12	3.375	2.750	3.400	2.425	2.500	0.06
K_2O	0.350	0.425	0.435	0.070	1.475	1.475	0.500	0.125	0.990	0.475	0.490	0.000	0.090	0.120	0.165	0.05	0.300	0.300	0.425	0.050	0.250	0.02
H_2O	0.640	0.755	0.705	0.875	1.240	1.570	0.800	0.775	1.185	1.435	0.435	0.565	0.760	0.650	1.105	0.31	1.075	1.105	1.445	0.670	0.525	0.06
TiO_2	0.720	0.830	0.380	0.500	2.675	1.080	1.520	0.555	1.270	3.870	2.910	0.470	0.590	2.355	2.590	0.04	0.410	1.120	2.310	1.485	2.920	0.17
P_2O_5	0.150	0.040	0.040	0.045	0.375	0.010	0.115	0.005	0.125	0.315	0.315	0.110	0.030	0.210	0.345	0.00	0.055	0.090	0.215	0.225	0.225	0.01
Sum	100.290	100.110	99.805	99.660	99.975	99.670	98.775	99.530	100.465	100.305	99.520	99.980	100.335	100.835	99.505	0.28	99.370	99.145	100.260	99.850	99.985	0.18
CO_2	<0.100	<0.100	<0.100	<0.100	<0.100	<0.100	<0.100	<0.100	<0.100	<0.100	<0.100	<0.10	<0.100	<0.100	<0.100		<0.100	<0.100	<0.100	<0.210	<0.100	
Q	28.0	26.3	45.4	29.8	24.8	35.5	29.4	27.6	33.5	28.1	21.8	26.0	26.1	30.6	32.3		58.7	31.2	31.6	35.5	35.4	
L	33.3	35.6	34.6	43.7	35.9	30.5	31.8	46.1	38.3	29.0	30.1	39.2	37.0	36.0	29.8		19.5	20.1	20.1	18.4	18.6	
M	38.7	38.1	20.0	26.5	39.3	34.0	38.8	26.3	28.2	42.9	48.1	34.8	36.9	33.4	37.9		21.8	48.7	48.3	46.1	46.0	
π	0.57	0.47	0.47	0.39	0.40	0.48	0.60	0.48	0.27	0.46	0.45	0.41	0.56	0.37	0.59		0.43	0.55	0.43	0.59	0.55	
k	0.07	0.07	0.07	0.01	0.23	0.26	0.00	0.01	0.13	0.11	0.10	0.00	0.02	0.02	0.06		0.05	0.06	0.07	0.00	0.07	
γ	0.18	0.26	0.16	0.24	0.17	0.12	0.21	0.04	0.06	0.12	0.15	0.19	0.00	0.16	0.16		0.25	0.28	0.28	0.25	0.27	
mg	0.71	0.67	0.52	0.57	0.46	0.65	0.57	0.65	0.32	0.32	0.41	0.43	0.49	0.33	0.44		0.52	0.67	0.47	0.52	0.43	
t	-11.2	-15.0	-6.8	-10.9	-11.2	-6.7	-12.9	-1.6	-7.5	-8.3	-13.1	-10.7	-3.5	-9.2	-10.4		-2.8	-10.5	-12.2	-8.6	-9.7	
si	105.9	105.7	197.3	125.0	106.4	137.0	109.7	110.7	148.4	114.0	113.8	109.2	97.3	129.9	121.4		230.5	102.3	107.7	115.6	117.2	
al	20.4	20.6	28.6	26.9	20.1	21.7	20.1	28.4	23.6	17.4	19.4	22.4	25.6	21.8	19.9		30.9	21.3	20.3	21.3	21.5	
fm	48.0	43.8	36.0	35.3	48.6	49.9	46.9	41.6	45.3	56.9	48.1	44.5	52.3	47.2	49.8		35.4	46.9	47.2	48.8	47.3	
c	26.1	28.4	25.1	26.0	22.6	19.1	27.9	20.0	17.6	19.4	25.1	23.8	15.8	20.8	25.2		21.5	25.7	24.4	24.4	25.0	
alk	5.5	7.2	10.3	11.8	8.7	9.3	5.1	10.0	13.5	6.3	7.4	9.3	6.3	10.2	5.1		12.2	6.1	8.1	5.5	6.2	

Q	-	-	18.1	-	-	2.1	-	-	2.8	1.3	-	-	-	0.1	2.6	31.4	4.9	8.5	9.1	11.9
Or	1.7	2.2	2.3	0.5	8.5	9.0	-	0.5	6.2	2.9	2.7	-	0.3	0.5	1.2	10.0	1.0	1.3	-	1.0
Ab	22.0	28.7	28.2	43.8	27.7	25.3	21.3	35.0	40.2	22.7	25.0	38.7	26.0	37.5	19.2	17.5	14.0	17.8	12.5	12.8
An	31.8	28.5	27.2	28.5	23.7	23.0	31.7	36.8	17.5	22.3	22.5	26.7	34.2	22.0	29.3	14.0	18.5	14.3	18.0	17.2
%-An	59	49	49	39	46	48	60	51	30	49	47	41	57	37	62	46	57	45	59	57
Ne	-	-	-	-	-	-	-	2.7	-	-	-	-	0.6	-	-	-	-	-	-	-
Cord.	-	-	-	-	-	-	-	-	-	-	-	-	8.3	-	-	-	-	-	-	-
Wo	-	10.4	-	7.8	3.8	-	-	-	-	-	1.5	7.8	-	-	-	-	-	-	-	-
Di	16.6	2.4	7.0	-	-	6.6	16.6	-	0.8	0.6	7.6	0.8	-	6.2	7.6	13.2	31.4	26.6	24.6	21.6
Opx	9.3	-	13.9	-	-	29.7	23.6	-	24.4	35.3	-	-	-	24.4	31.9	11.1	24.3	20.0	29.4	25.2
Ol	15.0	24.0	-	15.5	27.6	-	0.8	22.0	-	-	30.4	19.9	26.3	-	-	-	-	-	-	-
Ti	1.5	1.8	0.9	0.9	5.7	2.4	3.3	-	2.4	8.7	5.7	0.9	-	5.1	5.7	0.9	2.7	5.7	3.9	6.9
Mt	1.8	2.0	2.4	3.0	2.2	1.9	2.4	2.6	3.2	5.6	4.1	4.9	3.9	3.9	1.9	1.7	3.0	5.6	2.3	3.4
Cp	0.3	-	-	-	0.8	-	0.3	-	2.5	0.6	0.5	0.3	-	0.3	0.6	0.2	0.2	0.2	0.2	0.2
Ru	-	-	-	-	-	-	-	0.4	-	-	-	-	0.4	-	-	-	-	-	-	-
Ortho- meta-basite					x	x	x		x	x	x			x	x		x	x	x	x
Para-	x	x	x	x				x				x	x			x				
Cpx_I -bearing	x	x	x	x	x	x	x	x								x	x		x	x
Cpx_{II}-bearing									x	x	x	x	x	x	x			x		

Too few chemical data are available to establish a simple relation between the mg-values for the minerals cpx_I and cpx_{II} and the corresponding rocks with certainty. However, the total iron content in cpx_{II} is mainly higher than in cpx_I, which results in the different magnetic susceptibilities of these clinopyroxenes. It is obvious that the total iron content of the bulk rock composition determines the total iron content of the clinopyroxene to be formed (Fig. 19).

Poverty in potassium is remarkable, though colourless mica is often abundant. One of the most striking examples of this phenomenon is RGM 109 773 of which the wt% K_2O is 0.000. whereas the vol% of mica is over 6. The paragonite or margarite share should be considerable in this mica (Burgerhout, unpublished M.Sc. thesis, Leiden University, 1975; Burgerhout, Kieft & Felius, in prep.).

Many authors are of the opinion that metamorphic rocks, with the exception of certain characteristically metasomatic rocks, have chemical compositions with primary characters, i.e. that a close material analogy exists between the majority of metamorphic rocks and their parent rocks. This analogy is such that the metamorphic rocks of igneous derivation can chemically correspond to magma types. The Niggli-norms of the analysed rocks show comparatively slight variations. We are always dealing with the compounds Ru, Cp, Kp, Ne, Q, Mt, Fa, Cal, Fo, and Cs, with the exception of sample RGM 135 510, in which case Cs is replaced by Sp. The normative compositions are those of gabbros of the calc-alkaline suite. Only two of the analyses produce normative nepheline; all contain normative pyroxene (diopside, orthopyroxene) and/or olivine. The mentioned metabasites have persistently low Fe^{3+}/Fe^{2+}-ratios. Numerous diagrams to differentiate chemically between igneous and sedimentary origin of metamorphic rocks are available. A modification of the al-(fm+c)-alk double tetrahedron (Burri, 1959) has been presented by Köhler & Raaz (1951). It is based on the concept that chemical parameters should express crystallochemical as well as petrogenetic considerations.

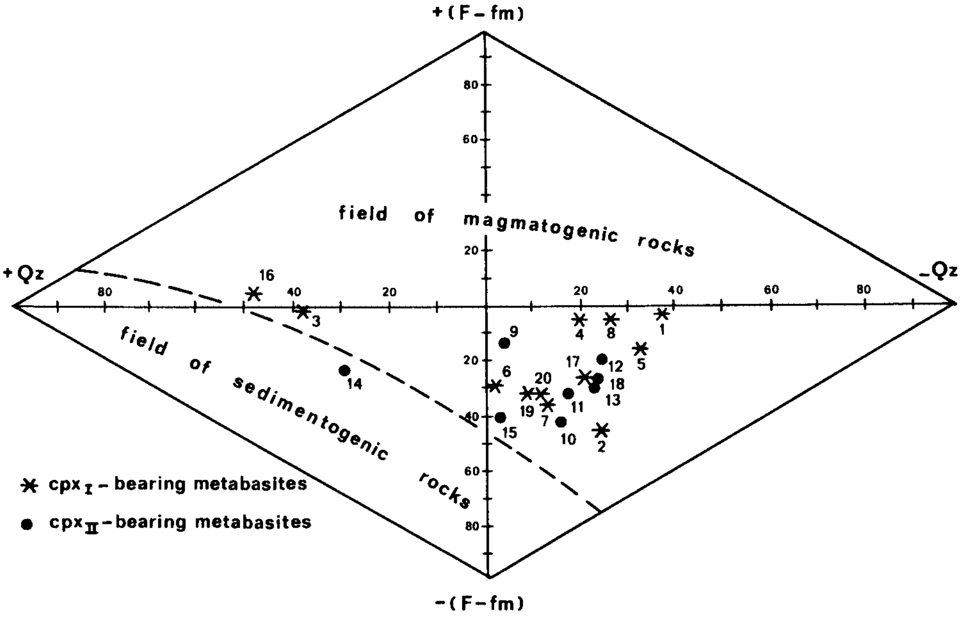

Fig. 20. Qz-(F-fm) diagram showing a modified double-tetrahedron (Köhler & Raaz, 1951) after Burri (1959), expressing the igneous or sedimentary origin of the chemically analysed metabasites from the Blastomylonitic Graben.

F-fm is the sum of the atomic equivalents of cations incorporated in feldspar molecules, and qz is the atomic value of the excess SiO_2, after saturation of all silicate molecules. The Köhler-Raaz plots of the present samples suggest mainly a magmatic descent (Fig. 20).

Misra (1971) distinguishes between para- and ortho-amphibolites by plotting Ti-content against iron enrichment-ratio (F) and Mn. The distinction between para- and ortho-metabasites in Table 19 is based on Misra's criteria combined with field data. When plotting the values of c and mg against each other (Leake, 1964, 1969), it appears that: a) no difference of importance exists between Misra's para- and ortho-rocks; moreover, it is to be assumed that the original sedimentary detritus is derived from magmatic rocks; b) cpx_I- and cpx_{II}-bearing metabasites define a magmatic differentiation trend indicated by a spreading of plots (Fig. 21). The cpx_I-bearing rocks are in the field of early to middle stage differentiates, whereas the cpx_{II}-bearing rocks form part of the middle to late stage differentiates. The trend line is based on the Karroo dolerite suite.

In the writer's opinion, the spreading of the plots of the present metabasites in an AFM-diagram emphasizes that they are early to middle stage differentiates of a tholeiitic to alkali-basaltic character with differentiation trend of decreasing mg (Nockolds & Allen, 1956). According to experimental studies by Green & Ringwood (1967) such magmas could be fractionated from olivine-normative magmas at a depth between 15 and 35 km.

Ophiolitic rocks from the Mediterranean and the Oman Mountains (Alleman & Peters, 1972), and the Papuan ophiolite suite are quoted for comparison (Fig. 22). The ophiolite province in eastern Papua (Thompson & Fisher, 1965) is interpreted by Davies (1971) as a plate of oceanic crust and mantle thrust over continental crust and platform sediments.

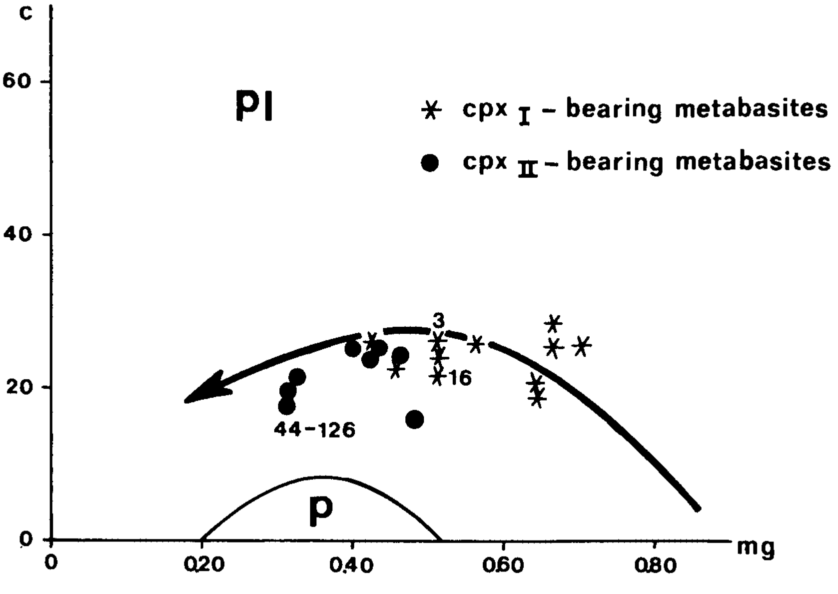

Fig. 21. Plot of c against mg (Niggli-values) of the chemically analysed cpx_I- and cpx_{II}-bearing metabasites from the Blastomylonitic Graben. The trend line is based on the Karroo dolerites (Leake, 1964, 1969). P= typical pelite and semi-pelite rocks; Pl= various pelite-limestone mixtures.

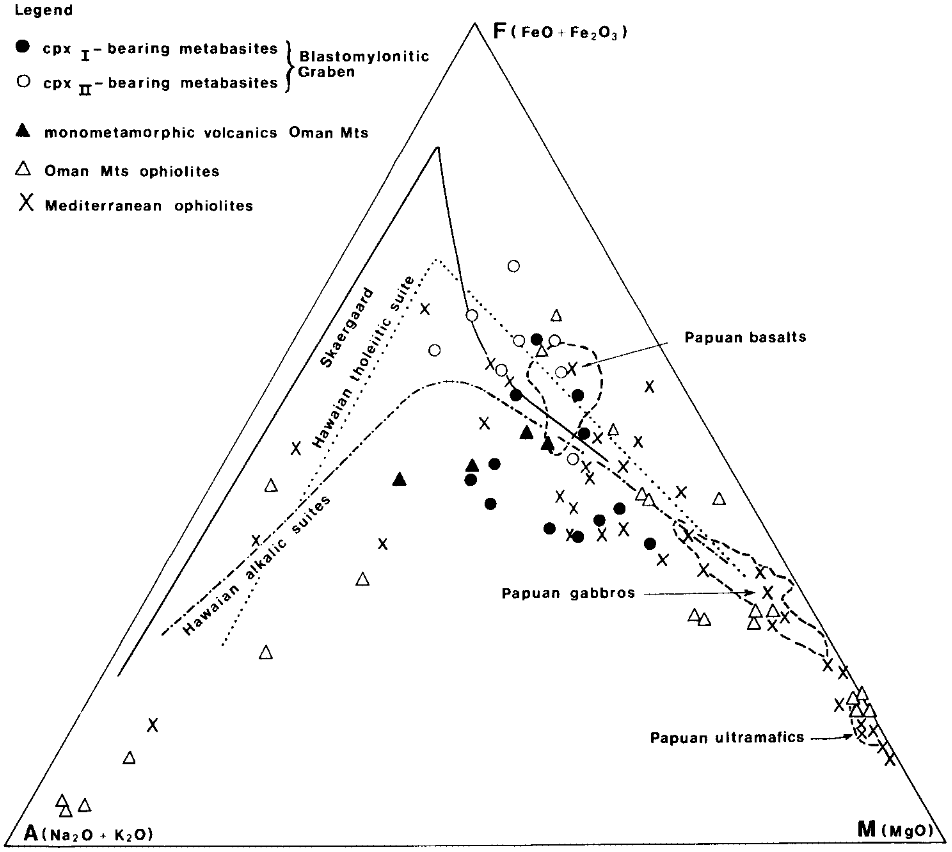

Fig. 22. Comparison of metabasites from the Blastomylonitic Graben with Mediterranean and Oman Mountains ophiolites (Alleman & Peters, 1972), with the Skaergaard intrusion (Kuno, 1968), the Papuan mafic and ultramafic rocks (Davies, 1971), and the Hawaiian basaltic suites.

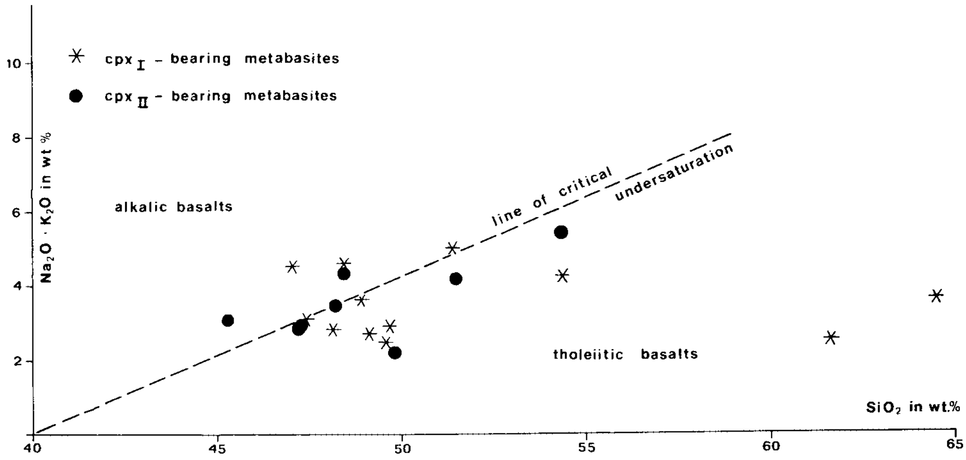

Fig. 23. Plot of metabasites from the Blastomylonitic Graben in the alkali/silica diagram. The boundary between the tholeiitic and the alkalic Hawaiian basaltic rocks is very close to the line of critical undersaturation (Macdonald & Katsura, 1964).

Finally, the present author has tried to define more fully the geological site in which originally magmatic rocks have been emplaced. In order to study compositional similarities with primary rocks from other areas, the method proposed by Ragland, Rogers & Justus (1968) has been adopted. Twenty-five chemical compositions of rocks mentioned by Misra & Griffin (1972) and three analyses (nrs. 40-42) by Ragland et al. (1968, Table 5 on p. 72) are compared with the average composition of the twenty presently analysed metabasites The analyses are recalculated as $a = \frac{(\%X\text{-}\%MB)}{\%MB}$ and $a^2 = \frac{(\%X\text{-}\%MB)^2}{\%MB}$, in which X = wt% oxide in the rock used for comparison and MB = wt% oxide in the present metabasite. The average composition and the range of the twenty metabasites are given in Table 27. Table 28 represents a list of rocks used for comparison with rank ordering. On a world wide scale the original magmatic rocks of the metabasites from the Blastomylonitic Graben in Galicia (Spain) seem to be — according to Ragland et al. (1968) — most closely similar to basalts from the Yellowstone area and to the Pacific and Atlantic tholeiites. However, it is evident from thin sections that some material transport took place, certainly during alterations succeeding the eclogite transformation. The various elements did behave differently in this respect. The deficiency of potassium is striking for the metabasites concerned. Some points in the alkali-diagram (chemical analyses 3 and 16 in Fig. 23) deviate strongly from the boundary line between the tholeiitic and Hawaiian alkali-basalts. This must be due to high Si-contents of the samples. In thin sections it has been noticed that some of the quartz was added during subsequent events. Kuno's at-

Table 27. Average composition and range of twenty chemical analyses from the metabasites of the Blastomylonitic Graben (Ragland et al., 1969).

oxide value:	average (%): [1]	range (%): (see Table 20)
SiO_2	50.98	45.22 - 64.50
Al_2O_3	16.10	12.24 - 21.14
TiO_2	1.56	0.38 - 3.87
Fe_2O_3		1.47 - 5.04
FeO	11.35	4.30 - 14.23
MgO	6.70	3.53 - 10.73
CaO	9.22	5.57 - 12.30
Na_2O	3.27	2.08 - 4.93
K_2O	0.44	0.00 - 1.48

[1]) Fe_2O_3 and FeO have been combined to give total iron as FeO with subsequent recalculation to give a sum of 100% for the oxides SiO_2 $+Al_2O_3+TiO_2+FeO+MgO+CaO+Na_2O+K_2O+MnO+P_2O_5$.

Table 28. List of rocks with rank ordening compared with the average composition of twenty analysed metabasites from Galicia, Spain.

Nr.:	n		a	Rank	a^2	Rank	Sum
M+G 21	6	Basalt from the Yellowstone area	0.93	1	1.04	1	2
M+G 1	10	Pacific and Atlantic tholeiite	1.20	2	1.62	4	6
M+G 6	11	Izu Peninsula, Japan, basalt	1.39	3	1.64	5	8
Ragl.42	2	Chill zone of Skaergaard intrusion	1.61	4	1.62	4	8
M+G 18	1	Chill zone of Palisades sill	1.76	7	1.17	2	9
M+G 2	181	Hawaiian olivine tholeiite	1.68	5	1.93	6	11
M+G 19	9	Snake River basalt, Idaho	1.81	8	1.50	3	11
Ragl.40	1	Chill zone of Stillwater Complex	2.08	10	2.08	7	17
M+G 17	15	Indian Deccan basalt	2.02	9	2.34	8	17
M+G 5	10	Thingmuli Vulcano Island	1.75	6	3.00	14	20
M+G 9	7	Japanese alkali-olivine basalt	2.54	13	2.54	9	22
Ragl.41	1	Chill zone of Bushveld lopolith	2.38	12	2.80	12	24
M+G 7	5	Basalt from peripheral district of South Island, New Zealand	2.83	15	2.57	10	25
M+G 3	8	Azores plag. and olivine basalts	2.88	16	2.74	11	27
M+G 11	28	Hawaiian alkali-olivine basalt	2.56	14	2.82	13	27
M+G 10	7	Hawaiian alkali-olivine basalt	2.29	11	3.31	17	28
M+G 13	7	Pribilof Island alkali basalt	2.91	17	3.17	16	33
M+G 25	36	Basin range alkali-olivine basalt	3.05	18	3.04	15	33
M+G 23	4	Alkali basalt from St. Helena	3.20	19	4.03	18	37
M+G 6	1	Bogoslof Island basalt	3.70	20	4.37	19	39
M+G 8	19	Basalt from the inner district of South Island, New Zealand	3.88	21	5.27	21	42
M+G 22	8	Carboniferous-Permian alkali-olivine basalt from Scotland	3.90	22	4.56	20	42
M+G 12	10	Pacific alkali basalt	4.72	24	6.33	22	46
M+G 16	2	Gough Island basalt	4.51	23	6.52	23	46
M+G 24	5	Alkali basalt from Tutuila	5.13	25	9.14	24	49
M+G 20	4	Basalts from Moon Craters, Idaho	5.52	26	9.28	25	51
M+G 14	3	Tristan da Cunha alkali basalt	5.65	27	11.36	26	53
M+G 15	10	Tristan da Cunha trachybasalt	7.92	28	18.90	27	55

n = number of analyses involved in calculating the average.
M+G = Misra & Griffin (1972).
Ragl. = Ragland et al. (1968).

tempt (Fig. 24) to classify basalts by means of the relation of $Al_2O_3/Na_2O + K_2O$ for given values of SiO_2 is less usefull for these rocks, because of the independently variable silica-content mentioned. The Niggli-ratio mg is significantly consistent in the respective cpx_I- and cpx_{II}-bearing rocks, indicating isochemical behaviour of the total iron and Mg contents.

Petrochemical representation of the major elements in accordance with

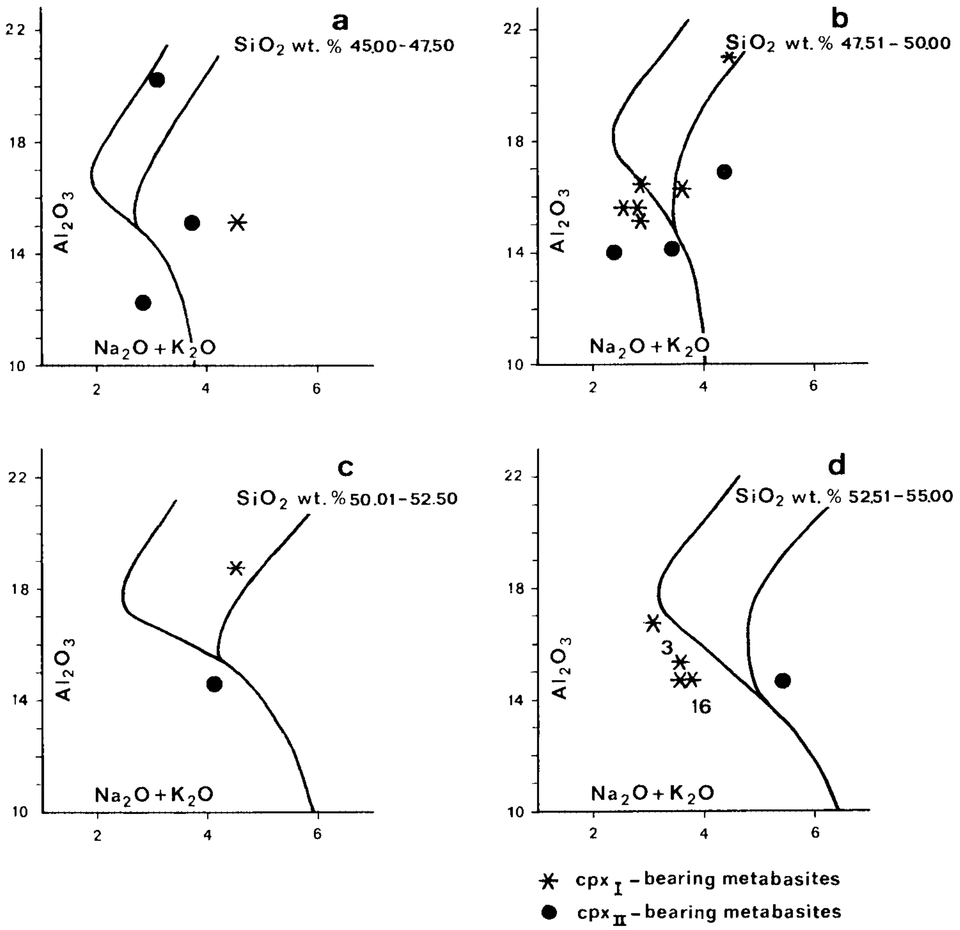

Fig. 24. Plot of the Al_2O_3/Na_2O+K_2O-ratio for given values of SiO_2 of the metabasites from the Blastomylonitic Graben. Values for tholeiitic magmatic rocks lay in the left hand field, for high-alumina basalts in the central field, and for alkali-olivine basalts in the right hand field (according to Kuno, 1960).

Miyashiro (1973), Green (1973), and Subbarao & Chandrasekharam (1976), did not lead to conclusive results. In this respect, it is usefull to mention van Calsteren (1977a), who on the basis of trace elements discriminated between older continental tholeiites and younger abyssal oceanic island basalts for the Cabo Ortegal metabasites.

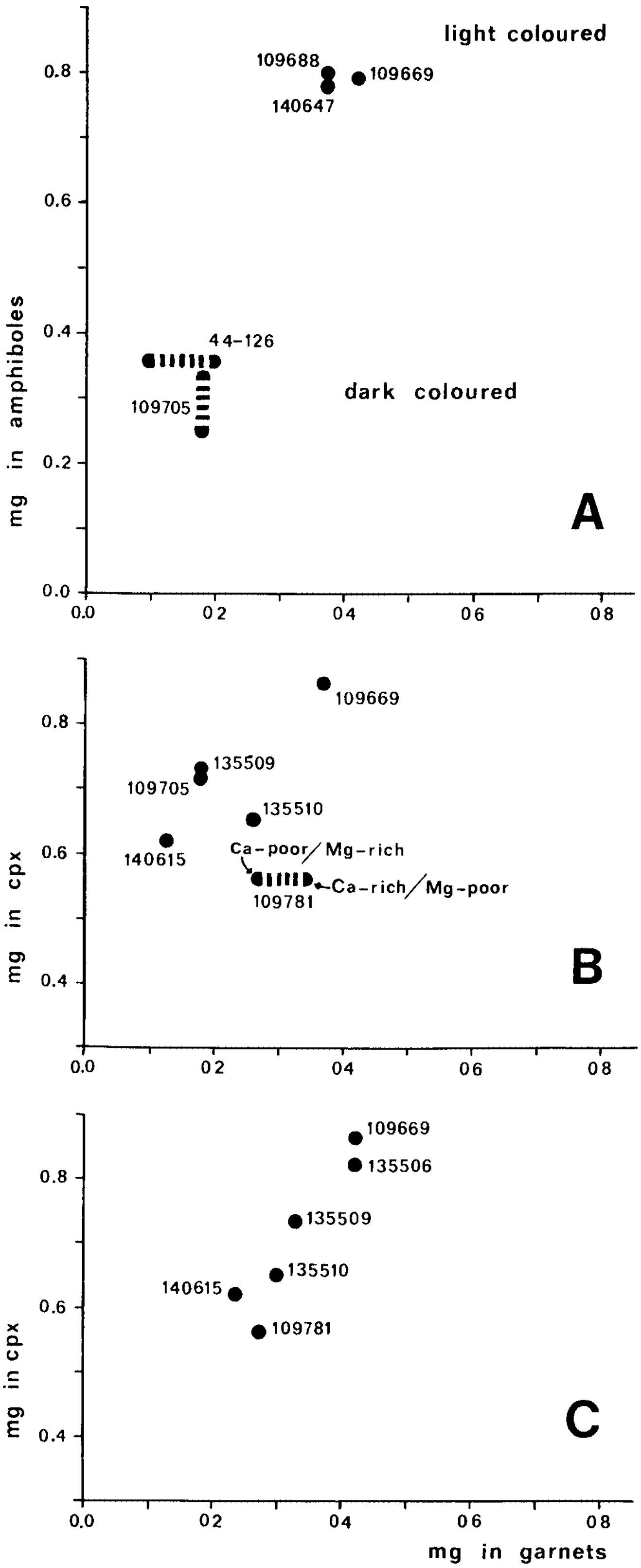
light coloured
109688
140647
109669
44-126
109705
dark coloured
mg in amphiboles
A
109669
135509
109705
135510
140615
Ca-poor/Mg-rich
Ca-rich/Mg-poor
109781
mg in cpx
B
109669
135506
135509
135510
140615
109781
mg in cpx
C
0.0
0.2
0.4
0.6
0.8
mg in garnets

Discussion on petrogenesis

Much literature exists on the interpretation of the physical conditions of eclogite formation. A complete review of all the literature is beyond the scope of this paper, only a few salient points will be noted. Turner (1968) and Winkler (1967) came to opposite conclusions with respect to the relevancy of Eskola's definition of the eclogite mineral facies. Whereas Turner stated that metamorphic facies refer to common mineral assemblages of associated rocks, and not to inferred metamorphic conditions, Winkler on the contrary emphasized the importance of the inferred conditions of formation. As a regular mineral association the existence of eclogite cannot be doubted, but opinions differ as to its significance in terms of metamorphic facies. Bands or lenses of eclogite occur in close association with rocks of the amphibolite, greenschist, or lawsonite-glaucaphane facies (Ghent & Coleman, 1973). On the other hand, eclogite occurs as inclusions in kimberlite and basalt, and furthermore as layers and lenses in ultramafic rocks (Eskola, 1920; Bobrievitch, Smirnov & Sobolev, 1960; and many others). Smulikowski (1965, 1968) is of the opinion that eclogites do not represent a mineral facies in the sense of Eskola, and Coleman states that in view of the rather compelling field evidence it would be advisable to abolish the concept of an eclogite metamorphic facies altogether.

Thermodynamic data allow the construction of a phase diagram showing that eclogite cannot originate under crustal conditions (Essene & Fyfe, 1967; Fry & Fyfe, 1969) in case $P_{H_2O} = P_{fluid} = P_{solid}$. It is evident from experimental studies on the origin of basalt magmas by Yoder & Tilley (1962) and on the transition from gabbro to eclogite by Green & Ringwood (1967, 1972) that close to the melting point of the basaltic system, amphibolite and amphibole-bearing assemblages are stable in the presence of excess water. Essene, Hensen & Green (1970) assume that amphibolite is stable instead of eclogite under condition of crustal metamorphism. However, is it evident from field investigations that many eclogites have been formed under crustal conditions. Examples are mentioned e.g. by Bearth from the Southern Swiss Alps (1959) and the Western Alps (1966); by Bryhni et al. (1970) from various parts of Norway; by Banna (1964, 1966) from the Bessi area of the Sanbagawa belt in Japan; and by Coleman & Lee (1963) and Coleman et al. (1965) from California, U.S.A. The eclogite formation is restricted to 'dry' rocks, where $P_{H_2O} < P_{solid}$ or $P_{H_2O} < P_{fluid}$, which agrees with the conditions necessary for the gabbro-eclogite transition (Green & Ringwood, 1967). Fry & Fyfe (1971) believe to have ascertained hydrothermal conditions for some eclogites formed in the earth crust occur in close relationship with metamorphic rocks of the amphibole, greenschists, or lawsonite-glaucophane facies. Within the crust, eclogites seem to be indicative of certain plate tectonic phenomena (Miyashiro, 1972, Ernst, 1973), where conditions of high pressure and relatively low temperature prevailed. Crustal eclogites are essentially formed under load pressures at least as high as the pressure necessary for the formation of the associated low-

Fig. 25. A. Mg-values of porphyroblastic amphiboles and garnet rims. However, the 44-126 garnets do not show a systematic variation from rim to core. B. Mg-values of clinopyroxenes and garnet cores. Variation of mg is given for the garnet of RGM 109 781. C. Mg-values of clinopyroxenes and garnet rims. Ca-rich/Mg-poor portion of garnet of RGM 109 781 plotted in the diagram agrees best with the linearity of the point pattern.

grade blueschists (Ghent & Coleman, 1973). According to current opinion, eclogites are unstable under glaucophane-schist, greenschist, or amphibole facies conditions where a free water phase is present. However, dense dry rocks — like eclogites — tend to produce an impermeable shell which protects the interior from hydration unless the body is subjected to intensive deformation (Brown & Fyfe, 1972).

As a first approximation eclogites are characterised by two minerals: omphacite and a more or less pyrope-rich almandine garnet. Smulikowski (1964) and Coleman et al. (1965) independently came to a tripartition of eclogites according to their geological occurrences. The end member compositions of the garnets appear to be mainly within the three component system almandine, pyrope, and grossular. Spessartine plays a subordinate role. Smulikowski (see Fig. 16D), and to some extent Coleman too, discerned a relation between the clinopyroxene composition and the geological occurrence. The clinopyroxene appears to be mainly a solid solution of diopside, jadeite, and a little acmite. Mottana, Sutterlin & May (1971) statistically confirmed the geological classification of eclogites by Coleman and Smulikowski on the basis of factor-analysis of their garnets and omphacites. Reasoning from the assumption that element partitioning in paragenetic minerals varies from type to type (Sobolev, 1964; Coleman et al., 1965; Banno & Matsui, 1965; and Essene & Fyfe, 1967), Banno (1970) proved the distribution coefficient of Fe and Mg between garnet and pyroxene to lend support to the geological eclogite classification. The said distribution coefficient appears to be useful as a geological thermometer distinguishing the various eclogite types.

Plotting the mg-values of clinopyroxene against those of the garnets of the corresponding rocks (Fig. 25A-C) reveals striking results. The relation between clinopyroxene and garnet rims suggests a more explicit linearity than the relation between clinopyroxene and garnet cores for five samples (RGM 109 669, 135 506, 135 509, 135 510, 140 615), which might indicate paragenetic co-stability between the clinopyroxene and the garnet rim rather than between the clinopyroxene and the garnet core.

As the metamorphism with increasing pressure becomes more favourable for garnet formation the maximum value of the ratio mg.W/MnO wt% (called g) will increase in garnetiferous amphibolites. This relation is demonstrated in the diagram of Fig. 26 derived from Leake (1972). The plots of the present eclogitic rocks, formed under high pressure conditions, accordingly are mostly situated outside the fields A and B shown in Fig. 26. The obvious linear relation between MnO-content and the mg-value is also in agreement with Leake's data (Fig. 27). This suggests a pre-metamorphic geochemical process of enrichment in Mn which could be connected with volcanic activity on the sea bottom (Krauskopf, 1967, p. 267).

Discriminating between FeO and Fe_2O_3 from electronprobe microanalyses is only possible by approximation. In fact the ACF-diagram is useless for closer comparison of minerals among themselves or minerals with rocks formed under similar conditions of pressure and temperature, and with slightly differing bulk compositions from the parent rocks. In the CFM-diagram paragenetic mineral pairs or mineral-rock combinations posses more or less parallel tie lines, regardless of their origin (Yoder & Tilley, 1962, p. 486; Black, 1974). The plots, of the

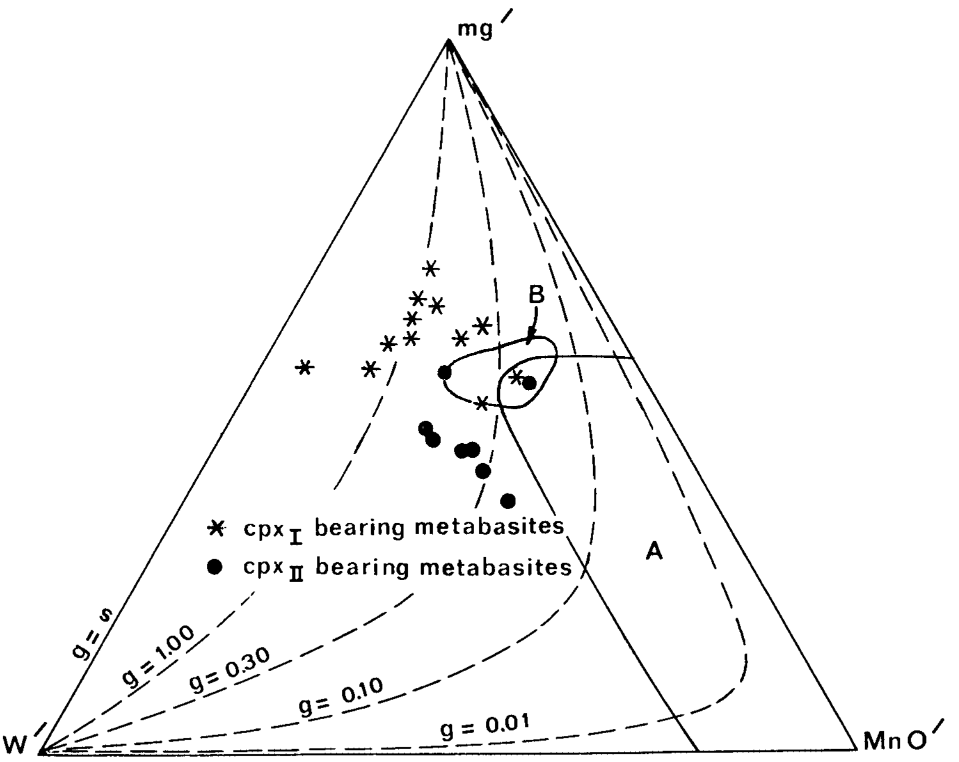

Fig. 26. Plot of metabasites from the Blastomylonitic Graben with respect to mg, MnO and w, converted to a total of 100, with indication of lines of equal g. The fields A and B are the compositions respectively of garnetiferous and cummingtonite-bearing striped amphibolites from Connemara, Western Ireland (Leake, 1972).

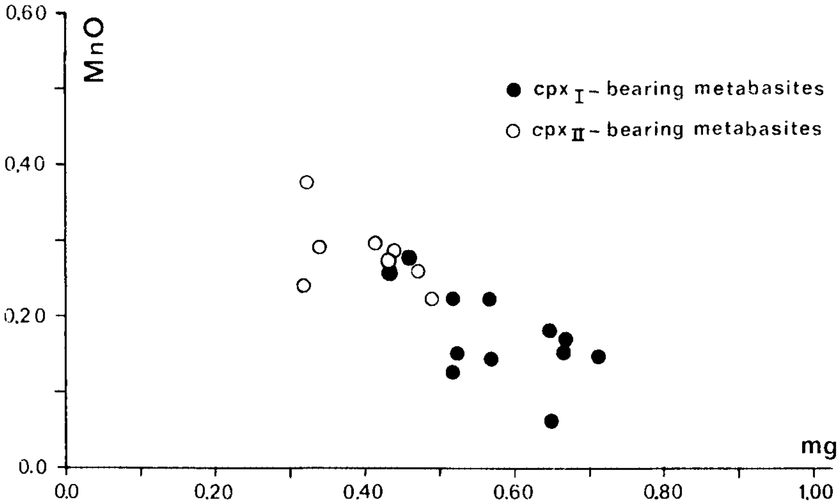

Fig. 27. Plot of the MnO content against the mg-values of metabasites from the Blastomylonitic Graben.

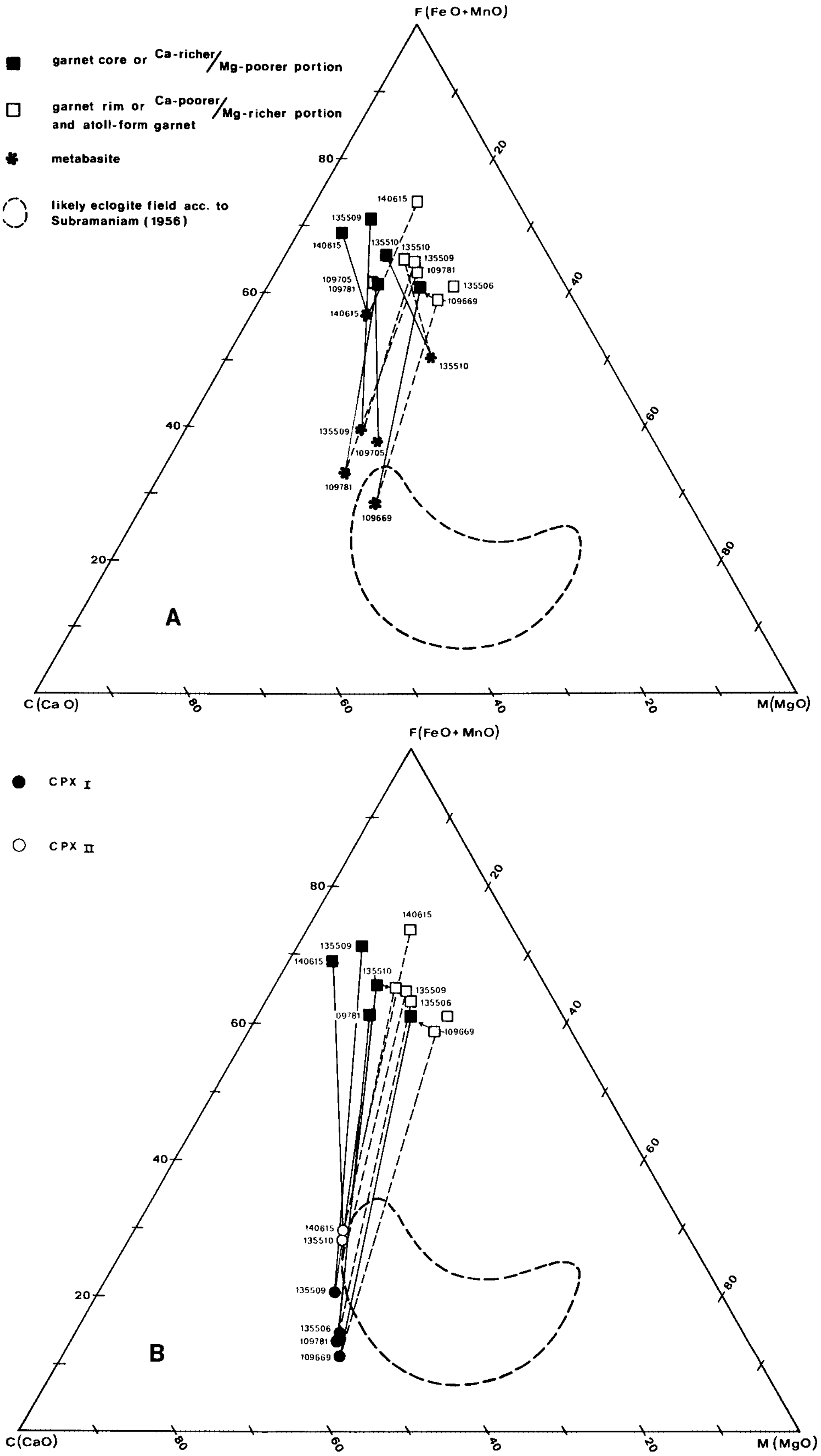
F(FeO+MnO)
garnet core or Ca-richer/Mg-poorer portion
garnet rim or Ca-poorer/Mg-richer portion and atoll-form garnet
metabasite
likely eclogite field acc. to Subramaniam (1956)
80
60
40
20
20
40
60
80
140615
135509
140615
135510
135510
135509
109781
109705
109781
135506
109669
140615
135510
135509
109705
109781
109669
A
C(CaO)
M(MgO)
F(FeO+MnO)
CPX I
CPX II
140615
135509
140615
135510
135509
135506
09781
109669
140615
135510
135509
135506
109781
109669
B
C(CaO)
M(MgO)

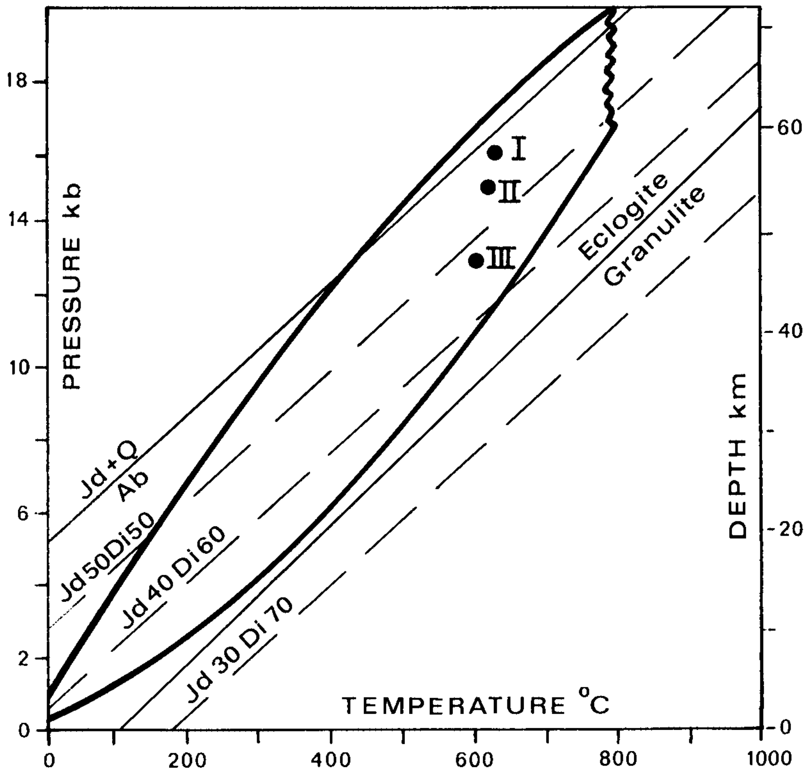

Fig. 29. P-T trajectory (with heavy outline) on prograde metamorphism for the type C eclogites of Coleman et al. (1965) according to Råheim & Green (1975). Points I, II and III are selected P, T and Jd values inferred from the chemical results of Tables 13 and 18: I= RGM 135 506: T= 625°C, P= 16 kb, Jd= 57.0% (Jd + Di = 100); II= RGM 135 509: T= 585°C, P= 13 kb, Jd= 57.8%; III= RGM 140 615: T= 610°C, P= 15 kb, Jd= 69.5%.

present eclogitic rocks (Fig. 28) fall outside the crescentic area outlining the bulk compositions of eclogite, as defined by Subramaniam (1956) with the exception of RGM 109 669.

It is obvious that the tie lines of corresponding mineral pairs such as clinopyroxene and garnet rims in the CFM-diagram show better parallelism than similar lines between clinopyroxene and garnet cores (Fig. 28B). This indicate paragenetic co-stability between garnet rims and corresponding clinopyroxenes, as confirmed by the relation of the mg-values of garnets and clinopyroxenes. Assuming that the rims and atolls are younger than the cores of garnets and that the paragenetic relationship of garnet rims and corresponding clinopyroxenes has been established, then, grosso modo, barroisitic amphibole (cf. p. 41), white mica, kyanite, and even zoisite can be considered also to belong to the paragenetic assemblage mentioned.

The conditions of pressure and temperature prevailing during the formation of garnet rims and clinopyroxene, which should correspond with the culmination of prograde metamorphism, are computed by approximation according to Råheim & Green (1974, Fig. 11). Referring to Fig. 17B, our garnets are mainly of the

---

Fig. 28. CFM-diagrams with plots of (A) rocks and accessory garnets, and of (B) garnets and corresponding clinopyroxenes.

group C-eclogites. Perchuk (1970) offered us a possibility to determine the temperature on the basis of Ca-partitioning in the garnet and clinopyroxene. Decrease in CaO from core to rim in the garnet may either be due to a drop in pressure or to an increase in temperature accompanied by little or no increase of pressure since K_D also decreases (Råheim & Green, 1975). The high jadeite-content of the clinopyroxene also points to high-pressure conditions. The results of three pairs (Fig. 29) are selected from calculations on coexisting garnet-clinopyroxene pairs from seven rock samples. The temperature (585-625°C) and pressure (13-16 kb) obtained appear to be in agreement with the content of the jadeite-component in the clinopyroxenes concerned (Jd + Di recalculated to sum of 100). The geothermal gradient during the culmination of this metamorphism should have been 11°C/km, which agrees with the theoretical and experimental conditions of formation for the group C-eclogites.

For the history of consecutive stages of mineral blastesis, alteration and deformation, the reader may be referred to Table 8. However, according to Winkler (1974, p. 27) the uralite and successive minerals of the amphibole + albite + epidote assemblage form part of another cycle of metamorphism and deformation.

The kinds of material transfer as observed in the present rocks is essentially indistinguishable from isochemical metamorphism (Sobolev, 1970, p. 235) with the possible exception of the potash- and silica-contents.

References

Alleman, F. & Tj. Peters, 1972. The Ophiolite-Radiolarite Belt of the North-Oman mountains. — Eclogae Geol. Helvetiae, 65: 657-697.

Althaus, E., 1967. The triple-point andalusite-sillimanite-kyanite. An experimental and petrologic study. — Contr. Miner. Petrol., 16: 29-44.

Anthonioz, P. M., 1970. Etude des complexes polymétamorphiques précambriens de Morais et Bragança (N.E. du Portugal). — Sci. Terre, 15: 145-166.

——, 1972. Les complexes polymétamorphiques précambriens de Morais et Bragança (N.E. du Portugal); étude pétrographique et structurale. — Mem. Serv. Geol. Portugal, N.S., 20: 1-185.

Aoki, K. & I. Kushiro, 1968. Some clinopyroxenes from ultramafic inclusions in Dreiser Weiher, Eifel. — Contr. Miner. Petrol., 18: 326-337.

Atherton, M. P. & W. M. Edmunds, 1966. An electron microprobe study of some zoned garnets from metamorphic rocks. — Earth Planetary Sci. Letters, 1: 185-193.

Aubouin, J., 1965. Géosynclinales. — Developments Geotectonics, 1: 1-355.

Banno, S., 1964. Petrologic studies on Sanbagawa crystalline schists in the Bessi-Ino district, central Sikoku, Japan. — Jour. Fac. Sci. Univ. Tokyo, 2, 15: 203-319.

——, 1966. Eclogite and eclogite facies. — Japanese Jour. Geology Geography, 37: 105-122.

——, 1970. Classification of eclogites in terms of physical conditions of their origin. — Phys. Earth Planet. Inter., 3: 405-421.

Banno, S. & Y. Matsui, 1965. Eclogite types and partition of Mg, Fe and Mn between clinopyroxene and garnet. — Proc. Japan. Acad. Tokyo, 41: 716-721.

Bearth, P., 1959. Über Eklogit, Glaukophanschiefer und metamorphen Pillowlaven. — Schweiz. Miner. Petrogr. Mitt., 39: 267-286.

——, 1966. Zur mineral faziellen Stellung der Glaukophangesteine der Westalpen. — Ibidem, 46: 13-24.

Bellière, J., 1971. Mylonites, blastomylonites et domaines polymétamorphiques. — Ann. Soc. Géol. Belgique, 94: 249-263.

Binns, R. A., 1967. Barroisite-bearing eclogite from Naustdal, Sogn og Fjordane, Norway. — Jour. Petrol., 8: 349-371.

Black, P. M., 1974. Mineralogy of New Caledonian metamorphic rocks. III. Pyroxenes and major elements partitioning between coexisting pyroxenes, amphiboles and garnets from the Ouégoa district. — Contr. Miner. Petrol., 45: 281-288.

Bobrievitch, A. P., G. I. Smirnov & V. S. Sobolev, 1960. On the mineralogy of xenoliths of grossular-pyroxene-disthene rock in kimberlite of Yakutia. — Geol. Geofiz., Akad. Nauk S.S.S.R., Sibirsk Otd., 3: 17-24 (translated from the Russian).

Borg, I. Y., 1967. Optical properties and cell parameters in the glaucophane-riebeckite series. — Contr. Miner. Petrol., 15: 67-92.

Brock, P. W. G., D. C. Gellatly & O. von Knorring, 1964. Mboziite, a new sodic amphibole end member. — Miner. Mag., 33: 1057—1065.

Brown, E. H. & W. S. Fyfe, 1972. The transition from metamorphism to melting: Status of the granulite and eclogite facies. — Proc. 24th Int. Geol. Congress, Sect. 2: 27-34.

Bryhni, I., D. H. Green, K. S. Heier & W. S. Fyfe, 1970. On the occurrence of eclogite in western Norway. — Contr. Miner. Petrol., 26: 12-29.

Bryhni, I. & W. L. Griffin, 1971. Zoning in eclogite garnets from Nordfjord, West Norway. — Ibidem, 32: 112-125.

Burri, C., 1959. Petrochemische Berechnungsmethoden auf äquivalenter Grundlage. — Birkhäuser Verlag, Basel: 1-334.

Calsteren, P. W. C. van, 1977a. Geochemistry of the polymetamorphic mafic-ultramafic complex at Cabo Ortegal (N.W. Spain). — (part of a thesis, in press).

Calsteren, P. W. C. van, 1977b. A mantle-plume model interpretation for the Paleozoic geology of Galicia with emphasis on the Cabo Ortegal area (N.W. Spain). — (part of a thesis, in press).

Calsteren, P. W. C. van, 1977c. Geochronological, geochemical and geophysical investigations in the high-grade mafic-ultramafic complex at Cabo Ortegal and other pre-existing elements in the Hercynian basement of Galicia (N.W. Spain). — (part of a thesis, in press).

Calsteren, P. W. C. van, N. A. I. M. Boelrijk, E. H. Hebeda, H. N. A. Priem, E. den Tex, E. A. Th. Verdurmen & R. H. Verschure, 1977. Isotopic dating of older elements (including the Cabo Ortegal mafic-ultramafic complex) in the Hercynian orogen of N.W. Spain: manifestations of a presumed early Paleozoic mantleplume. — (in press).

Capdevila, R., 1969. Le métamorphisme régional progressif et les granites dans le segment hercynien de Galice nord-orientale (NW de l'Espagne). — Thèse Univ. Montpellier: 1-430.

Clark, J. R., D. E. Appleman & J. J. Papike, 1968. Bonding in eight ordered clinopyroxenes isostructural with diopside. — Contr. Miner. Petrol., 20: 81-85.

Clarke, J. R. & J. J. Papike, 1968. Crystal-chemical characterization of omphacites. — Amer. Miner., 53: 840-868.

Coleman, R. G. & D. E. Lee, 1963. Glaucophane-bearing metamorphic rock types of the Cazadero area, California. — Jour. Petrol., 4: 260-301.

Coleman, R. G., D. E. Lee, L. B. Beatty & W. W. Brannock, 1965. Eclogites and eclogites: their differences and similarities. — Bull. Geol. Soc. Amer., 76, 5: 483-508.

Coombs, D. S., C. A. Landis, R. J. Norris, J. M. Sinton, D. J. Borns & D. Craw, 1976. The Dun Mountain Ophiolite Belt, New Zealand, its tectonic setting, constitution, and origin, with special reference to the southern portion. — Amer. Jour. Sci., 276: 561-603.

Cooper, A. F., 1972. Progressive metamorphism of metabasic rocks from the Haast Schist Group of Southern New Zealand. — Jour. Petrol., 13: 457-492.

Davies, H. L., 1971. Peridotite-gabbro-basalt complex in eastern Papua: An overthrust plate of oceanic mantle and crust. — Bull. Bur. Mineral Res. Geol. Geophys. Australia, 128: 1-48.

Deer, W. A., R. A. Howie & J. Zussman, 1962-1964. Rock forming minerals. Vol. I-V. — Longmans, London.

Dobretsov, N. L., V. S. Sobolev, N. V. Sobolev & W. Khlestov, 1974. The facies of metamorphism at high pressures. (Translated from the Russian by D. A. Brown). — Australian Nat. Univ., Canberra, Dept. Geol. Publ., 266 (1975): 1-361.

Dudley, P. P., 1969. Electron microprobe analyses of garnet in glaucophane schists and associated eclogites. — Amer. Miner., 54: 1139-1150.

Edwards, A. B., 1960. Textures of ore minerals. — Australian Inst. Mining Metall. Engineers, Melbourne, 2nd. edit.

Engels, J. P., 1972. The catazonal poly-metamorphic rocks of Cabo Ortegal (NW Spain), a structural and petrofabric study. — Leidse Geol. Meded., 48: 83-133.

Engels, J. P., J. J. M. W. Hubregtse, P. Floor & E. den Tex, 1974. Precambrian complexes in the Hercynian orogen of the northwestern Iberian Peninsula. — P.I.C.G. Précambrien des zones mobiles de l'Europe, Conf. Lib., 1972, Praha: 163-173.

Ernst, W. G., 1968. Amphiboles, crystal chemistry, phase relations and occurrence. In: Monographic series of theoretical and experimental studies. Minerals, rocks and anorganic materials, Vol. I, subseries: Experimental mineralogy. — Springer, Heidelberg-Berlin-New York: 1-125.

——, 1973. Blueschist metamorphism and P-T regimes in active subduction zones. — Tectonophysics, 17: 255-272.

Eskola, P., 1920. The mineral facies of rocks. — Norsk Geol. Tidsskr., 6: 143-194.

Essene, E. J. & W. S. Fyfe, 1967. Omphacite in Californian metamorphic rocks. — Contr. Miner. Petrol., 15: 1-23.

Essene, E. J., B. J. Hensen & D. H. Green, 1970. Experimental study of amphibolites and eclogite stability. — Phys. Earth Planet. Inter., 3: 378-384.

Fediukova, E. & Z. Vejnar, 1971. Optic and cryptic zoning of garnets in West-Bohemian amphibolites. — Lithos, 4: 205-212.

Fonteilles, M., 1965. Sur la profondeur de formation des veines à disthène géodique de la région Baud (Morbihan) et sur la signification des veines à disthène en général. — Bull. Soc. Franç. Miner. Cristallogr., 88: 281-289.

Fry, N. & W. S. Fyfe, 1969. Eclogites and water pressure. — Contr. Miner. Petrol., 24: 1-6.

Fry, N. & W. S. Fyfe, 1971. On the significance of the eclogite facies in alpine metamorphism. — Verhand. Geol. Bundesanst., 2: 257-265.

Ghent, E. D. & R. G. Coleman, 1973. Eclogites from southwestern Oregon. — Bull. Geol. Soc. Amer., 84: 2471-2488.

Gibbs, G. V. & C. T. Prewitt, 1968. Amphibole cation site disorder. — Papers Proc. 5th. Gen. Meet. Int. Miner. Assoc., Cambridge, 1966: 334-335.

Gilbert, M. C., 1966. Synthesis and stability relations of the hornblende pargasite. — Amer. Jour. Sci., 264: 698-742.

Green, D. H. & A. E. Ringwood, 1967. An experimental investigation of the gabbro to eclogite transformation and its petrological applications. — Geochimica Cosmochimica Acta, 31: 767-833.

Green, D. H. & A. E. Ringwood, 1972. A comparison of recent experimental data on the gabbro-garnet granulite-eclogite transition. — Jour. Geol., 80: 277-288.

Green, N. L., 1973. The diagram MgO/Al_2O_3 vs. (Na_2O+K_2O)/total $FeO+TiO_2$. A distinct geochemical separation of the calc-alkaline and tholeiitic rock series. — Canadian Mineralogist, 12: 144.

Harte, B. & K. J. Henley, 1966. Occurrence of compositionally zoned garnets in regionally metamorphosed rocks. — Nature, 210: 689-692.

Heritsch, F., 1927. Studien über den Chemismus der Granaten. — N. Jb. Miner. Geol. Paläont., Beil.-Bd. 55A: 60-91.

Heritsch, H. & E. Kahler, 1961. Strukturuntersuchungen an zwei Kluftkarinthinen. Ein Beitrag zur Karinthinfrage. — Tschermaks Miner. Petrogr. Mitt., 7: 218-234.

Hess, H. H., 1966. Notes on operation of Frantz isodynamic magnetic separator. — Princeton Univ., U.S.A.

Himmelberg, G. R. & J. J. Papike, 1969. Coexisting amphiboles from blueschist facies metamorphic rocks. — Jour. Petrol., 10: 102-114.

Holdaway, M. J., 1971. Stability of andalusite and the aluminium silicate phase diagram. — Amer. Jour. Sci., 271: 97-131.

Hollister, L. S., 1966. Garnet-zoning: An interpretation based on the Rayleigh fractionation model. — Science, 154: 1647-1651.

——, 1969. Contact metamorphism in the Kwoiek area of British Columbia: An endmember of the metamorphic process. — Bull. Geol. Soc. Amer., 80: 2465-2494.

Hubregtse, J. J. M. W., 1973a. Petrology of the Mellid area, a Precambrian polymetamorphic rock complex, Galicia, NW Spain. — Leidse Geol. Meded., 49: 9-31.

——, 1973b. Distribution of elements in some basic granulite-facies rocks. With special reference to coexisting minerals in a garnet-bearing metagabbro and a clinopyroxene-garnet-amphibole gneiss from the Mellid area, Galicia, NW Spain. — Proc. Kon. Ned. Akad. Wet., Afd. Nat., 1, 27, 1: 1-68.

Kaesberry, E. J., P. W. C. van Calsteren & R. P. Kuijper, 1976. Early Paleozoic mantle diapirism in Galicia. — Tectonophysics, 31: 61-65.

Klein, C., 1968. Coexisting amphiboles. — Jour. Petrol., 9: 281-330.

——, 1969. Two-amphibole assemblages in the system actinolite-hornblende-glaucophane. — Amer. Miner., 54: 212-237.

Knowles, C. R., J. V. Smith, A. E. Bence & A. L. Albee, 1969. X-ray-emission microanalysis of rock-forming minerals. VII. Garnets. — Jour. Geol., 77: 439-451.

Köhler, A. & F. Raaz, 1951. Über eine neue Berechnung und graphische Darstellung von Gesteinsanalysen. — N. Jb. Miner., Mh.: 247-263.

Krauskopf, K. B., 1967. Introduction to Geochemistry. — McGraw-Hill, New York: 1-721.

Kuno, H., 1960. High-alumina basalt. — Jour. Petrol., 1 & 2: 121-145.

——, 1968. Basalts. In: H. H. Hess (ed.). The Poldervaart treatise on rocks of basaltic composition. Vol. 2: 623-688. — Interscience Publ., New York.

Kurat, G. & H. G. Scharbert, 1972. Compositional zoning in garnets from granulite facies rocks of the Moldanubian Zone, Bohemian Massif of Lower Austria, Austria. — Earth Planetary Sci. Letters, 16: 379—387.

Kushiro, I., 1965. Clinopyroxene solid solutions at high pressures. — Carnegie Inst. Washington, Yearbook 64: 112-120.

Lange, H., 1963. Zur petrographischen Gliederung amphibolitischer und eklogitischer Gesteine. — Bergakademie Deutschland, 2: 92-96.

Leake, B. E., 1964. The chemical distinction between ortho- and para-amphibolites. — Jour. Petrol., 5: 238-254.

——, 1965a. The relationship between composition of calciferous amphibole and grade of metamorphism. In: W. S. Pitcher & G. W. Flinn (eds). Controls of Metamorphism. — Oliver & Boyd, Edinburgh: 299-318.

——, 1965b. The relationship between tetrahedral aluminium and the maximum possible octahedral aluminium in natural calciferous and subcalciferous amphiboles. — Amer. Miner., 50: 843-851.

——, 1968. A catalog of analyzed calciferous and subcalciferous amphiboles together with their nomenclature and associated minerals. — Geol. Soc. Amer., Spec. Paper 98: 1-210.

——, 1969. The discrimination of ortho- and para-charnockitic rocks, anorthosites and amphibolites. — Indian Miner., 10: 89-104.

——, 1971. On aluminous and edenitic hornblendes. — Miner. Mag., 38: 389-407.

——, 1972. Garnetiferous striped amphibolites from Connemara, western Ireland. — Ibidem, 38: 649-665.

Linthout, K. & C. Kieft, 1970. Preliminary note on a mboziite of metamorphic origin. — Ibidem, 37: 629-631.

Lotze, F., 1945. Zur Gliederung der Varisziden der Iberischen Meseta. — Geotekt. Forsch., 6: 78-92.

MacDonald, G. A. & T. Katsura, 1964. Chemical composition of Hawaiian lavas. — Jour. Petrol., 5: 82-133.

Matte, Ph., 1968. La structure de la virgation hercynienne de Galice (Espagne). — Trav. Lab. Géol. Fac. Sci. Grenoble, 44: 1-28.

Matthes, S., P. Richter & K. Schmidt, 1969. Die Eklogitvorkommen des kristallinen Grundgebirges in NE Bayern. II. Der Pyroxen der Eklogite und Eklogitamphibolite des Münchberger Gneisgebietes. — N. Jb. Miner., Abh. 112: 1-46.

Matthes, S., P. Richter & K. Schmidt, 1970. Idem. III. Der Disthen (Kyanite) der Eklogite und Eklogitamphibolite des Münchberger Gneisgebietes. — Ibidem, 113: 111-137.

Matthes, S., P. Richter & K. Schmidt, 1974. Idem. VII. Ergebnisse aus einer Kernbohrung durch den Eklogit-Körper des Weissensteins. — Ibidem, 120: 270-314.

Matthes, S., P. Richter & K. Schmidt, 1975. Idem. IX. Petrographie, Geochemie und Petrogenese der Eklogite des Münchberger Gneisgebietes. — Ibidem, 126: 45-86.

Misra, S. N., 1971. Chemical distinction of high-grade ortho- and para-metabasites. — Norsk Geol. Tidsskr., 51: 311-316.

Misra, S. N. & W. L. Griffin, 1972. Geochemistry and metamorphism of dolerite dikes from Austvagy in Lofoten. — Ibidem, 52: 409-425.

Miyashiro, A., 1953. Calcium-poor garnet in relation to metamorphism. — Geochemica Cosmochimica Acta, 4: 179-208.

——, 1957. The chemistry, optics and genesis of the alkaliamphiboles. — Jour. Fac. Sci. Univ. Tokyo, 2, 11: 57-83.

——, 1972. Metamorphism and related magmatism in plate tectonics. — Amer. Jour. Sci., 272: 629-656.

——, 1973. The Troodos Ophiolitic Complex was probably formed in an island arc. — Earth Planetary Sci. Letters, 19: 218-224.

Mons, W. & P. Paulitsch, 1970. Garnet orientation in different metamorphic facies. In: P. Paulitsch (ed.) Experimental and natural deformation. — Springer, Heidelberg, Berlin.

Monster, C., 1967. Petrografie van het gebied in de omgeving van Bayo (Coruña, Spanje). — Unpublished report, Leiden.

Morgan, B. A., 1970. Petrology and mineralogy of eclogite and garnet amphibolite from Puerto Cabello, Venezuela. — Jour. Petrol., 11: 101-145.

Mottana, A. & A. D. Edgar, 1969. The significance of amphibole composition in the genesis of eclogites. — Lithos, 3: 37-49..

Mottana, A., P. G. Sutterlin & R. W. May, 1971. Factor analysis of omphacites and garnets: A contribution to the geochemical classification of eclogites. — Contr. Miner. Petrol., 31, 238-250.

Murgoci, G., 1922. Sur la classification des amphiboles bleues et de certaines hornblendes. — C. R. Hebdom. Séance Acad. Sci., Paris, 175: 426-429.

Nandi, K., 1967. Garnets as indices of progressive regional metamorphism. — Miner. Mag., 36: 89-93

Newton, R. C., 1966. Kyanite-sillimanite equilibrium at 750° C. — Science, 15: 1222-1225.

Nockolds, S. R. & R. Allen, 1956. The geochemistry of some igneous rock series. — Geochimica Cosmochimica Acta, 9: 34-77.

Parga-Pondal, I., 1966. La investigación geológica en Galicia. — Leidse Geol. Meded. 36: 207-210.

Perchuk, L. L., 1970. Pyroxene-garnet equilibrium and the depth facies of eclogites. — Internat. Geology Rev., 10: 280-318.

Phillips, R., 1963. The recalculation of amphibole analyses. — Miner. Mag., 33: 701-711.

Powell, D. & J. E. Treagus, 1970. Rotational fabrics in metamorphic minerals. — Ibidem, 37: 801-814.

Priem, H. N. A., N. A. I. M. Boelrijk, R. H. Verschure, E. H. Hebeda & E. A. Th. Verdurmen, 1970. Dating events of acid plutonism through the Paleozoic of the western Iberian Peninsula. — Eclogae Geol. Helvetiae, 63: 255-274.

Raase, P., 1974. Al and Ti contents of hornblende, indicators of pressure and temperature of regional metamorphism. — Contr. Miner. Petrol., 45: 231-236.

Ragland, P. C., J. J. W. Rogers & J. S. Justus, 1968. Origin and differentiation of Triassic dolerite magmas, North Carolina, U.S.A. — Ibidem, 20: 57-80.

Råheim, A. & D. H. Green, 1974. Experimental determination of temperature and pressure dependance of the Fe-Mg partition coefficient for coexisting garnet and clinopyroxene. — Ibidem, 48: 179-203.

Råheim, A. & D. H. Green, 1975. P, T paths of natural eclogites during metamorphism, a record of subduction. — Lithos, 8: 317-328.

Rast, N., 1965. Nucleation and growth of metamorphic minerals. In: W. S. Pitcher & G. S. Flinn (eds) Controls of Metamorphism. — Oliver & Boyd, Edinburgh: 73-102.

Richardson, S. W., M. C. Gilbert & P. M. Bell, 1969. Experimental determination of kyanite-andalusite equilibria; the aluminium silicate triple-point. — Amer. Jour. Sci., 267: 259-272.

Ross, M., J. Papike & P. W. Weiblen, 1968. Exsolution in clinoamphiboles. — Science, 159: 1099-1102.

Rubbens, I. B. H. M., 1963. Resultaten van kartering en petrografisch onderzoek in het 'Complejo Antiguo'. Galicië, Spanje. — Unpublished report, Leiden.

Saxena, S. K., 1968. Distribution of elements between coexisting minerals and the nature of solid solution in garnet. — Amer. Miner., 53: 994-1014.

Scharbert, H. G., 1954. Die eklogitische Gesteine des südlichen Groszvenediger-gebietes (Osttirol). — Jb. Geol. Bundesanst., 97: 39-63.

Schmid, R., 1966. Granatchemismus als Indicator des Metamorphosengrades in der Zone Ivrea-Verbano (Norditalien). — Schweiz. Miner. Petrogr. Mitt., 46: 683-687.

Schouten, C., 1934. Structures and textures of synthetic replacements in 'open space'. — Econ. Geol., 29: 611-658.

Skinner, B. J., 1956. Physical properties of endmembers of the garnet group. — Amer. Miner., 41: 428-436.

Smellie, J. A. T., 1974. Formation of atoll garnets from the aureole of the Ardara pluton, Co. Donegal, Ireland. — Miner. Mag., 39: 878-888.

Smith, J. V., 1966. X-ray emission microanalysis of rock-forming minerals. VI. Clinopyroxenes near the diopside-hedenbergite join. — Jour. Geol., 74: 463-477.

Smulikowski, K., 1964. An attempt at eclogite classification. — Bull. Acad. Polonaise Sci., Série Sci. Géol. Géogr., 12: 701-703.

——, 1965. Chemical differentiation of garnets and clinopyroxenes in eclogites. — Ibidem, 13: 11-18.

——, 1968. Differentiation of eclogites and its possible causes. — Lithos, 1: 89-101.

Sobolev, N. V., 1964. Paragenetic types of garnet. — Izd. Nauka, Moscow (in Russian).

Sobolev, V. S. (ed.), 1970. The facies of Metamorphism. (Translated from the Russian by D. A. Brown). — Australian Nat. Univ., Canberra, Dept. Geol. Publ., 214 (1972): 1-416.

Springer, G., 1967. Die Berechnung von Korrekturen für die quantitative Elektronenstrahl-Microanalyse. — Forts. Miner., 45B: 103-146.

Spry, A., 1969. Metamorphic textures. — Pergamon Press, Oxford-London-Edinburgh: 1-350.

Sriramadas, A., 1957. Diagrams for the correlation of unit cell edges and refractive indices with the chemical composition of garnets. — Amer. Miner., 42: 294-298.

Stockwell, C. H., 1927. An X-ray study of the garnet group. — Ibidem, 12: 327-344.

Sturt, B. A., 1962. The composition of garnets from pelitic schists in relation to the grade of regional metamorphism. — Jour. Petrol., 3: 181-191.

Subbarao, K. V. & D. Chandrasekharam, 1976. Some comments on the origin of the Troodos Massif, Cyprus. — N. Jb. Miner., Mh., 8: 379-387.

Subramaniam, A. P., 1956. Mineralogy and petrology of the Sittampundi Complex, Salem district, Madras State, India. — Bull. Geol. Soc. Amer., 67: 317-390.

Tex, E. den & P. Floor, 1967. A blastomylonitic and polymetamorphic 'Graben' in western Galicia (NW Spain). — Etages tectoniques, Colloque de Neuchâtel, 1966: 169-678.

Tex, E. den & P. Floor, 1971. A synopsis of the geology of western Galicia. In: L. Montadert et al. (eds), Histoire structural du Golfe de Gascogne. — Edit. Technip, Paris, 1, 3: 1-14.

Thompson, J. E. & N. H. Fisher, 1965. Mineral deposits of New Guinea and Papua, and their tectonic setting. — VIII Commonwealth Mining Metall. Congress, Australia-New Zealand, Proc. Gen., 6.

Tröger, E., 1959. Die Granatgruppe: Beziehungen zwischen Mineralchemismus und Gesteinsart. — N. Jb. Miner., Abh., 93: 1-44.

——, 1967. Optische Bestimmung der gesteinsbildenden Minerale. II. Textband — E. Schweizerbart'sche Verl., Stuttgart: 1-822.

——, 1971. Idem. I. Bestimmungstabellen. Ibidem: 1-188.

Turner, F. J., 1968. Metamorphic Petrology. — McGraw-Hill, London, etc.: 1-403.

Vogel, D. E., 1966. Nature and chemistry of the formation of clinopyroxene-plagioclase symplectite from omphacite. — N. Jb Miner., Mh., 6: 185-189.

——, 1967. Petrology of an eclogite-bearing polymetamorphic rock complex at Cabo Ortegal, NW Spain. — Leidse Geol. Meded., 40: 121-213.

——, 1969. Catazonal rock complexes in the polymetamorphic terrain at Cabo Ortegal (NW Spain). — Geol. Assoc. Canada, Spec. Paper no. 5: 83-88.

Vogel, D. E. & C. Bahezre, 1965. The composition of partially zoned garnet and zoisite from Cabo Ortegal, NW Spain. — N. Jb Miner., Mh. 5: 140-149.

Wagner, R. H. & E. Martinez-Garcia, 1974. The relation between geosynclinal folding phases and foreland movements in northwest Spain. — Studia Geol., 7: 131-158.

Wegmann, C. E., 1935. Zur Bedeutung der Migmatiten. — Geol. Rundschau, 26: 305-350.

Wenk, E., H. Schwander & W. Stern, 1974. On calcic amphiboles and amphibolites from the Lepontine Alps. — Schweiz. Miner. Petrogr. Mitt., 54: 97-149.

White, A. J. R., 1964. Clinopyroxenes from eclogites and basic granulites. — Amer. Miner., 49: 883-888.

Winkler, H. G. F., 1967. Petrogenesis of metamorphic rocks. — Springer Verlag, Berlin-Heidelberg-New York.

Wit, M. de & D. F. Strong, 1975. Eclogite-bearing amphibolites from the Appalachian mobile belt, northwestern Newfoundland: Dry versus wet metamorphism. — Jour. Geol., 83: 609-627.

Wolff, P. M., 1948. Multiple Guinier cameras. — Acta Crystall., 1: 207-211.

Wright, W. J., 1938. The composition and occurrence of garnets. — Amer. Miner., 23: 436-449.

Yoder, H. S. & C. E. Tilley, 1962. Origin of basalt magmas: An experimental study of natural and synthetic systems. — Jour. Petrol., 3: 342-532.

Zwaan, P. C., 1955. On the determination of pyroxenes by X-ray powder diagrams. — Leidse Geol. Meded., 14: 167-276.

——, 1961. Some notes on the identification of pyrope-almandine garnets. — Proc. Kon. Akad. Wet., B, 64, 2: 305-312.

Manuscript received 4 May 1977.

Plates

Plates 1 to 4 show photographs of thin sections. Plate 5 shows X-ray emission photographs of garnets; the photographs were made at the Free University in Amsterdam. Plate 6 is a detailed drawing of a thin section of sample RGM 109 684.

Abbreviations: ab= albite, act= actinolite, amp= amphibole, ap= apatite, bi= biotite, cpx= clinopyroxene, ep= epidote, gar= garnet, ilm= ilmenite, ms= white mica, q= quartz, ru= rutile, sulf= sulfide, tit= titanite, ur= uralite, zois= zoisite.

Plate 1

Fig. 1. Zoned structure in β-zoisite of RGM 109 684. The plane of the thin section is perpendicular to the folding axis of the rock. Crossed polarizers.

Fig. 2. Zoned structure in α-zoisite of RGM 109 688. Crossed polarizers.

Fig. 3. A fan-shaped swarm of zoisite crystals inclosed in light-coloured amphibole poikiloblasts. See also the explanation of text figure 5A (RGM 109 669). Crossed polarizers.

Fig. 4. Eclogitic rock consisting of clinopyroxene, garnet, amphibole, quartz, and rutile. A deformed pyroxene porphyroblast shows amphibole in the fractures. The linearly arranged amphibole blebs show simultaneous extinction (RGM 140 617). Crossed polarizers.

Plate 1

1

2

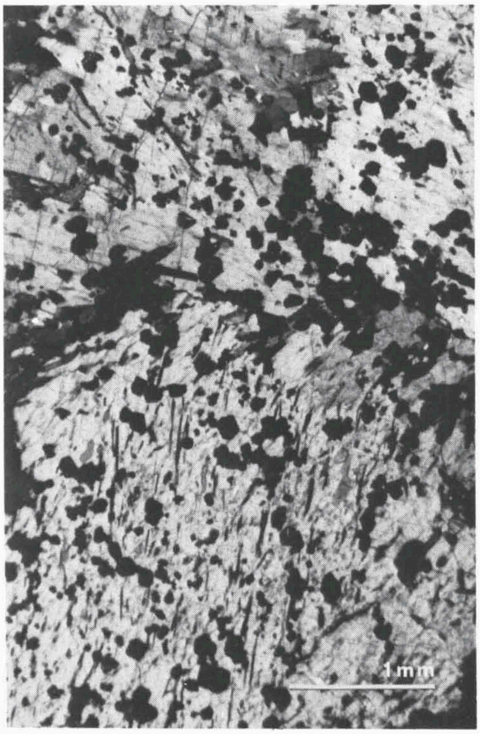

3

4

Plate 2

Fig. 1. Eclogitic rock altered by subsequent stages of metamorphism into an assemblage of partly uralitized clinopyroxene, garnet, white mica, amphibole, epidote, albite, quartz, and apatite. Notice the albite film along the grain boundaries of quartz and mica (RGM 135 509). Plane polarized light.

Fig. 2. Garnet-amphibolitic rock in an advanced stage of uralitization and subsequent albitization. The assemblage albite + mica + actinolite replaces the garnet (RGM 140 505). Plane polarized light.

Fig. 3. Originally eclogitic rock in which dispersed garnet rests survived two obvious alteration stages. The older one shows cores of uralite remnants in the assemblage of dark-coloured amphibole, albite, epidote, and titanite with rutile-ilmenite cores (RGM 140 623). Plane polarized light.

Fig. 4. Eclogitic rock rich in light-coloured amphibole. The clinopyroxene shows some uralitization (RGM 109 688). Plane polarized light.

Plate 2

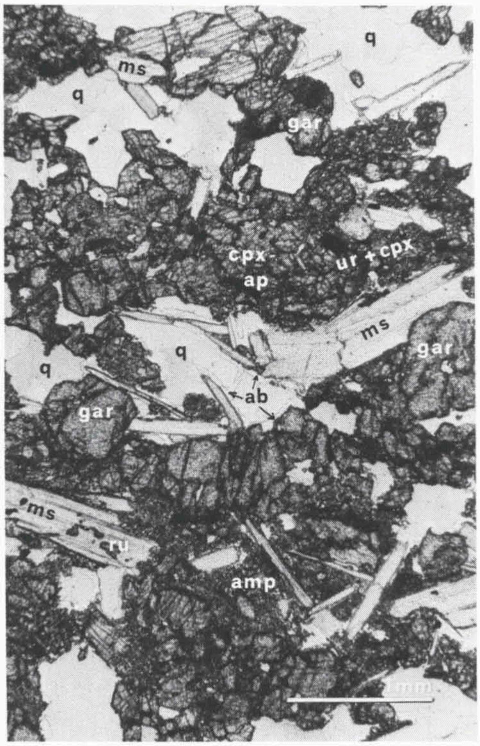
q
ms
q
gar
cpx
ap
ur + cpx
ms
gar
q
q
ab
gar
ms
ru
amp
1mm

1

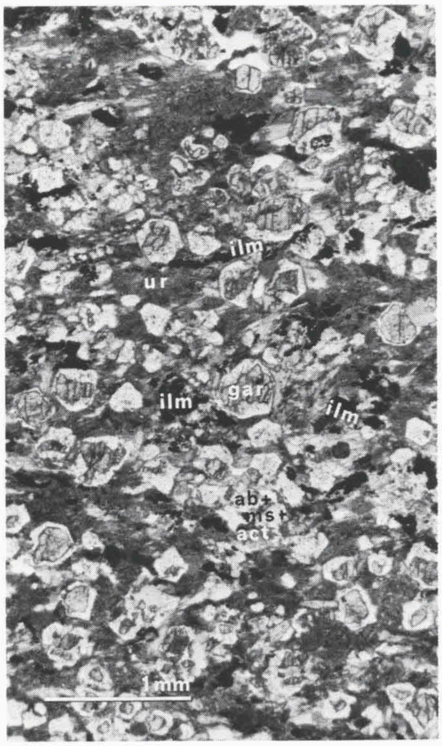
ilm
ur
ilm
gar
ilm
ab+
ms+
act
1mm

2

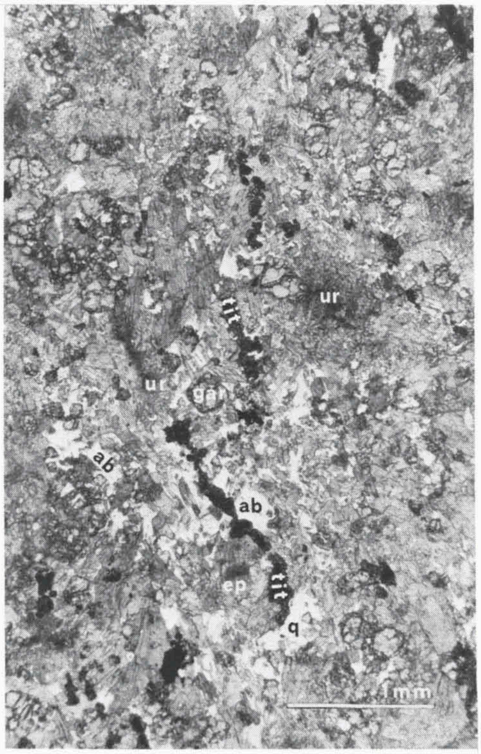
ur
tit
ur
gar
ab
ab
ep
tit
q
1mm

3

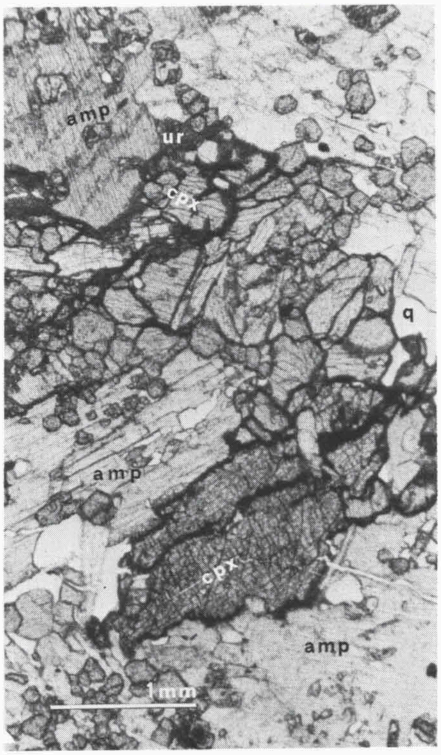
amp
ur
cpx
q
amp
cpx
amp
1mm

4

Plate 3

Fig. 1. Uralite patches with strings of ilmenite (with rutile core and titanite rim) in a boudinaged groundmass of amphibole, albite, epidote, etc. Also in the groundmass albite porphyroblasts with folded fibrous amphibole are found (RGM 140 290). Crossed polarizers.

Fig. 2. This is an example of thorough intergrowth of amphibole and clinopyroxene. Comb-like garnet aggregates are apparently resorption remnants within the composite porphyroblast. It is remarkable that the garnet is more idioblastically shaped towards the granoblastic than towards the porphyroblastic clinopyroxene (Ru 8). Crossed polarizers.

Fig. 3. Albite veinlet in an altered rock (RGM 109 705). The veinlet shows successive stages of alteration. For further explanation see the text on page 31.

Plate 3

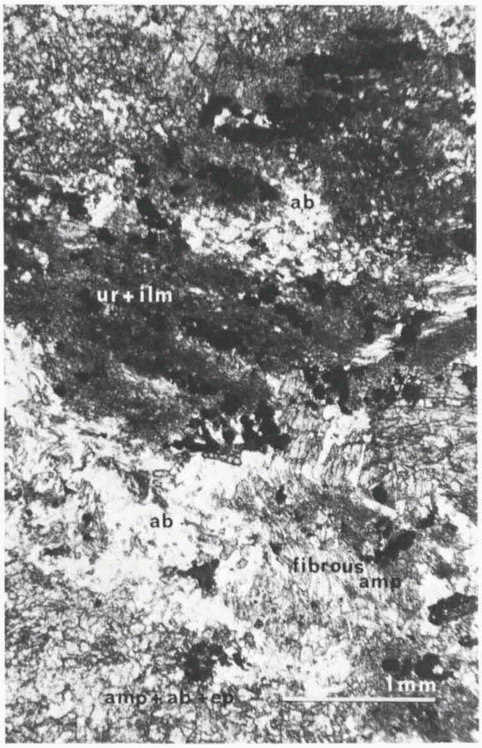
ab
ur + ilm
ab
fibrous amp
amp + ab + ep
1 mm

1

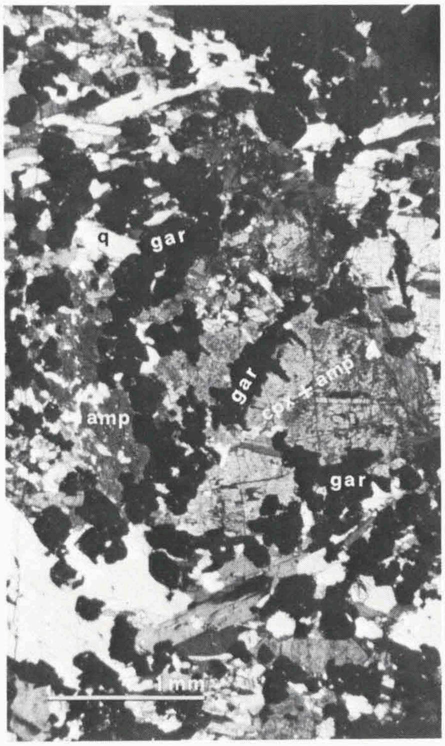
q
gar
gar
cpx + amp
amp
gar
1 mm

2

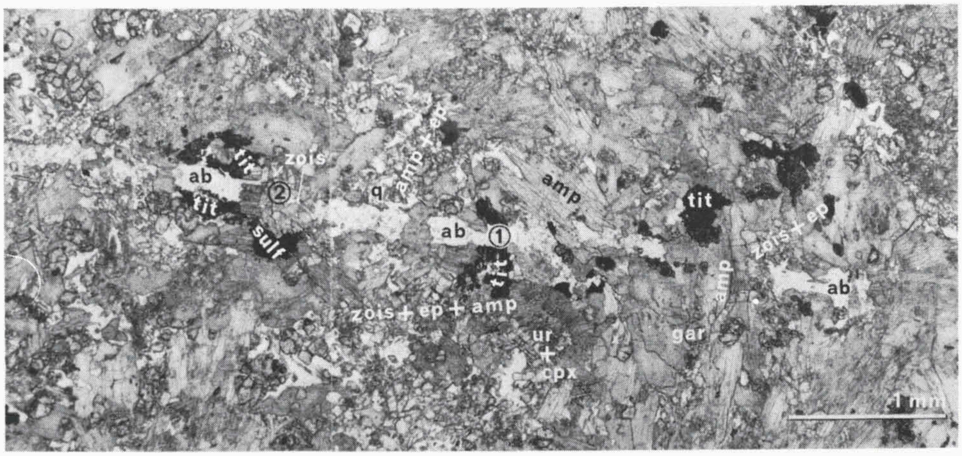
tit
zois
ab
②
tit
sulf
q
amp + ep
amp
ab
①
tit
tit
zois + ep
amp
ab
zois + ep + amp
ur + cpx
gar
1 mm

3

Plate 4

Fig. 1. The eclogitic rock of Ru 12 shows the older type of deformation. Plane polarized light.

Figs. 2, 3. Two examples of intensively altered and deformed eclogitic rocks (RGM 140 290 and RGM 109 744, respectively). For further explanation see the text on page 31. Plane polarized light.

Plate 4

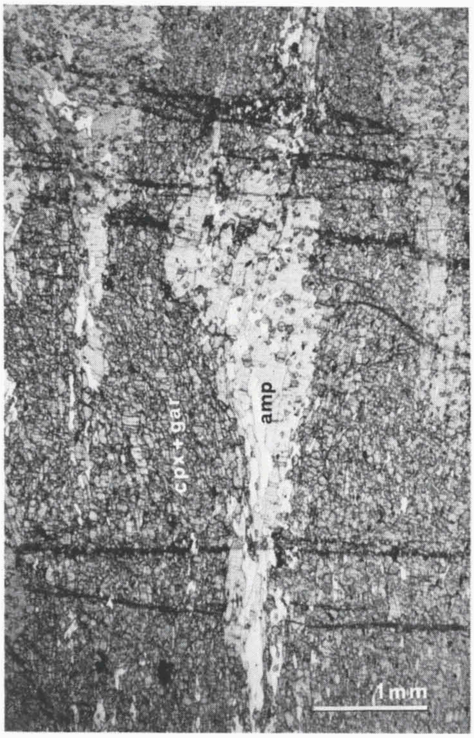
cpx + gar
amp
1mm

1

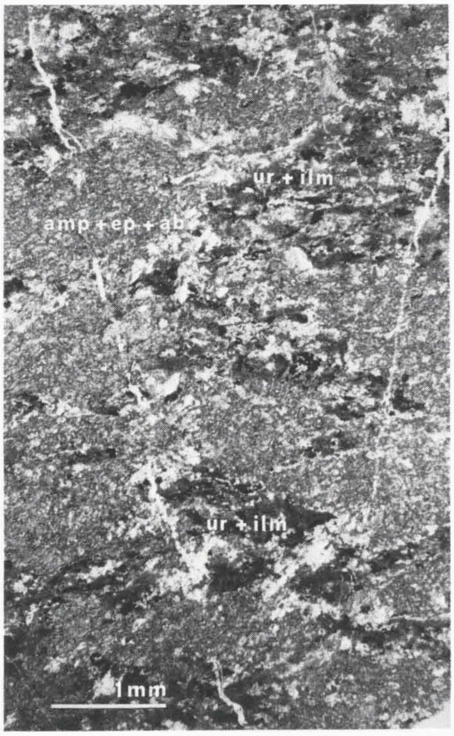
ur + ilm
amp + ep + ab
ur + ilm
1mm

2

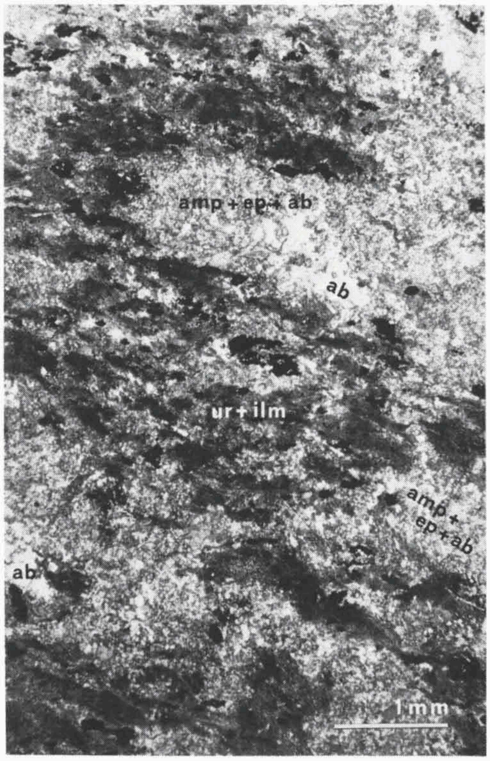
amp + ep + ab
ab
ur + ilm
amp + ep + ab
ab
1mm

3

Plate 5

Fig. 1. Mn Kα X-ray emission photograph of a garnet of sample RGM 135 510, 20 kV. Garnet with Mn-enrichment in the rim (middle).

Fig. 2. Ca Kα X-ray emission photograph of a garnet of sample RGM 140 615, 20 kV. Irregular Ca-partitioning in the garnet.

Fig. 3. Mn Kα X-ray emission photograph, 20 kV. Garnet from zone 2 as mentioned on page 32 (sample RGM 109 684). The small garnets outside the garnet-rich band have rather irregular zoned structure. The MnO-percentage is varying (maximal 3.2 wt%). The cores of these garnets are usually richer in Mn and Ca, and poorer in Fe and Mg than the rims.

Plate 5

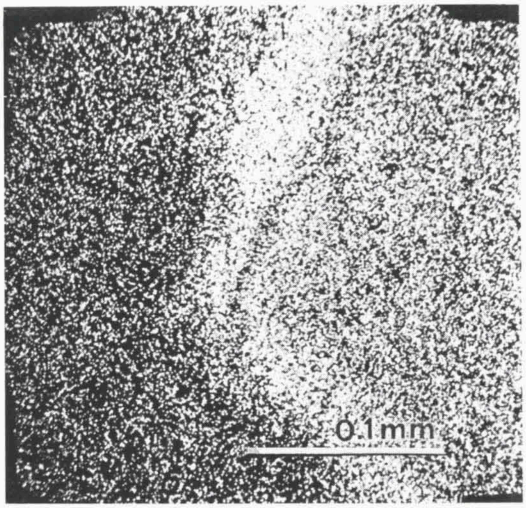

1

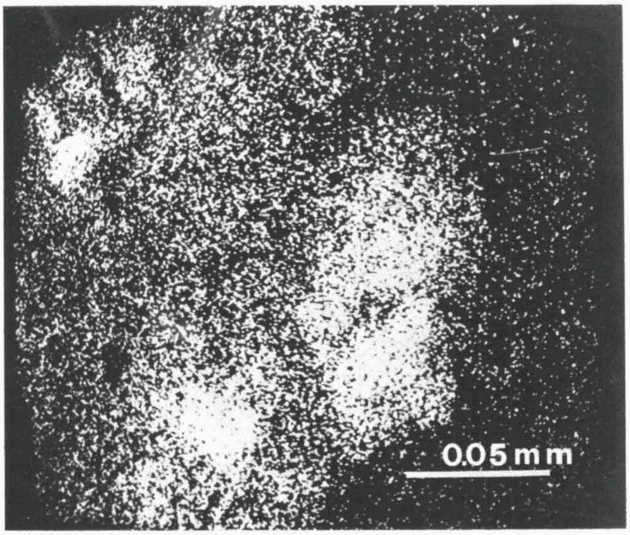

2

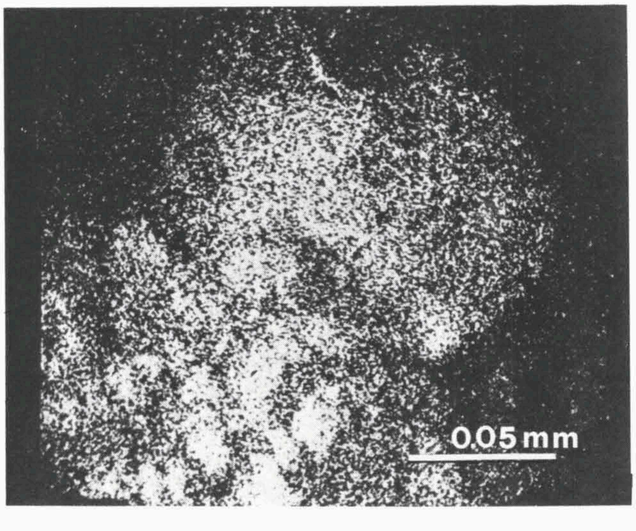

3

Plate 6

A drawing in colour after microphotographs of a thin section from sample RGM 109 684. The folding axis, as mentioned on page 32, is perpendicular to the plane of the thin section.

Plate 6

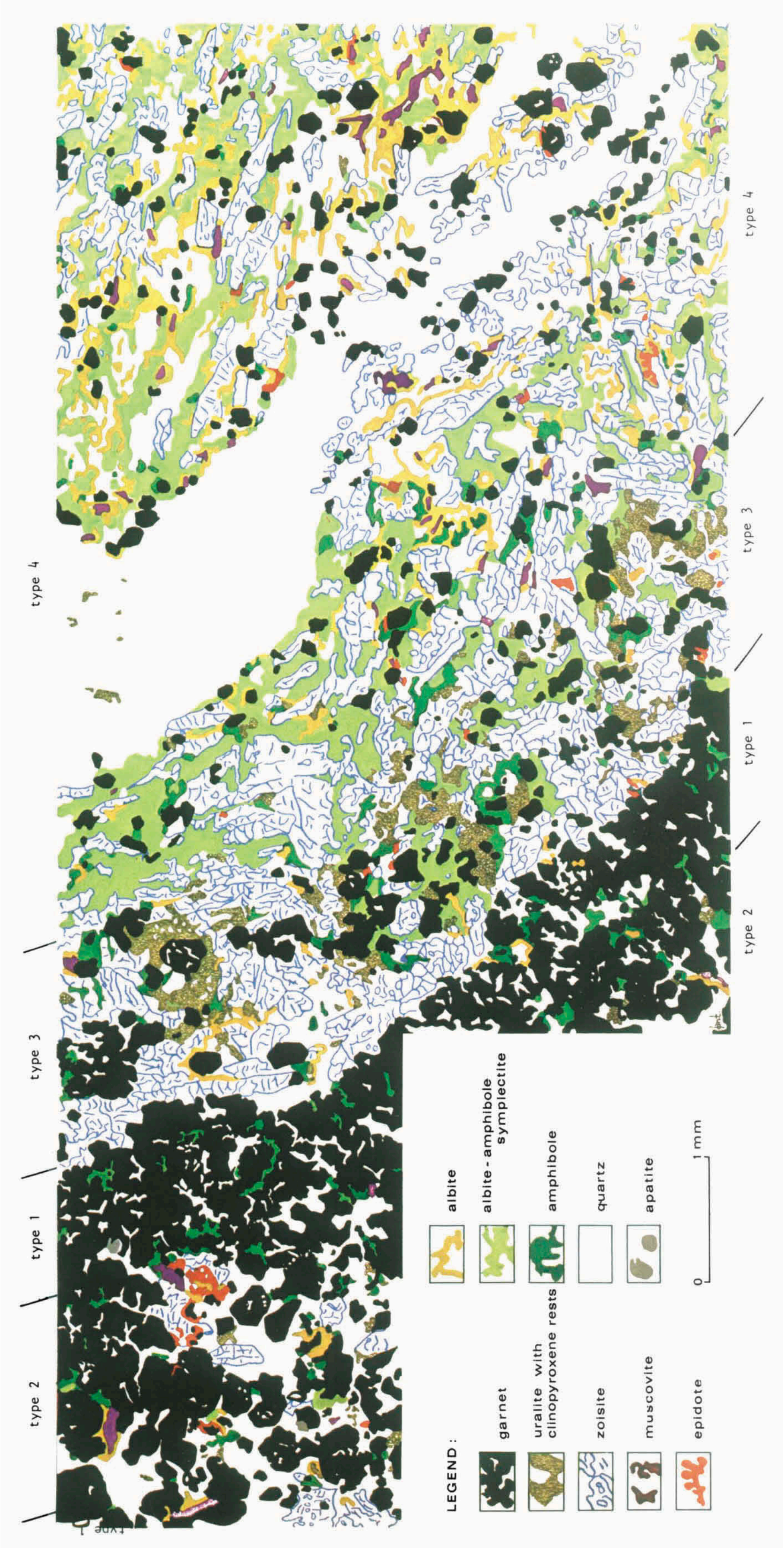
type 2
type 1
type 3
type 4
type 2
type 1
type 3
type 4
LEGEND:
garnet
uralite with clinopyroxene rests
zoisite
muscovite
epidote
albite
albite - amphibole symplectite
amphibole
quartz
apatite
0
1 mm